From the Institut für klinische Molekularbiologie
(Directors: Prof. Dr. med. Schreiber, Prof. Dr. med. Rosenstiel,
Prof. Dr. rer. nat. Franke)
at the University Medical Center Schleswig-Holstein, Campus Kiel
at Kiel University

# Autophagy and endoplasmic reticulum stress coordinate protective interleukin-22 signals in the intestinal epithelium.

Dissertation
to acquire the doctoral degree (Dr. med.)
at the Faculty of Medicine

at Kiel University

presented by
**Florian Tran**
from **Kiel**

Kiel, 2018

1st Reviewer: Prof. Dr. Philip Rosenstiel

2nd Reviewer: Prof. Dr. Stefan Rose-John

Day of oral examination: 08.05.2019

Approved for printing, Kiel, 01.03.2019

Signed: _____

Prof. Dr. Johann Roider

(Chairperson of the Examination Committee)

**This work is dedicated to my parents.**

# Table of contents

# 1 Introduction

## 1.1 Preamble

The presented study was designed to gain insight into the pathophysiology of chronic intestinal inflammation as a characteristic of inflammatory bowel disease (IBD) using several models of intestinal inflammation. In detail, this study focused on interactions of pathophysiological signalling pathways involved in IBD development in preclinical model systems. In the following we will address epidemiology, clinical features and recent pathophysiological concepts of IBD including fundamental previous studies this work is based on.

## 1.2 Inflammatory bowel disease

### 1.2.1 Clinical features

Inflammatory bowel disease is a chronic disease characterised by a relapsing-remitting course of intestinal inflammation. Two main subentities are known: Crohn's disease (CD) and ulcerative colitis (UC). IBD is caused by a multifactorial interplay of genetic susceptibility and misbalanced host-microbiota interactions (1). Even though CD and UC share several genetic risk factors and have similar epidemiology, they differ in anatomical sites of inflammatory activity, macroscopic and microscopic appearance of inflamed bowel and degree of inheritance (2). Macroscopically, CD is characterised by skipping lesions which can involve the entire gastrointestinal tract and transmural inflammation resulting in frequent development of fistulas (2). By contrast, UC only affects the colorectum and inflammation is confined to the mucosa (2). On microscopic level, non-caseous epithelioid granulomas are typical for CD, while crypt abscesses and goblet cell differentiation defects are hallmarks of UC histology (2). Both IBD entities are associated with other autoimmune disorders like primary sclerosing cholangitis (PSC), primary biliary cirrhosis (PBC) and other extraintestinal manifestations like oligoarthritis or sacroileitis, uveitis, erythema nodosum, liver manifestations and psychiatric disorders (2). Moreover, chronic inflammation favours oncogenesis, resulting in higher colorectal cancer risk in UC and to a smaller extent CD patients (2, 3).

### 1.2.2 Environmental factors

IBD is a typical multifactorial disease with both inherited and environmental contributions to the pathogenesis of the disease. IBD is more prevalent in western European or northern American countries. The incidence steeply rises, particularly in emerging country like China and India, pointing towards a critical role of high socioeconomic levels rather than geographic factors in the aetiology of IBD (4, 5). This hypothesis is underscored by findings from migrant studies, which demonstrated increased risk of developing IBD (and other multifactorial disorders) for immigrants from low prevalence regions moving to countries with higher IBD prevalence (6).

Smoking has been identified as the most prominent modulator of disease development. Active smokers are at higher risk in developing Crohn's disease in a dose-dependent manner while they are paradoxically protected against the development of UC (7-9). Nutrition habits have dramatically changed over the last century and have hence been implicated in the development of intestinal inflammation (10). A high-fat "Western" diet containing high amounts of sugars, fats and oils is associated with an increased risk for the development of CD (11), while for each single compound both protective and risk associations were found (12). Hence, most findings from the dietary studies remain inconclusive and do not point towards general protective or deleterious factors. However, Chassaing *et al.* showed that two commonly used food emulsifiers (carboxymethylcellulose and polysorbate-80) in manufactured products perturb intestinal microflora and raze the epithelial barrier and hence promote intestinal inflammation as well as metabolic disorders (13).

Indeed, intestinal dysbiosis in IBD patients hinted towards the microbial gut flora as a potential mediator of IBD development (14, 15). Usage of antibiotics in early childhood disturbs physiological development of a balanced microbial community, which is associated with increased vulnerability to the development of IBD (16). While most studies fail to pinpoint certain microbes as definite causes of IBD, they revealed perturbed composition of the gut bacterial (and viral/fungal) community due to dysfunction of a host defence mechanism or environmental factors. Interestingly, a study by Lupp *et al.* demonstrates colonic microbial changes in inflamed intestines irrespective to the trigger – be it in response to chemical triggers, genetic predispositions or infectious agents (17). This study fuels the current discussions on the disturbed microenvironment as a result or bystander of intestinal inflammation,

leading to a yet unsolved “hen and egg”-problem. Strategies to cure IBD by restoring “healthy” gut microbial communities, e.g. via faecal microbial transfer (FMT), have very ambiguous outcomes at the current stage (18); at best, a non-stable induction of remission can be achieved by intensive FMT (19).

In sum, environmental components potentially influence disease development and outcome as risk factors, however it is difficult (and currently impossible) to pinpoint down a specific trigger in an affected individual.

### 1.2.3 Genetic factors

A myriad of studies linked genetic factors to disease development. Using novel genome sequencing methods, large-scale genetic studies identified over 200 single-nucleotide polymorphisms (SNPs) which confer increased risk for the development of IBD (20). Moreover, some IBD risk genes have been associated with other autoimmune disorders like primary sclerosing cholangitis (21), asthma bronchiale and type I diabetes and susceptibility to mycobacterial infections (22), pointing at least partly to a unifying immunological principle which is disturbed in the development of chronic inflammatory disease.

The most well known risk genes associated with high risk for Crohn’s disease are nucleotide-binding oligomerization domain-containing protein 2 (*NOD2*) (23), coding for a pathogen-associated molecular pattern (PAMP)-recognising receptor, and autophagy-related protein 16-1 (*ATG16L1*), a critical scaffold protein involved in autophagy (24). Many of these genes found can be categorised in genes involved in innate immune regulation and maintenance of barrier integrity. These genes can also be functionally clustered e.g. to cytokine signalling (e.g. *IL23R*, *JAK2*, *TYK2*, *IL7R*), autophagy (e.g. *ATG16L1*, *IRGM*, *LRRK2*) and endoplasmic reticulum (ER) stress related genes (e.g. *ORMDL3*, *XBP1*). Indeed, the genetic landscape reveals a strong contribution of epithelial signals in IBD pathophysiology. While IBD was initially regarded as a primarily immune cell driven disorder (25), the concept of epithelial dysfunction has emerged as a major regulator in disease development. In particular, barrier-enhancing cytokines, epithelial ER stress and autophagy were some of the most intensely investigated mechanistic processes, which are highlighted in the following chapters.

Familial observation studies revealed the impact of inheritance on IBD with the highest individual risk for IBD development in first-degree relatives of IBD patients (26). In these constellations, a high concordance rate (70.1-83.8%) in disease type, extent and extraintestinal manifestations can be observed (27). In twin studies including monozygotic twins, high concordance rates in CD (around 25%) were observed, with a smaller extent in UC (28, 29), thus underscoring the impact of the genetic architecture to the genesis of IBD.

A very small proportion of IBD has been described to be mono- or oligogenic diseases with mutations e.g. in genes encoding for X-linked inhibitor of apoptosis protein (*XIAP*) (30), interleukin-10 (*IL10*) (31) or interleukin-10 receptor (*IL10R*) (32) as underlying causes. These monogenic IBD syndromes generally have very early onset (< 6 years of age) with a more severe, complicated and therapy-refractory disease course (33). Despite a small number of patients suffering from mono/oligogenic IBD syndromes, these cases are potentially treatable by targeted therapeutic approaches calling for in-depth functional studies of the underlying biology. For instance, abatacept treatment in cytotoxic T-lymphocyte-associated protein 4 (*CTLA4*)-mutated patients has shown efficacy in case series (34). However, most IBD cases are considered as non-Mendelian polygenic disorders, thus complicating genetic risk estimates and calling for more complex therapeutic approaches.

### 1.2.4 Current therapeutic approaches

Due to the complexity of IBD pathophysiology no causal therapy has been successfully developed yet. Current therapeutic strategies involve rather unspecific immunosuppression and targeted antagonism of inflammatory cytokines to restrain but not cure inflammation (35).

Mesalazine (or 5-aminosalicylic acid), an anti-inflammatory aminosalicylate, and budesonide, a topically effective corticosteroid without systemic effects, are first-line therapeutics in IBD and can be given orally or as an enema for lower bowel conditions (36). In case of stronger disease activity, systemic corticosteroids, azathioprine, methotrexate and 6-mercaptopurine are commonly used immunosuppressive drugs to induce and maintain remission (37). Relevant adverse events include unspecific immunosuppression leading to increased vulnerability to

infections (38), along with toxicity of the drugs (e.g. myelosuppression) (37) and stigmatising Cushing's syndrome, which includes diabetes, abdominal obesity, high blood pressure and round red face (39).

In severe IBD cases, therapeutic recombinant antibodies targeting specific immune pathways (e.g. TNFα, IL-23) are the current mainstay in the treatment of IBD. Although they are more expensive drugs than conventional immunosuppression, their usage leads to reduced healthcare costs due to reduced hospitalization and surgery (40). Prototypically, blocking of tumor necrosis factor alpha (TNFα), one of the key inflammatory cytokines in inflammatory diseases, has been shown to be effective in IBD treatment (41), therefore anti-TNFα antibodies like infliximab, adalimumab, certolizumab pegol and golimumab are included in induction and maintenance therapy schemes (42-44). In the following, other mechanistic targets have been identified in IBD therapy: Vedolizumab, a recombinant antibody against α4β7-integrin, blocks immune cell infiltration from gut vessels and is effective as an escalation therapy (45). Ustekinumab (anti-IL12/IL-23 antibody) has been approved for IBD therapy which targets the p40 subunit shared by IL-12 and IL-23 (46). Very recently, tofacitinib (small molecule Just Another Kinase (JAK) inhibitor) (47) has been approved by the FDA for UC treatment since June 2018. Further promising drugs which are under development are etrolizumab (anti-αEβ7-integrin antibody) (48) and ozanimod (RPC-1063, sphingosine-1-phosphate receptor agonist) (49).

## 1.3 The role of IL-22 in intestinal inflammation

IL-22 is a cytokine of the IL-10 superfamily first described in 2000 (50). Due to structural similarity to IL-10, IL-22 deploys its function via binding the transmembrane receptor complex consisting of the subunits IL-22R1, which is also shared by IL-20 and IL-24 from the same cytokine family, and IL-10R2 (50). IL-22 is a tissue-protective cytokine in intestinal mucosal immunity, but has also been implicated to play a role in psoriasis (51), hepatitis (52), pancreatitis (53), chronic lung (54) and joint inflammation (55). The main effects of IL-22 are assigned to its downstream activation of intracellular JAK-signal transducer and activator of transcription (STAT) signalling, particularly STAT3 (56). Main physiological consequences of IL-22-dependent STAT3 activation in intestinal epithelial cells are related to antimicrobial peptide (57) expression, promotion of epithelial regeneration (56) and

posttranslational modification of secreted proteins (58). Indeed, IL-22 was found to be the strongest inducer of STAT3 in the intestinal epithelium, thus IL-22 is regarded as the strongest tissue protective cytokine in intestinal inflammation (56). As such, IL-22 is regarded as the archetypical barrier protective cytokine, which bears high potential for therapeutic exploitation in immune-related diseases, e.g. IBD (59) and graft versus host disease (GvHD) (60). STAT1 and STAT5 activation upon IL-22 stimulus is weaker than STAT3 activation (61), however evidence pointing towards an important role of STAT1 in IL-22 signalling has been put forward. Type I interferons like interferon (IFN)α and IFNβ synergistically enhance IL-22-dependent STAT1 signalling and thus potentiate the pro-inflammatory properties of IL-22 in the intestine (60, 62). Additionally, activation of the mitogen-activated protein kinase (MAPK) pathways and the phosphoinositide 3-kinase (PI3K)-Akt-mechanistic target of rapamycin (mTOR) pathway may also play important roles in IL-22 downstream signalling (61, 63).

While epithelial cells of barrier organs (e.g. skin, lung, intestine) are the primary receiver of IL-22 signals, IL-22 is secreted from a plethora of immune cells circulating in the underlying mucosal tissue. Hence, IL-22 is one of only a few unidirectional cytokine bridging immune cell signals with epithelial functions. In detail, IL-22 has been shown to produced by T cells, in particular T helper 1 ($T_h1$), $T_h17$ (64, 65), $T_h22$ (66, 67), $CD8^+$ T cells, natural killer T (NKT) and γδT cells (68). Other cellular sources are neutrophilic polymorph nuclear (PMN) cells (69) and innate lymphoid cells (ILCs) like NK cells, lymphoid tissue inducer (LTi) cells, and natural cytotoxicity triggering receptor $(NCR)^+$ ILCs (70, 71) .

Expression of IL-22 is controlled by several mechanisms. While the aryl hydrocarbon receptor (AhR) is a transcriptional regulator of *IL22* expression (72, 73), pro-inflammatory cytokines like IL-17, IL-12, IL-23 and IL-6 (64) promote IL-22-dependent effects. In particular, IL-23 licenses production of IL-22 through binding to its receptor IL-23R on dendritic cells (74). Our working group demonstrated that intestinal epithelial cell (IEC)-specific expression of *Il23r* also orchestrates IL-22 production in the intestinal mucosa in a murine model, underpinning the complexity of regulatory crosstalks between various cell types in gut inflammation (75). Intriguingly, loss of *Il23r* in IECs diminished inducible IL-22 levels in the intestinal mucosa, resulting in a severe experimental colitis due to the insufficiency of IL-22-dependent protective

signals (75). In general, IL-22 is highly expressed in inflammatory conditions, e.g. IBD or rheumatoid arthritis (55). Higher numbers of IL-22 producing cells in intestinal mucosa of IBD patients (76) can be found, but also systemically elevated levels of IL-22 are positively correlated with disease activity (77). Mice lacking *Il22* expression succumb in an experimental colitis model using dextrane sodium sulphate (DSS), hereby demonstrating the regenerative impact of IL-22 in intestinal inflammation (78). However, IL-22 and its downstream effects seem to be tightly regulated by a natural antagonist called IL-22 binding protein (IL-22BP), which is a soluble single-chain IL-22R not encoded by *IL22R1* (79) and expressed in several tissues including the intestinal mucosa. In an acute inflammatory state, IL-22BP is down-regulated (78), presumably to disinhibit tissue-protective IL-22 effects. On the contrary, a carcinogenesis promoting role of IL-22 due to increased epithelial proliferation and inhibition of cellular differentiation has been described in the gut (78), liver (80) and connective tissue (81). Thus, the role of IL-22 in the context of intestinal inflammation seems to be ambiguous. Despite these findings, efforts are made to establish IL-22 or IL-22-dependent signalling as therapeutic targets in IBD treatment. IL-22Fc (UTTR1147A) is a recombinant fusion protein of IL-22 with the Fc part of human immunoglobulin (Ig) G4 antibodies which passed pre-clinical safety and pharmacological studies in mice, rats and cynomolgus monkeys (59). Currently, a phase Ib study with intravenous UTTR1147A in healthy volunteers and volunteering patients with UC and CD is evaluating safety of this therapy (ClinicalTrials.gov identifier: NCT02749630).

## 1.4 The intestinal epithelium – a multitalented barrier

The intestinal epithelium is a monolayer containing a variety of specialised cells, which (in a homeostatic state) meet the demands of both proper nutritional function and sufficient protection against luminal harmful stimuli, e.g. invading microbes (82). Most of the defence mechanisms originate from the epithelial cells either by providing a physical barrier, cell intrinsic strategies or secreted components for host protection (figure 1-1). While the epithelial architecture varies along the whole gastrointestinal tract (82) I will focus on the small and large intestine as these are the main sites of IBD activity (2) and point out the unifying principles of epithelial biology that are present at all sites of the intestine. The secretory defence line, mainly consisting of

mucins (83), immunoglobulins and antimicrobial peptides (AMP) (75, 84-86) is important as physical and immunological host barrier in antimicrobial defence. However, as it would be beyond the scope, I did not address their interesting role in intestinal inflammation in this thesis work.

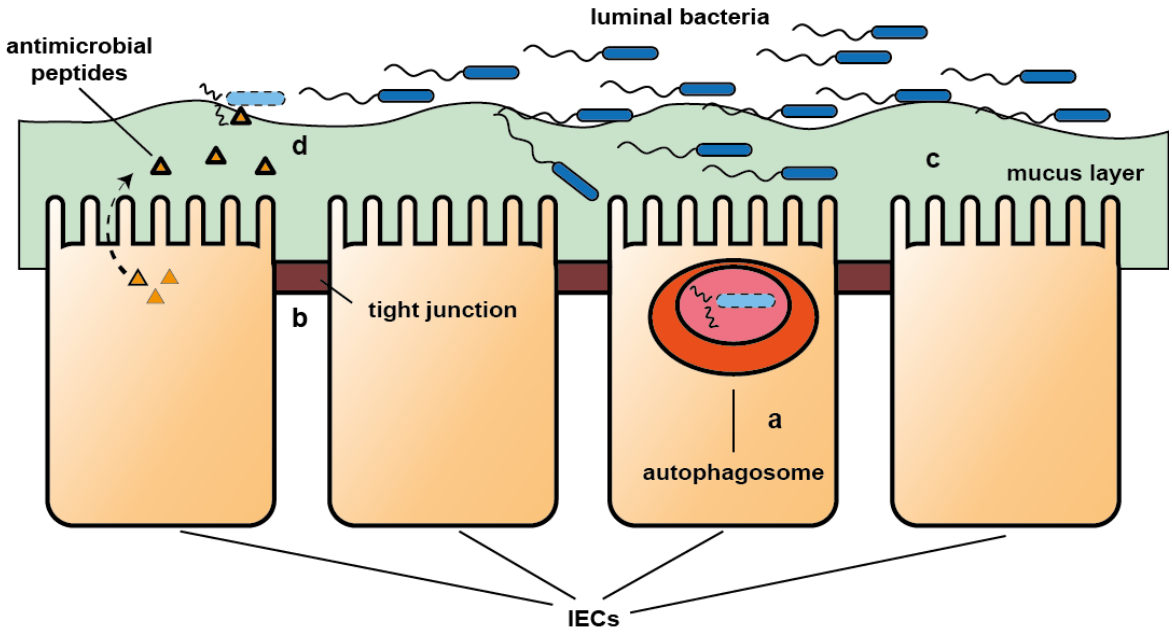


**Figure 1-1: Main defence strategies of the intestinal epithelial barrier**

(a) IECs and their innate defence mechanisms like autophagy, (b) tight junctions, (c) the mucus layer and (d) antimicrobial peptides contribute to the barrier function of the intestinal epithelium.

### 1.4.1 Epithelial integrity as a stronghold of host-defence against pathogens

The small intestinal epithelium is spread along the crypt-villus axis. In the villus part, mainly enterocytes and goblet cells with interspersing M-cells and enteroendocrine cells are located, whereas the crypt fraction also harbours Paneth cells, intestinal stem cells (ISC) and the highly proliferative transit-amplifying cell zone (TAC) (82). Immune cells are in close communication with the epithelium; some even reside in the barrier itself, so-called intraepithelial lymphocytes (87). In contrast, the colonic epithelium forms no villi but only crypts, containing more goblet cells but otherwise similar distribution of epithelial cell types and a functionally similar subset of cells in the crypt bottom as in the small intestine (82).

Specialised cellular contacts including tight junctions, adhering junctions and desmosomes, are essential for the integrity of epithelial tissues as well (82). IBD patients displayed lower expression of tight junction proteins like occludin and ZO-1, causing an increased gut permeability, which may contribute to intestinal inflammation (88, 89).

### 1.4.2 Cell death & regeneration: Cellular fate towards harmful stimuli

Harmful stimuli like irradiation, pathogens, chemicals, humoral signal or nutritional deprivation lead to cellular stresses like oxidative stress and ER stress. If the cellular damage is irreversible, cellular fate is skewed towards cell death. Defects of the epithelial layer, e.g. by cellular death or by tissue wounding leads to a defective physical and immunological barrier function and thus favour an inflammatory phenotype of the intestine (90). In particular, epithelial cell death is a hallmark of intestinal inflammation and has therefore extensively been studied. For instance, TNFα is a key pro-inflammatory cytokine in IBD which can induce an immunogenic type of epithelial cell death called necroptosis besides classic apoptosis in murine models and in CD patients (91). Necroptosis is a programmed cell death modality characterised by cellular lysis and efflux of intracellular contents without blebbing and is therefore distinct to caspase-mediated apoptosis. Genetic deletion of epithelial caspase-8, one of the critical regulators of apoptosis, led to necroptotic cell death upon TNFα and subsequent spontaneous ileitis and high susceptibility to experimental colitis (91). Other inflammatory cytokines (like interferon gamma (IFNγ) (92)) and cellular stress signals can contribute to death of epithelial cells, e.g. uncontrolled ER stress (93), autophagy defects (94) and excessive inflammasome activation (95).

Epithelial regeneration is an adaptive proliferative response toward tissue damage aiming to minimize the epithelial barrier defects and re-establish containment of potential harmful stimuli within the intestinal lumen. Epithelial regeneration exploits the molecular principles of cellular proliferation by orchestrating simultaneous proliferation and differentiation on an epithelial cell type specific level (e.g. stem cells, transit amplifying cells, goblet cells, Paneth cells). The crypt bottom, which forms a niche for stem cell, is crucial for epithelial regeneration: Intestinal stem cells (ISC) are

the stem cell pool for all epithelial cell types, and their function is critically dependent on the interspersed Paneth cells (96). Stem cell proliferation is dependent on canonical Wnt and STAT3 signalling (97, 98).

Importantly, interleukin (IL)-22 (which activates STAT3) promote epithelial regeneration by boosting the function and protection of the stem cell niche (60, 98). Vice versa deletion of STAT3 in the intestinal epithelium (*Stat3*$^{\Delta IEC}$ mice) attenuates regenerative capacity, ultimately leading to defective wound healing in an inflammatory setting and thus perpetuating disease (56). As described before, these tissue protective properties of IL-22 gave rise to the rationale of designing recombinant IL-22-based treatments (59). This outstanding role of IL-22 in proliferation is underscored by increased tumorigenesis in the intestine (78) and the biology of psoriasis, another inflammatory disorder of the skin: Here, IL-22 is the driving force of keratinocyte hyperproliferation and hence IL-22 inhibition is under evaluation as a novel therapy concept (99).

In this context, Leucine-rich repeat -containing G-protein coupled receptor 5 (LGR5) is a marker surface receptor implicated in Wnt signalling and mainly expressed in ISC (100). The natural ligand of LGR5 is R-Spondin1, which was shown to boost Wnt-signalling in synergy with Wnt3a (101). However, the definite cellular source of R-Spondin1 remains to be investigated. Transforming growth factor beta (TGFβ) signalling is another critical stimulatory axis for stem cell function (102). Bone morphogenetic protein 4 (BMP4), a member of the TGFβ superfamily and exclusively expressed in the intravillus mesenchyme, repressed *de novo* crypt formation (102). Transgenic overexpression of the antagonist noggin led to overt proliferation and de novo crypt generation in a mouse model (102). Epidermal growth factor (EGF) was shown to drive intestinal epithelial proliferation as well (103).

Moreover, the Hippo-Yes-associated protein (YAP) pathway has been implicated in stemness and regeneration (104). By contrast, TAC are the most proliferative cell type amongst the intestinal epithelial cells (IEC) and contribute to rapid epithelial turnover (82). ISC and TAC function are linked in an mTORC1-dependent fashion (96). Whereas homeostatic epithelial proliferation under physiological conditions is mainly driven by cell intrinsic signalling programs epithelial wound healing greatly depends on exogenous regenerative stimuli secreted from residing cells in the intestinal mucosa.

The knowledge of the underlying molecular event of stem cell proliferation has empowered Sato *et al.* to implement *in vitro* three-dimensional epithelial culture models, which are referred as intestinal organoids (105). After isolation of the stem cell niche, they were embedded into a gel-like collagen matrix and stimulated with epidermal growth factor (EGF), R-spondin1 and noggin, which essentially maintain intestinal stemness by activating the EGF receptor (EGFR) and Wnt pathways and suppressing transforming growth factor-beta (TGFβ) signalling, respectively. As a consequence, stem cells autonomously divide and their offspring form crypt-like structures with clear polarization and differentiate into all known intestinal epithelial cell types. This technology has been transferred to other tissues like hepatic (106) and even neuronal tissues (107). Also, human organoids are effectively investigated (108). Organoids represent an adequate model for studying intestinal epithelial biology and have been used for biomedical purposes like drug screenings, bio-banking (109), transplantation (110) etc. As exemplified in this work, intestinal organoids are increasingly often used to study the epithelial biology.

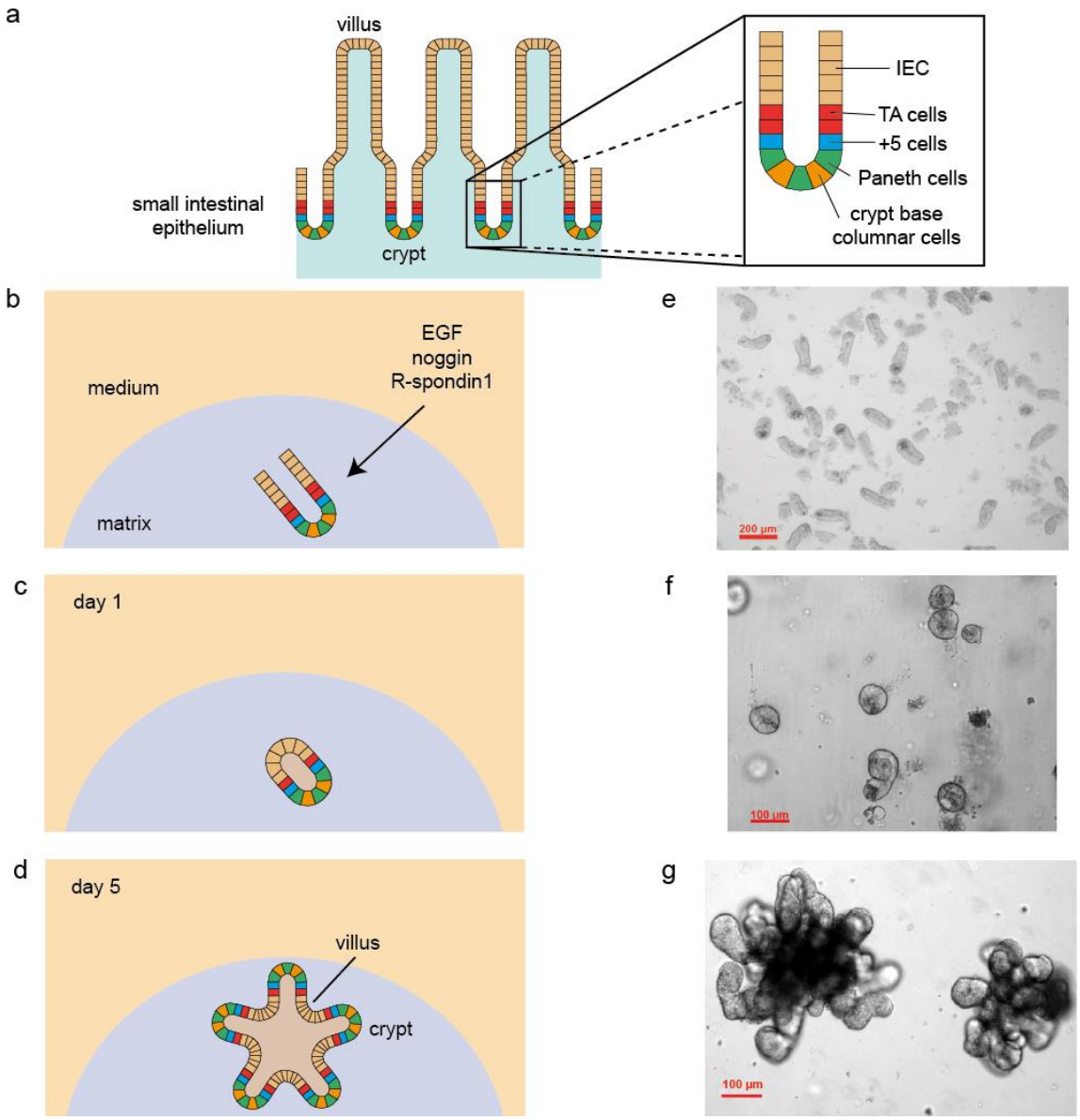


**Figure 1-2: Conception of intestinal organoid cultures**

(a) Scheme of small intestinal epithelium architecture. Crypts provide the stem cell niche, were Paneth cells and different stem cell subsets like Lgr5$^{+}$ +5 cells and crypt base columnar cells reside. Next to the crypt base transit amplifying (TA) cells can be found, which serve for massive tissue renewal at baseline conditions. (b) Isolated crypts were embedded into a collagen matrix, which is then overlaid by stem cell medium containing EGF, noggin and R-spondin1. (c) Crypts develop cystic formations after one day in culture, providing cellular luminal-basolateral polarity. (d) Evolved crypt-derived organoids with multiple crypt-like stem cell niches and villus-like epithelium. (e) Freshly isolated epithelial crypts in suspension. (f), (g) Corresponding microscopic captures to (c) and (d).

### 1.4.3 Innate strategies to cope with microbial invasion

Intestinal epithelial cells have intrinsic strategies to react to microbial pathogen invasion. Both intra- and extracellular pattern recognition receptors like Toll-like receptors (TLRs), NOD and NOD-like receptors, cyclic GMP-AMP synthase (cGAS) etc. mediate anti-infective response upon sensing of microbial molecules (111). In addition, these receptors serve as adaptors or scaffolds for effector mechanisms in intestinal epithelial cells like autophagy induction and generation of reactive oxygen species (ROS) (111). In brief, the induction of bactericidal ROS like hydrogen peroxide ($H_2O_2$) or superoxide ($O^{2-}$) have been implicated in host defence against intracellular pathogens (112). Recently, our working group has shown that NOD2-dependent ROS generation, in particular of $O^{2-}$, is crucial for antibacterial defence (113).

Cytosolic DNA is a danger signal for either massive DNA damage with extrusion of DNA fragments from the nucleus to the cytoplasm (114) or for the presence of intracellular microbes (115). Several receptors sense microbial nucleic acid, e.g. TLR9 (116), absent in melanoma 2 (AIM2) (117), cGAS (118) and retinoic acid inducible gene (RIG)-I (119). cGAS detects double stranded (ds)DNA to produce the second messenger cyclic guanosine monophosphate-adenosine monophosphate (cGAMP). cGAMP in turn can also be produced by viable intracellular bacteria and is sensed by the ER-resident stimulator of interferon genes (STING), which leads to phosphorylation of TANK-binding kinase 1 (TBK1) and thus ultimately mediate a type-I interferon signal to counteract microbial infections (120). STING signalling has been implicated in inflammatory diseases (115) and cancer biology (121) and is hence extensively studied. In particular, the idea of an intrinsic sensing of harmful signals like dsDNA (be it through release of damaged DNA from the cytosol/mitochondrion or through external stimulation like viral infection) which induces a strong inflammatory program is focussed in recent work as therapeutic target (122). Concurring with this, RIG-I senses cytosolic (viral) ss/dsRNA to activate downstream melanoma differentiation antigen (MDA)5 and mitochondrial antiviral-signaling protein (MAVS) to ultimately induce IFN-I production (119).

Another potent mechanism limiting microbial propagation across the epithelium is the induction of autophagy and xenophagy of intracellular pathogens (123). Intriguingly, NOD2 recruits ATG16L1 to the plasma membrane for induction of xenophagy,

suggesting requirement of physical protein-protein interaction for proper ATG16L1-dependent xenophagy (124). The role of autophagy in IBD and the composition of the related ER stress machinery will be detailed in chapter 1.5.

## 1.5 Autophagy and ER stress resolution – critical mechanisms in epithelial homeostasis

### 1.5.1 ER stress

The endoplasmic reticulum (ER) is the cellular organelle required for synthesis and primary post-translational processing (e.g. *N*-linked glycosylation and disulphide bond formation) of nascent secretory and transmembrane proteins. It forms a reticular plexus communicating with the outer lipid bilayer of the nuclear membrane (125). Accumulation of un-/misfolded proteins, e.g. in a state of high secretory activity, leads to their aggregation in the ER and subsequent cellular stress called ER stress, which can direct cellular fate towards cell death (125). To control excessive ER stress and to avoid severe tissue damage due to cellular malfunction, evolutionary highly conserved signalling pathways, summarised as the unfolded protein response (UPR), guard either re-establishment of cellular homeostasis or serve as checkpoint for programmed cell death if excessive ER stress cannot be resolved (125). Considering this, it is not surprising that highly secretory cells (like Paneth cells) are the most vulnerable cell types to ER stress and have the strongest UPR activation within tissues (93).

The folding capacity of the ER can be modulated by several intrinsic and extrinsic factors like hypoxia (126), ROS (127), saturated fatty-acids (128) pathogens (129) and ageing (130). A particular role of the ER has been pinpointed in the context of viral infections as replicating viruses perturb ER function for production of viral proteins (131). Other pathogens selectively modulate distinct UPR pathways to ensure their survival (132). ER stress can be experimentally induced e.g. by tunicamycin (inhibition of N-glycosylation) or thapsigargin (calcium efflux from the ER) (133).

Mechanistically, three ER resident transmembrane proteins integrate UPR activity: inositol-requiring enzyme 1α (IRE1α, ERN1), PKR-like ER kinase (PERK, EIF2AK3) and activating transcription factor 6 (ATF6) (125). Binding immunoglobulin protein

(BiP, GRP78, HSPA5), a chaperone, represses the activity of these three ER stress sensors in a compensatory state, but associates with misfolded proteins under ER stress conditions and which ultimately lead to disinhibition of the UPR (134) (see figure 1-3).

One important regulator of ER stress, XBP1, has been identified as an important IBD risk factor (93). Under ER stress conditions, IRE1α, an endonuclease, splices *XBP1* to generate the *spliced XBP1* (*XBP1s*) form which after translation acts as a protective transcriptional factor for chaperones and other ER-resident proteins (135). Vice versa *XBP1* negatively regulates IRE1, thus propagating pro-inflammatory signalling and cell death e.g. via JNK (136) and development of colitis-associated carcinogenesis (93, 137). Besides splicing of XBP1, activated IRE1 cleaves aberrant mRNA with its endonuclease domain which is called regulated IRE1-dependnet decay (RIDD). Together with p-eIF2α, a downstream regulator of PERK, cleaved mRNA fragments after RIDD prevent further accumulation of misfolded proteins (138, 139). Moreover, ER stress impairs epithelial regeneration by suppressing stem cell markers and proliferative activity, another hallmark of intestinal inflammation (140).

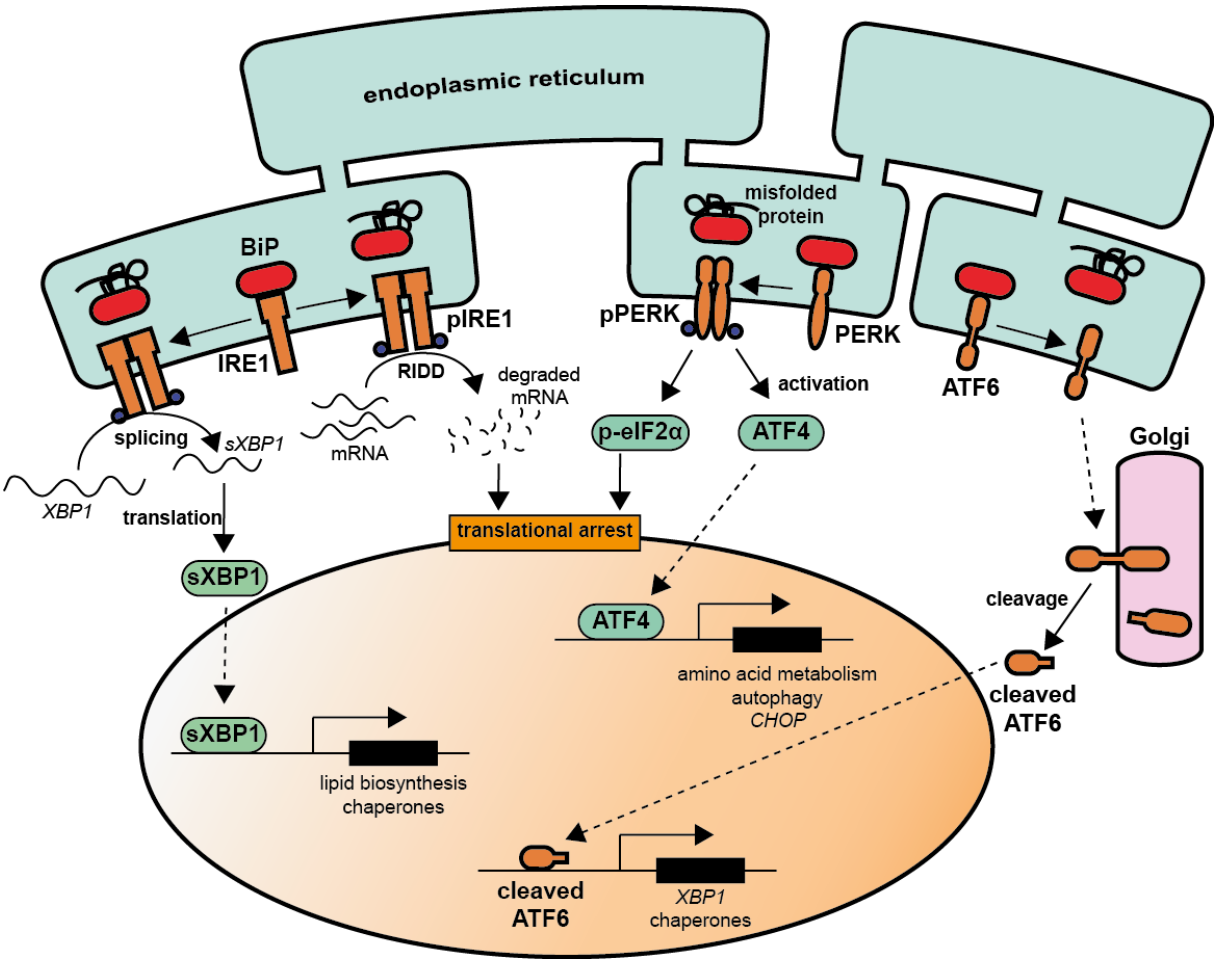


**Figure 1-3: Conception of the unfolded protein response (modified from (125) with permission from Springer Nature)**

Three ER-resident transmembrane proteins propagate critical stress signals upon accumulation of misfolded proteins in the ER: BiP recognises and binds to misfolded proteins dissociating from IRE1, PERK and ATF6, thereby disinhibiting their downstream signals, culminating in binding of the transcription factors XBP1s, ATF4 and cleaved ATF6 to target genes encoding for cell-protective mechanism like chaperones or cell death induction (e.g. *CHOP* (141)). In parallel, regulated IRE-dependent decay (RIDD) of mRNA and p-eIF2α downstream of pPERK lead to translational arrest/attenuation.

## 1.5.2 Autophagy

Autophagy is a “cannibalistic” mechanism serving to cope with stressful condition (e.g. starvation) due to the orderly degradation of subcellular components and pathogens. It serves various purposes in housekeeping cellular function, for instance recycling of unused and senescent cellular components in a state of starvation (142). Three different autophagy types are described (see figure 1-4): The classic mode

termed as macro-autophagy serves degradation of cytoplasmic cargo enveloped in a double membrane-bound vesicle called autophagosome via fusion with lysosome, referred to as autolysosome (142). However, micro-autophagy describes a process in which cytosolic components are directly engulfed by lysosomes (142). Finally, translocation of proteins complexed with chaperone proteins (e.g. Hsc70) via lysosomal-associated membrane protein 2A (LAMP-2A) across the lysosomal membrane has been referred to as chaperone-mediated autophagy (143). Most recent work focuses on the role of macro-autophagy, which therefore is hereinafter referred to as “autophagy”.

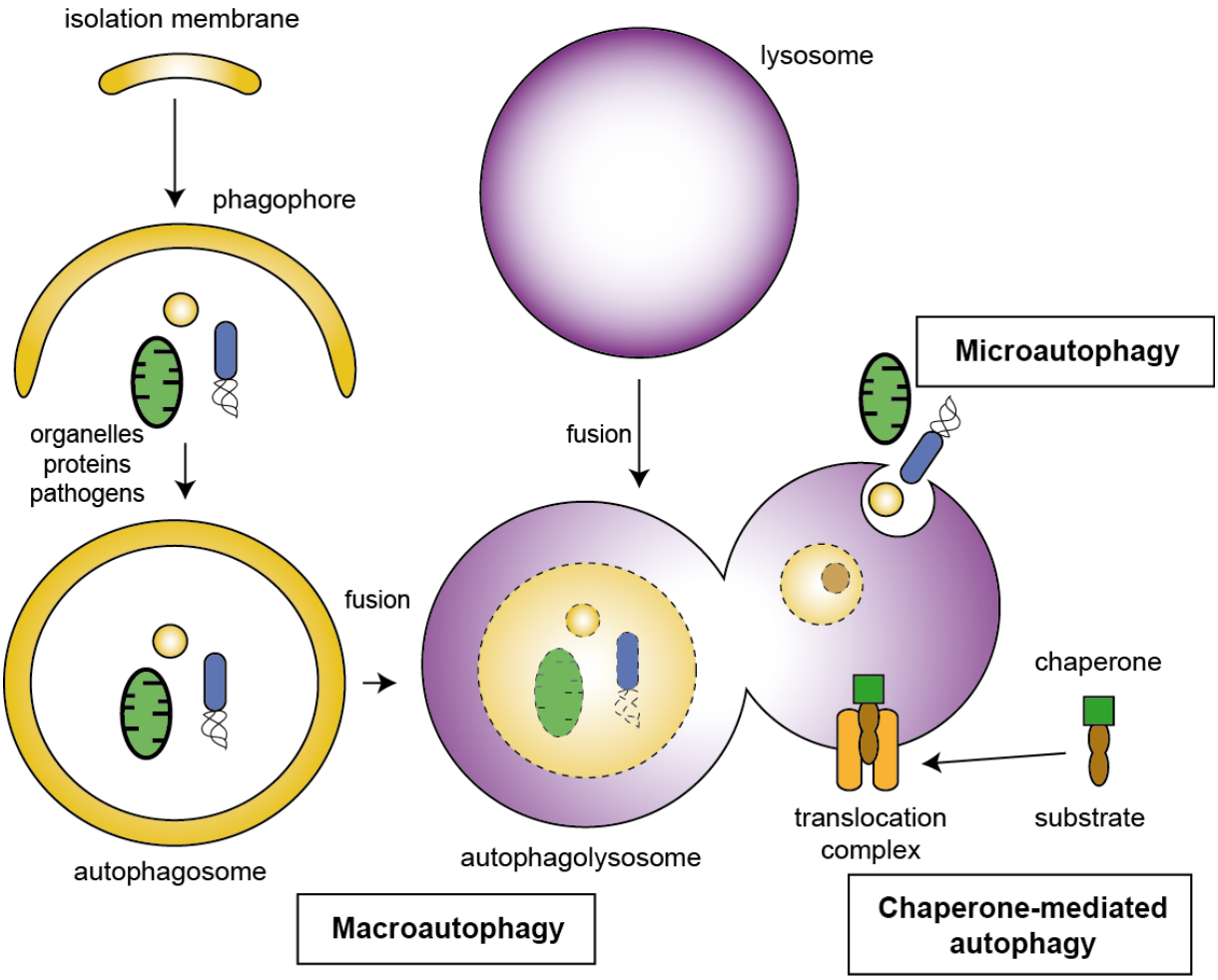


**Figure 1-4: Conception of the main types of autophagy (modified from (143) with permission from Springer Nature)**

Three main subtypes of autophagy are depicted in this graphic: Nascent isolation membranes, consisting of phospholipid bilayer double membranes, engulf dispensable organelles, proteins and pathogens, finally isolating them in autophagosomes. Fusion with lysosomes results in degradation of the isolated structures, a process called macroautophagy. Small amounts of these organelles or proteins can be directly taken up by lysosomes through endocytosis (microautophagy). Certain substrates can be translocated into lysosomes for degradation through specific transporters and chaperones (chaperone-mediated autophagy).

Macroautophagy is targeted towards certain aged organelle structures e.g. mitochondria (then referred to as mitophagy) (144), ER membrane (ER-phagy/reticulophagy) (145) or pathogens (xenophagy) (123). Impaired mitophagy has been associated with degenerative diseases like Parkinson's disease, suggesting a role of dysfunctional removal of cellular compartments in the aetiology of human disease (146). Selective autophagy requires specific adaptor molecules for the

autophagosomes to target specific sites. Optineurin has been linked to ER-phagy (130, 147) and mitophagy (148) in context of both neurodegeneration und inflammatory diseases like IBD. Interestingly, also protein complexes can be targeted, as exemplified by the role of the tripartite motif (TRIM) family in targeting regulatory elements of the innate immunity like NLRP3 (inflammasome formation) or IRF3 (type I interferon response) (149) (150). Autophagy is controlled by different pathways, including Beclin-1 (151) and mTOR (152).

Defective autophagy has been associated with many inflammatory and degenerative conditions like IBD. Autophagy-related 16-like 1 (ATG16L1) is a pivotal autophagy regulator, with the T300A variant conferring risk for the development of CD (24). ATG16L1 is required for the assembly of various autophagy-related gene (ATG) products like ATG5, ATG7, ATG10 and ATG12 to form a complex essential for autophagosome formation. The *ATG16L1*$^{T300A}$ (refseq number: rs2241880) variant can be cleaved by caspase 3, leading to loss of protein function (153). In ER stress conditions, Paneth cells are susceptible to impaired autophagy within epithelial tissue as shown by loss of functional lysozyme$^{+}$ granules in IEC-specific knockout of *Atg16l1* in mice (154). Both loss of *Atg16l1* and knock-in of human *ATG16L1*$^{T300A}$ variants resulted in decreased stemness in the intestine and diminished regenerative capacity (153). Interestingly, a recent study linked *Atg16l1* deficiency with immunogenic necroptotic cell death in the context of viral infections, providing another mechanistic explanation for ATG16L1 genotype-dependent disease susceptibility (94). ATG16L1 has also been implicated as an immune nexus as deficient *Atg16l1* in immune cells like bone marrow derived macrophages or dendritic cells unchained inflammatory processes like inflammasome and NF-κB activation (153). Other confirmed autophagy-related risk genes are for instance immunity-related GTPase family M protein (*IRGM*) (155) and leucine-rich repeat kinase 2 (*LRRK2*) (156) which, however, are less intense investigated.

### 1.5.3 The interplay of autophagy and ER stress in intestinal inflammation

Autophagy and UPR are not isolated processes, but indeed have molecular interdependencies on many levels. UPR induces autophagy via the PERK-eIF2α signalling branches (and the downstream factors activating transcription factor 4 (ATF4) and C/EBP homologous protein (CHOP)) (157) and IRE1α activation (158). In addition, UPR pathways can restrain mTOR activity via AMP kinases (AMPK) to induce autophagy (159).

Autophagy induction acts as compensatory machinery in order to repress overt ER stress and subsequent UPR activation. In the scenario of intestinal inflammation, epithelial ER stress as in *Xbp1*$^{\Delta IEC}$ mice induces autophagy in an eIF2α-dependent fashion which in turn controls IRE1α activity (see figure 1-5). Concomitant knockout of *Atg16l1* or *Atg7* ultimately disinhibits UPR activity, resulting in spontaneous excessive cellular death and severe transmural ileitis in young adult *Atg16l1*$^{\Delta IEC}$*/Xbp1*$^{\Delta IEC}$ mice, reminiscent of the classic CD phenotype (160). The aforementioned Paneth cell disorder might be causative for this phenomenon as mice harbouring a Paneth cell-specific deletion of *Xbp1* have a similar phenotype. Also, aged *Atg16l1*$^{\Delta IEC}$ mice phenocopied *Atg16l1*$^{\Delta IEC}$*/Xbp1*$^{\Delta IEC}$ mice, presumable due to chronic accumulating ER stress associated with age (130). In line with these murine *in vivo* data, Deuring *et al.* demonstrated high expression levels of ER stress markers like GRP78 and p-eIF2α in Paneth cells of CD patients harbouring *ATG16L1*$^{T300A}$ variants correlate with more fistula and need for intestinal surgery (161). However, the detailed mechanism by which autophagy controls ER stress are not fully understood.

Cytokines regulate and modify ER stress. A recent study demonstrated the role of IL-10 in attenuating experimental colitis via suppression of epithelial ER stress (162). The same working group showed that IL-22 ameliorates ER stress in ß cells (163). These findings point towards an ER stress-modulating role of cytokines of the IL-10 family, in particular of the protective cytokine IL-22. IL-22 has also been implicated in autophagy regulation and depending on cellular context, can suppress and promote autophagy (164, 165). In this study, I dissected the role of IL-22 in autophagy and ER stress regulation in a preclinical model of intestinal inflammation.

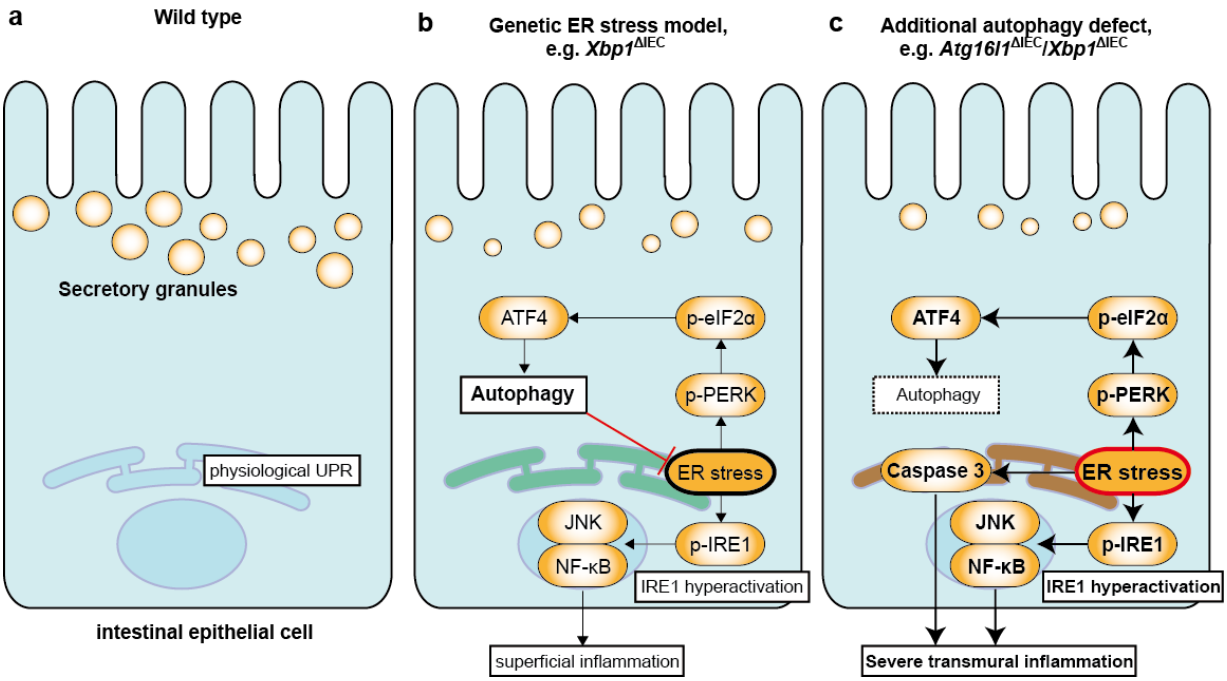


**Figure 1-5: Interplay of autophagy and ER stress in the intestinal epithelium (modified from (125) with permission from Springer Nature)**

(a) Intestinal epithelial cells display physiological UPR in order to maintain ER homeostasis while producing secretory proteins. (b) Genetic distortion of critical nexus of the UPR like deletion of *Xbp1* destabilises the homeostasis towards ER stress, resulting in a NF-κB/JNK-dependent inflammatory phenotype. Autophagy activation downstream of the PERK branch restrains ER stress as a compensatory mechanism. (c) Additional disruption of essential autophagy components like *Atg16l1* disinhibited ER stress, ultimately leading to caspase 3-mediated cell death and severe (transmural) intestinal inflammation.

# 2 Aim of the study

The aim of the following was to study the impact of two fundamental cellular homeostatic principles, namely UPR and autophagy, on the fine tuning of cytokine induced epithelial proliferation. The following preliminary data from other studies gave rise to the design of the hypothesis:

- Epithelial ER stress and defective autophagy are associated with impaired regeneration of the epithelial barrier.
- IL-22 promotes epithelial proliferation via activation of JAK/STAT pathway
- IL-10, a cytokine structurally related to IL-22, has been shown to promote epithelial regeneration via mechanism involving the alleviation of epithelial ER stress.

Based on these findings we postulated that pro-regenerative effects of IL-22 are mediated via alleviation of epithelial ER-Stress in a STAT1/STAT3-dependent manner. In particular, I addressed the following key questions:

- Does experimental ER stress and autophagy inhibition interfere with the regenerative function of IL-22?
- Does IL-22 vice versa modulate epithelial ER stress or autophagy?
- Do IL-22 effects differ *in vitro* and *in vivo* in the context of genetically determined epithelial ER stress or autophagy defects?
- If yes, what are the molecular switches in intestinal epithelial cells proficient vs. deficient for *Atg16l1* and *Xbp1*?

For this purpose, three different experimental models were employed in this study: Human colon carcinoma cell lines for *in vitro* studies, primary intestinal organoids (as a novel *ex vivo* model for intestinal epithelial tissue) and genetically modified mice to study *in vivo* effects of IL-22.

# 3 Materials & Methods

## 3.1 Material

All materials used are listed in the appendix. Antibodies and primers are listed in the appropriate methodological chapters.

## 3.2 Methods

### 3.2.1 Animals

*Il23r*$^{fl/fl}$*;VillinCre* (*Il23r*$^{\Delta IEC}$), *Atg16l1*$^{fl/fl}$*;VillinCre* (*Atg16l1*$^{\Delta IEC}$), *Xbp1*$^{fl/fl}$*;VillinCre* (*Xbp1*$^{\Delta IEC}$) and *Atg16l1*$^{fl/fl}$;*Xbp1*$^{fl/fl}$*;VillinCre* (*Atg16l1*$^{\Delta IEC}$/*Xbp1*$^{\Delta IEC}$) mice have been described previously (75, 93, 160). In brief, *Il23r*$^{fl/fl}$ (*Il23r*$^{fl}$) mice were generated by targeted insertion of *LoxP* sites flanking the exon 4 of the *Il23r* gene (Genoway, Lyon, France). *Atg16l1*$^{fl/fl}$ (*Atg16l1*$^{fl}$) mice were generated by insertion of *LoxP* sites flanking the exon 1 of the *Atg16l1* gene (Genoway, Lyon, France). *Xbp1*$^{fl/fl}$ (*Xbp1*$^{fl}$) mice were generated by targeted insertion of LoxP sites flanking the exon 2 of the *Xbp1* gene. *VillinCre* animals (strain: B6.SJL-Tg(Vil-cre)997Gum/J) were purchased from Jackson Laboratory. Conditional knockout of *Atg16l1* and *Xbp1* in the intestinal epithelium was established by crossing *VillinCre* mice with *Atg16l1*$^{fl}$ or *Xbp1*$^{fl}$ mice, resulting in specific deletion of *Atg16l1* (*Atg16l1*$^{\Delta IEC}$) and *Xbp1* (*Xbp1*$^{\Delta IEC}$) in the intestinal epithelium. *Atg16l1*;*Xbp1*;*VillinCre* double knockout mice were created by crossing *Atg16l1*$^{fl}$ mice with *Xbp1*$^{\Delta IEC}$. Transgenic WD40-truncated *Atg16l1* (*Atg16l1*$^{\Delta WD40}$) mice were generated in collaboration with Genoway (166). In brief, a Stop-polyadenylation signal cassette was inserted into the exon 10 of *Atg16l1*, leading to ubiquitous expression of truncated *Atg16l1* mRNA missing the C-terminal region encoding for the WD40-repeat domain.

Mice harbouring a missense mutation in exon 6 of *Tmem173 (Tmem173*$^{gt}$), resulting in an isoleucine-to-asparagine change in amino acid 199(167), and *Mda5* knockout (*Mda5*$^{-/-}$) mice were raised at the University Hospital Bonn and kindly provided by Gunter Hartmann (Bonn University) for organoid experiments. Intestinal organoids derived from *Ripk3*$^{-/-}$ and *Ripk1*$^{D138N}$ mice were created in Cologne, cryo-preserved and kindly provided by Manolis Pasparakis (University Hospital of Cologne) for further experiments. *Mlkl*$^{-/-}$ mice were raised at Kiel University and kindly provided by

Stefan Krautwald (Department of Nephrology, University Hospital Schleswig-Holstein, Campus Kiel).

Genotyping strategies for each transgenic mice strain have previously been established and were carried out as described before(93, 119, 160, 166-169).

All mice were provided with food and water *ad libitum* and maintained in a 12-h light-dark cycle under standard conditions (21°C ± 2°C with 60 % ± 5 % humidity) at Kiel University (*Il23r*$^{\Delta IEC}$, *Xbp1*$^{\Delta IEC}$, *Atg161*$^{\Delta IEC}$, *Atg16l1*$^{\Delta WD40}$, *Mlkl*$^{-/-}$), the University of Cambridge (*Xbp1*$^{\Delta IEC}$/*Atg16l1*$^{\Delta IEC}$), the University Hospital Bonn (*Tmem173*$^{gt}$, *Mda5*$^{-/-}$) and the University of Cologne (*Ripk3*$^{-/-}$, *Ripk1*$^{D138N}$).

## 3.2.2 Animal experiments

Weight- and gender-matched mice backcrossed for at least 6 generations were used at an age of 8 to 14 weeks for all experiments. For experiments including application of recombinant murine IL-22 and anti-IFNAR antibody or DSS experiments equal numbers (min. n=5 per genotype) of male and female animals were employed. Procedures involving animal care were conducted in conform to national and international laws and policies and appropriate permission. All experiments were carried out in accordance with the guidelines for Animal Care of the Kiel University and the University of Cambridge (for experiments involving *Atg16l1*$^{\Delta IEC}$/*Xbp1*$^{\Delta IEC}$ mice). Mice were sacrificed by cervical dislocation. For mRNA and protein extraction, tissues were snap-frozen in liquid nitrogen and stored at -80°C.

### 3.2.2.1 Systemic administration of IL-22 in *Atg16l1*$^{fl}$ mice

Age- and gender-matched wild type (*Atg16l1*$^{fl}$) mice at the age of 8-14 weeks received intraperitoneal administration of 2 µg of recombinant murine IL-22 (rmIL-22, Peprotech, Rocky Hill, United States) dissolved in 200 µl sterile PBS or equal volumes of sterile PBS without rmIL-22 (with n=3 animals per treatment group) once. Mice were sacrificed after 24 h post-injection. Crypts from small intestines and colons were collected and subsequently snap frozen and stored at -80°C for further analysis.

The described animal experiment was approved by the Animal Investigation Committee of the University Hospital Schleswig-Holstein (Campus Kiel; acceptance no.: V 242-72241.121-33 (125-9/13)).

### 3.2.2.2 Systemic administration of IL-22 and anti-IFNAR antibody and DSS colitis in *Atg16l1*$^{\Delta IEC}$ mice

Age- and gender-matched *Atg16l1*$^{fl}$ and *Atg16l1*$^{\Delta IEC}$ mice at the age of 8-14 weeks received intraperitoneal administration of 2 µg of recombinant murine IL-22 (rmIL-22 Peprotech, Rocky Hill, United States) dissolved in 200 µl sterile PBS or equal volumes of sterile PBS without rmIL-22 (with n=5-8 animals per treatment group) on 6 or 10 consecutive days, respectively. In an additional treatment group, *Atg16l1*$^{\Delta IEC}$ mice received both rmIL-22 and a neutralising anti-IFNAR antibody (MAR1-5A3, BioXcell, West Lebanon, United States) (170) intraperitoneally, while anti-IFNAR was administered on the indicated experimental day after the dextran sodium sulphate (DSS) treatment. Body weight was assessed on a daily base. For induction of experimental acute colitis, a myriad of well-established protocols exists (171). In this study, mice were supplied with 2 % DSS dissolved in autoclaved tap water in place of regular drinking water (n=5-8 animals per treatment group). Dependent on the experimental scheme, 2 % DSS were supplied either for 4 days before sacrifice or for 5 days followed by 5 days of regular drinking water before sacrifice. Organs and isolated intestinal crypts were collected and subsequently snap frozen and stored at -80°C for further analysis. For histological analysis, intestinal tissues were fixed in 10% formalin at 4°C overnight for further processing as described below.

The described animal experiments were approved by the Animal Investigation Committee of the University Hospital Schleswig-Holstein (Campus Kiel; acceptance no.: V 242-72241.121-33 (125-9/13) including a notification of amendment).

### 3.2.2.3 Systemic administration of IL-22 in *Atg16l1*$^{\Delta IEC}$/*Xbp1*$^{\Delta IEC}$ mice

Age- and gender-matched *Atg16l1*$^{fl}$/*Xbp1*$^{fl}$ or *Atg16l1*$^{\Delta IEC}$/*Xbp1*$^{\Delta IEC}$ mice at the age of 8 to 12 weeks were treated with either 2 µg rmIL-22 or PBS via intraperitoneal injection (n=5-8 animals per treatment group) every other day for 13 days (7 injections in total) before being sacrificed for histological assessment and intestinal epithelial cell isolation as described below. The described animal experiments were approved by the School of Clinical Medicine, Central Biomedical Resources (University of Cambridge) after provision of a regulated procedures study plan and a hazardous substance risk assessment according to UK standards. The internal study number allocated was 2560-54 (MT).

### 3.2.3 Isolation of primary intestinal epithelial tissue and organoid cultures

Isolation of primary epithelial cells, especially for long-term culture purpose and irrespective of genetic background was approved by the Animal Investigation Committee of the University Hospital Schleswig-Holstein (Campus Kiel; acceptance no.: V 312-72241.121-33 (Internal no: 716)) if not included within other approved animal investigation proposals.

#### 3.2.3.1 Isolation of primary intestinal epithelial cells and crypts

To obtain epithelial tissue from murine intestine, different isolation methods were applied. In general, mice were euthanised and the intestine was isolated. After removal of Peyer's patches and mesenteric fat the intestines were longitudinally opened and flushed with ice-cold PBS.

For intestinal epithelial scrapings, the intestinal epithelium was collected by scraping off the superficial mucosa using a glass slides and then snap frozen in liquid nitrogen for further analysis.

For isolation of intestinal epithelial cells, intestines were cut into small pieces, transferred into 50 ml falcons and incubated in HBSS containing 1mM DTT for 10 min at room temperature with intermittent shaking to gently remove luminal mucus. Supernatant was removed and tissue was washed with PBS once and then digested with dispase (1 U/ml in RPMI with 2% FBS) for 30 minutes at 37°C whilst shaking (250 rpm). Debris was removed with a 100µm cell strainer, and cells were collected by centrifugation for 5 min at 1500rpm.

The isolation of small intestinal crypts was established by Sato *et al.* (172) in order to establish long-term cultures of intestinal organoids. Based on the protocol used by Yilmaz *et al.* (96), intestines were flushed, cut open longitudinally, dissected into pieces of less than 0.5 cm of length and incubated on ice for 10 minutes in 10 mM EDTA dissolved in PBS whilst intermitting shaking. After sedimentation, the supernatant containing detritus, mucus and villi was discarded and 10 mM EDTA was substituted again. After three repeats, 4°C cold PBS was substituted to the small intestine pieces. The suspension was shaken vigorously for 30 seconds, incubated on ice for 5 minutes. This procedure was repeated to detach intestinal crypts from the

lamina propria. The suspensions were filtered through a cell strainer with 100 µm pores twice to separate intestinal crypts from the villi fraction. Crude preparation, including five repetition steps of shaking and only one step of straining, increased the amount of villi and lamina propria cells. This was used to investigate overall mucosa cells.

Calculation of crypt numbers in the suspension was performed by microscopic assessment of crypt counts in a 5 µl-droplet of suspension. After centrifugation with 300 x g at 4°C, the pellet contains intestinal crypts which were snap frozen for further analysis or used for organoid cultures.

### 3.2.3.2 Establishment of intestinal organoid cultures

For the establishment of intestinal organoids, the pelleted crypt fraction after the isolation described above was suspended in a mixture of Matrigel® (BD Bioscience/Heidelberg, Germany) and ice-cold PBS (2:1) to a concentration of 5-10 crypts/1 µl gel mix. 100 µl of the suspension were plated out onto pre-cooled 24-well plates and incubated at 37°C for 15 minutes to let the gel polymerise. Afterwards, 1000 µl of intestinal stem cell medium based on the protocol of Sato *et al.* were added. In essence, the medium based on Advanced DMEM/F12 (ADF) medium contained 10 % FBS, 10 mM HEPES, 1 % penicillin/streptomycin, murine EGF, murine Noggin and human R-Spondin 1 (see figure 1-2) (172). Medium was changed every other day and organoids were passaged every five to eight days. For passaging organoids, medium was removed and the well was flushed with 1 ml of ice-cold PBS. After pipetting up and down for 5 to 10 times the organoid-containing gel dissociated from the well and suspensions were collected in a 15 ml falcon. After centrifugation at 300 x g for 5 minutes the supernatant and excessive Matrigel were removed, leaving a loose pellet of organoids which was then vigorously suspended in 100 µl of cold PBS to break down organoids to single crypt structures. Afterwards, crypts were again seeded out in 2:1 Matrigel/PBS mix. Organoids were subjected to stimulation experiments after a minimum of two passages. Cryopreservation and thawing of organoids was performed according to manufacturer's protocol of StemCell Technologies using CryoStor™ CS10 (catalogue number #07930).

### 3.2.4 Quantification of cell death in intestinal organoids

Organoids derived from mice of indicated genotypes were seeded out into 24-well plates. After approximately three to five days, organoids reached a size with multiple crypt-like buds and were treated with indicated stimulants for indicated time.

To evaluate epithelial cell death, medium was changed and the gel was washed once with PBS. The gel was collected in 1.5 ml tubes, suspended in 1 ml of ice-cold PBS and the pelleted after centrifugation at 4°C for 5 minutes at 400 x g. Supernatants as well as the upper layers of the gel remnants were removed. Lower layers of the gel pellet containing organoids were incubated in TrypLE Express (ThermoFischer Scientific, Steineich, Germany) for 5 min at 37°C to dissociate cells, followed by washing steps using ice-cold PBS. 250,000 cells were incubated in staining solution containing 2 µl PI in 100 µl PBS each and then subjected to flow cytometry analysis using BD FACSCalibur™ (San Jose, United States) and BD CellQuest™ Pro Software. The gating strategy involved plotting FL-2H for PI fluorescence intensity against forward scatter (FSC) to distinguish $PI^{high}$ vs $PI^{low}$ populations which are assumed to be dead vs living cells. These gates excluded cellular clumps with did not dissociate well after TrypLE Express treatment. Dead cells were then first quantified as fraction of dead cells (= dead cells/total single cells). Cell death induction by stimulants were then determined as *% change dead cells*, while the fraction of dead cells in the treatment control wild type organoids served as the baseline cell death rate (% change dead cells = fraction of dead cells after treatment – fraction of wild type dead cells at baseline).

To visualise dead cells in organoids, 1 µl of PI was added to 500 µl medium for 4 hours. Medium was then removed and replaced by PBS. Merged images with a bright-field image overlaid by a RFP-filtered fluorescence channel capture (red fluorescent cells indicate $PI^{+}$ dead cells) were generated using Zeiss Axio Vert.A1 observer (Jena, Germany) and Zeiss AxioVision LE software. Images are shown at indicated magnification.

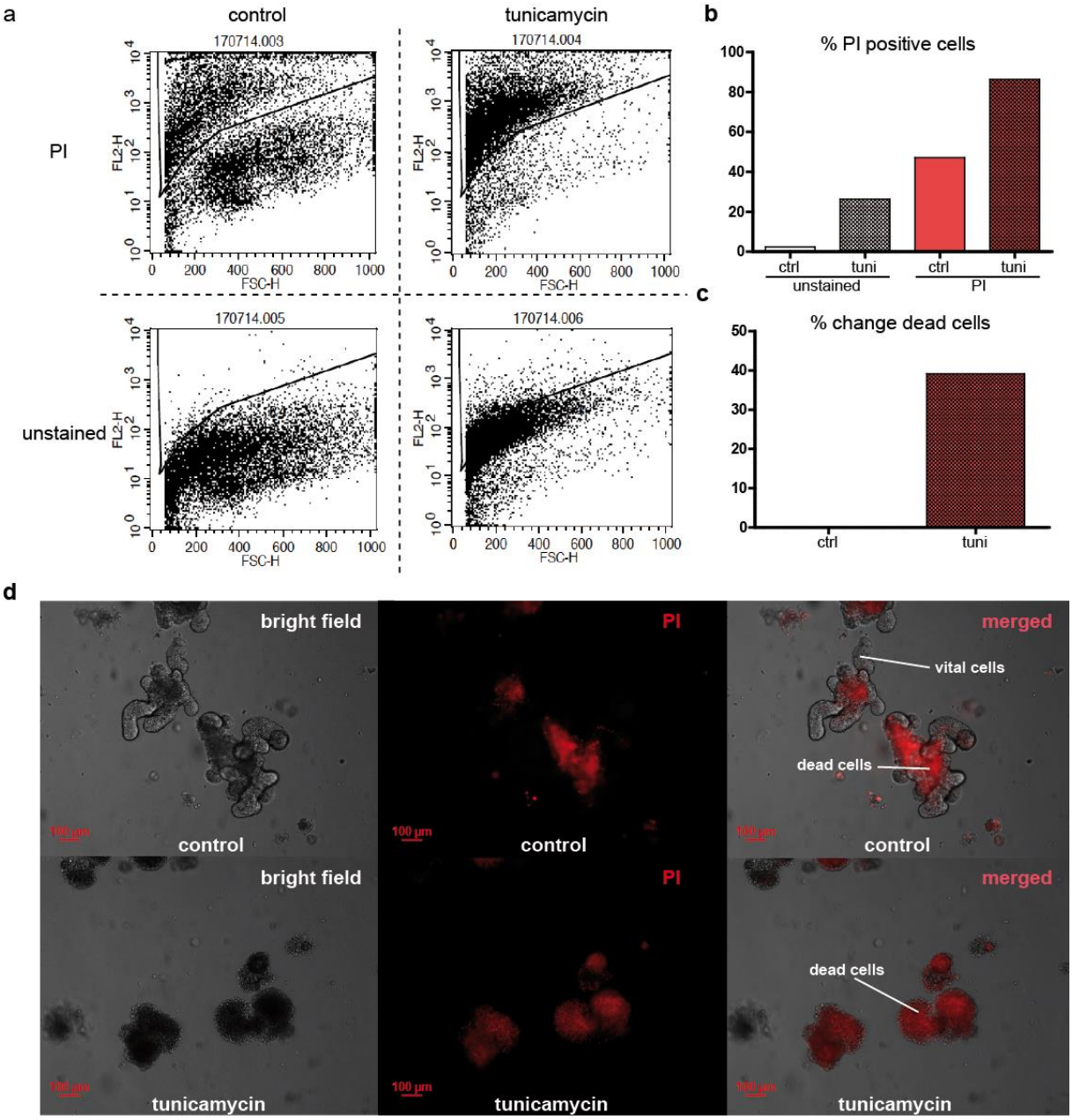


**Figure 3-1: Quantification and visualisation of cell death in intestinal organoids**

(a) FACS plot of wild type organoids treated with tunicamycin (1 µg/ml) for 24h or DMSO control, with or without prior incubation with PI (2 µl/100 µl PBS) for 10 minutes. FL-2H was plotted against FSC-H. Gate includes $PI^{high}$ cells, which are considered as dead. (b) Corresponding analysis of gated $PI^{high}$ cells, each group n=1. (c) Calculated % change dead cells compared to DMSO controls. (d) Visualisation of cell death in organoids from the same experiment as in (a). Bright field images, RFP-filtered fluorescence detection captions (for PI) and merged images are shown. Bars indicate 100 µm.

### 3.2.5 Cell culture

HT-29 and Caco-2 human colorectal adenocarcinoma cells were seeded in 6-well, 12-well and 24-well plates. Using CRISPR/Cas9 technology (173), an *ATG16L1* deficient Caco-2 cell line was established by Dr. Johannes Kuiper and kindly provided for this work. Cells were cultured in DMEM + 10 % FCS or MEM + 20 % FCS, respectively, until a fully confluent cellular monolayer established. Prior to stimulation, cells were serum-starved by incubating DMEM + 1% medium or MEM + 1% FCS for 24 h.

### 3.2.6 Scratch assays

Scratch assays were performed based on the protocol of Liang *et al.* (174) In detail, epithelial cells were seeded out into 6- or 12-well plates and cultured until fully confluent cellular monolayers established. The medium was removed and cells were gently washed with 37°C warm PBS once. Using a scalpel, a line was cut on the bottom of each well to support later re-identification of assessed wound areas. To create an epithelial wound, a P100 pipette tip was used to rapidly scratch the cellular layer (Figure 3-2). The wounds were then washed with warm PBS for three times to remove dissociated cells before incubation in proper medium and condition. Epithelial wound closure was assessed by imaging using Zeiss Axio Vert.A1 (Jena, Germany) and digital measurement of the cell free area using AxioVision LE (Zeiss) software. The relative wound closure after indicated time interval is calculated as followed: *Relative wound closure* = 1 – (*wound area*/*starting wound area*).

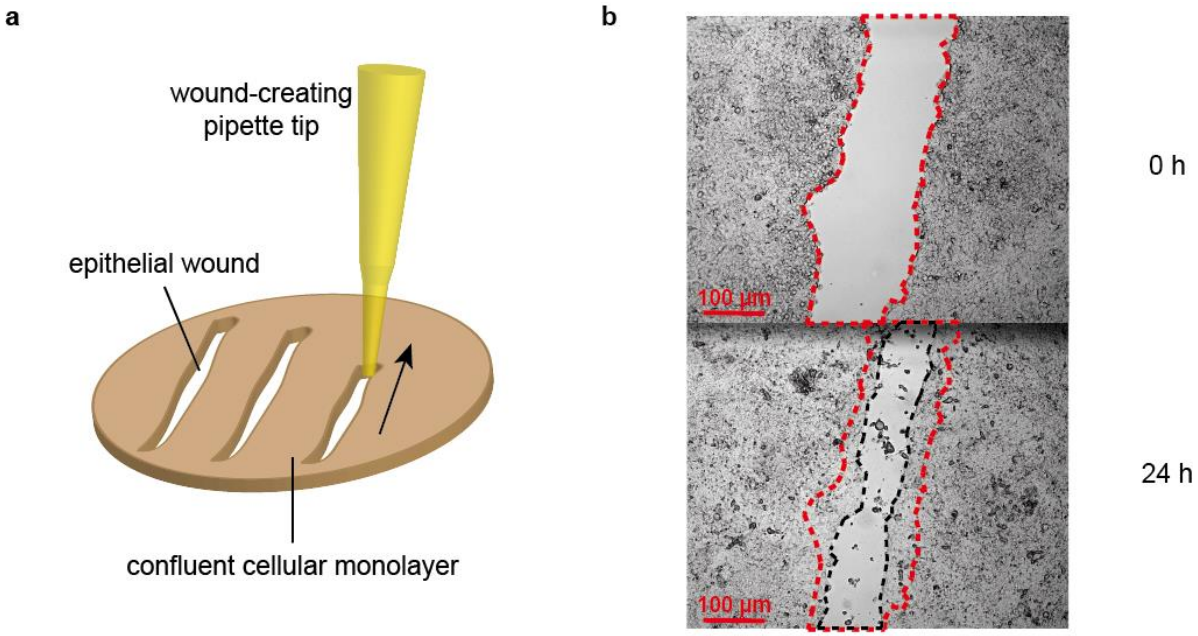


**Figure 3-2: Conception of epithelial scratch assays**

(a) Scheme of epithelial scratch assays using a P100 pipette tip. Cell lines were cultured until confluence before wounding. (b) Unstimulated HT-29 cell layer directly after wounding and after 24h of regeneration. Red bars indicate 100 µm.

### 3.2.7 Histopathological analyses of murine intestinal tissue

After cervical dislocation, the entire small intestine or colon was excised and separated longitudinally into two equal parts. The longitudinal section was rolled up, starting with the distal part thereby having the distal ileum at the very inner layer and the proximal intestine at the very outer layer. The entire specimen was fixed in 10% formalin. Paraffin sections were cut and stained with hematoxylin/eosin. Histological scoring was performed in a blinded fashion by two independent observers. The histological score displays the combined score of inflammatory cell infiltration and tissue damage as described elsewhere (175). A semi-quantitative scoring system was used for the assessment of spontaneous intestinal inflammation, computed as a sum of five histological subscores. The histological subscores were determined as followed (for each parameter: 0, absent; 1, mild; 2, moderate; 3, severe): mononuclear cell infiltrate, crypt hyperplasia, epithelial injury/erosion, granulocyte infiltrates and transmural inflammation (0, absent; 1, submucosal; 2, one focus extending into muscularis and serosa; 3 up to five foci extending into muscularis and serosa; 4, diffuse).

### 3.2.8 Immunohistochemistry and immunofluorescence

For immunohistochemical (IHC) and immunofluorescence (IF) staining, 5 µm sections of paraffin-embedded colon/ileum swiss rolls were deparaffinised with Xylol substitute (Roth) and incubated in citric buffer for 3 minutes.

For IHC, sections were blocked with blocking serum (Vectastain ABC Kit) for 20 minutes. Primary antibodies (anti-γH2AX, rabbit, Cell Signalling Technologies (Leiden, The Netherlands), #9718, used in 1:1,000 dilution) were incubated overnight. Sections were washed, incubated with biotinylated secondary antibodies and afterwards with DAB substrate (Vectastain ABC Kit).

For IF staining, sections were blocked in PBS containing 5% BSA and 0.2% Triton-X for 30 minutes after removal of citric buffer and before incubation of a primary antibody overnight at 4°C (see table 1). Secondary antibodies conjugated with fluorophores were added after washing steps with PBS for 45 minutes. Then, tissue was then counterstained with DAPI and DRAQ5 and then mounted with fluorescence mounting medium (DAKO). For IF staining of Caco-2 cells, cells were fixed on cover slides using 4 % paraformaldehyde for 30 minutes at room temperature. After washing steps, cells were permeabilised for 3 minutes at room temperature using PBS containing 1 % Triton X-100 and 5 % BSA. Cells were blocked using 5 % goat serum for at least 60 minutes at room temperature. The further staining procedure was identical to the IF protocol for tissues.

**Table 1: Antibodies used for immunofluorescence staining**

| Primary antibody | Host specificity | Working dilution | Company | Article number |
|---|---|---|---|---|
| dsDNA | mouse | 1:1,000 | Santa Cruz Biotechnology (Heidelberg, Germany) | sc-58749 |
| phospho-TBK1 | rabbit | 1:1,000 | Cell Signalling Technologies (Leiden, The Netherlands) | #13647 |
| E-cadherin (clone 36) | mouse | 1:200 | BD Biosciences (Heidelberg, Germany) | #610182 |
| | | | | |
| **Secondary antibody** | **Host specificity** | **Working dilution** | **Company** | **Article number** |
| anti-mouse Alexa Fluor 488 | goat | 1:10,000 | Invitrogen (Darmstadt, Germany) | A11029 |
| anti-rabbit Alexa Fluor 555 | goat | 1:10,000 | Invitrogen (Darmstadt, Germany) | A21430 |

For TUNEL assay, slides were subjected to ApopTag® Plus Peroxidase In Situ Apoptosis Detection Kit (Merck Millipore) according to manufacturer's protocol. 50 randomly distributed intestinal crypts were analysed for $TUNEL^+$ cells and numbers were normalised to the number of crypts. Slides were visualised by an AxioImager Z1 microscope (Zeiss, Jena, Germany). Pictures were captured by a digital camera system (AxioCam HrC/HrM, Zeiss). Measurements were made using a semi-automated image analysis software (AxioVision version 08/2013).

## 3.2.9 Protein detection and analysis

### 3.2.9.1 Protein extraction and quantification

Cells and tissues were lysed using 40-100 µl SDS-based DLB buffer + 1 % Halt™ Protease inhibitor cocktail (ThermoFischer Scientific, Steineich, Germany) before 5 minutes incubation at 95°C and followed by sonification for 5 seconds. To remove cell remnants, lysates were centrifuged at 16.000 x *g* for 15 minutes at 4°C and supernatants were transferred into a new tube. For protein extraction of organoids, Matrigel was removed by several centrifugation steps at 4°C followed by lysis as described above. If not in use, lysates were stored at -80°C.

For quantification of protein concentrations, the colorimetric DC™ Protein Assay (Bio-Rad, Munich, Germany) based on the Lowry method (176) was used according to the manufacturer's protocol. The absorbance at 750 nm was measured using the microplate reader Infinite M200 Pro (Tecan, Männedorf, Switzerland) and the appropriate software i-control™ 1.9 (Tecan, Männedorf, Switzerland).

### 3.2.9.2 Sodium dodecyl sulphate polyacrylamide gel electrophoresis (SDS-PAGE)

Before immunoblot analysis, equal amounts of lysates (15-20 µg of total protein) were supplemented with 5x SDS loading dye and heated at 95°C for 5 minutes. Lysates were then transferred on self-prepared polyacrylamide gels before electrophoresis. The used gel consists of a 12 or 15 % separation gel, which is overlaid by a 3 % stacking gel (Table 2).

**Table 2: Formulation of used stacking and separation gel for SDS-PAGE**

| components | 12 % separation gel | 15 % separation gel | 3 % stacking gel |
|---|---|---|---|
| distilled water | 3.5 ml | 2.5 ml | 1.95 ml |
| buffer | 2.5 ml (**separation**) | 2.5 ml (**separation**) | 0.75 ml (**stacking**) |
| 30% bisacrylamide (35.7:1) | 4 ml | 5 ml | 0.3 ml |
| TEMED | 10 µl | 10 µl | 3 µl |
| 10 % APS | 100 µl | 100 µl | 30 µl |

Electrophoresis was performed in 1x Tris/Glycine/SDS (TGS) buffer at 15 mA for 30 minutes followed by 60 minutes at 30 mA.

### 3.2.9.3 Immunoblot analysis

After electrophoretic separation, proteins were transferred onto polyvinylidene fluoride (PVDF) membranes (GE Healthcare, Munich, Germany) using a semi-dry immunoblotting technique at 0.1 A for 45 minutes. Protein loaded membranes were blocked with 5 % blotting grade blocker (non-fat dry milk, Bio-Rad, Munich, Germany) or bovine serum albumin (BSA) in 1x Tris-buffered saline (TBS) supplemented with 0.1 % Tween 20 (T/TBS) for 1 hour at room temperature. Membranes were then incubated with specific primary antibodies over night at 4°C (Table 3).

**Table 3: Primary antibodies used for immunoblot analysis**

| Primary antibody | Host specificity | Working dilution | Company | Article number |
|---|---|---|---|---|
| ATG16L1 | mouse | 1:500 | MBL International (Woburn, United States) | M150-3 |
| STING | rabbit | 1:1,000 | Cell Signaling Technologies (Leiden, The Netherlands) | #13647 |
| phospho-TBK1 | rabbit | 1:1,000 | Cell Signaling Technologies (Leiden, The Netherlands) | #5483 |
| TBK1 | rabbit | 1:1,000 | Cell Signaling Technologies (Leiden, The Netherlands) | #3504 |
| LC3BI/II | rabbit | 1:1,000 | Novus Biologicals (Cambridge, United Kingdom) | NB100-2331 |
| β-Actin | mouse | 1:10,000 | Sigma (Munich, Germany) | A-5441 |
| GAPDH | mouse | 1:10,000 | Santa Cruz Biotechnology (Heidelberg, Germany) | sc-59541 |

Afterwards, membranes were washed with T/TBS three times and incubated to an appropriate horseradish peroxidase (HRP)-conjugated secondary antibody for 1 hour at room temperature (Table 4).

**Table 4: Secondary antibodies used for immunoblot analysis**

| Secondary antibody | Host specificity | Working dilution | Company | Article number |
|---|---|---|---|---|
| rabbit-HRP | sheep | 1:3,000 | GE Healthcare (Hamburg, Germany) | NA931V |
| mouse-HRP | sheep | 1:3,000 | GE Healthcare (Hamburg, Germany) | NA934V |

Membranes were washed with T/TBS three times, again and protein was detected by chemiluminescence using Amersham ECL™ Prime Western Blot Detection Reagents (GE Healthcare, Hamburg, Germany) or Pierce ECL™ Plus Western Blotting Substrate (ThermoFischer Scientific, Darmstadt, Germany). Chemiluminescence of the protein bands were captured on Amersham Hyperfilm ECL (GE Healthcare, Hamburg, Germany) which were developed using Curix 60 (AGFA, Mortsel, Belgium). If necessary, membrane stripping was performed in 50 ml stripping buffer containing 0.6 % β-mercaptoethanol for 20-40 minutes at 55°C.

### 3.2.10 Enzyme-linked immunosorbent assay (ELISA)

To determine human IL-8 concentrations secreted from stimulated cell cultures, supernatants were subjected to the human IL-8 ELISA Kit according to manufacturer's protocol from ThermoFischer Scientific (Darmstadt, Germany).

### 3.2.11 mRNA extraction, cDNA synthesis and gene expression analysis

mRNA isolation of PBS washed cells, snap frozen tissue and PBS washed Matrigel containing organoids was performed using commercial RNA isolation kit (RNEasy Kit Mini, Qiagen, Hilden, Germany). RNA concentration was measured using the NanoDrop spectrometer ND1000 (PeqLab, Erlangen, Germany). cDNA synthesis was performed using RevertAid Premium cDNA Synthesis Kit (ThermoFischer Scientific, Darmstadt, Germany) according to manufacturer's protocol. Gene expression analysis was subjected to the cDNA samples using SYBR Green qRT-PCR or TaqMan assays (Table 5) which were purchased from Applied Biosystems

(Darmstadt, Germany). Primer sequences were retrieved using Primer3 software version 0.4.0(177, 178), except for those individually referenced (Table 6). The design criteria involved exon-exon span, a length of 20-25 bases, an optimal annealing temperature of 60°C and an amplicon size of 200-400 basepairs (bp). Synthesis of primers was carried out by Microsynth (Lindau, Germany).

**Table 5: List of TaqMan Assays used for quantitative real-time PCR**

| Gene Name | Species | TaqMan Probe ID |
|---|---|---|
| *Reg3g* | Mus musculus | 01181783 |
| *Reg3b* | Mus musculus | 00440616 |
| *Atg16l1* | Mus musculus | 00513085 |
| *Lgr5* | Mus musculus | 00438905 |
| *Actb* | Mus musculus | 00607939 |

**Table 6: List of primers used for quantitative real-time PCR**

| Primer | Sequence | Reference |
|---|---|---|
| mu_*Actb* for | 5'- GATCGGTGGCTCCATCCTGGC | |
| mu_*Actb* rev | 5'- CGCAGCTCAGTAACAGTCCGCC | |
| mu_*Gapdh* for | 5'- CCGGGGCTGGCATTGCTCTCA | |
| mu_*Gapdh* rev | 5'- CTTGCTCAGTGTCCTTGCTGGGG | |
| mu_*Xbp1* for | 5'- AGCAGCAAGTGGTGGATTTG | Kaser *et al.* (93) |
| mu_*Xbp1* rev | 5'- GAGTTTTCTCCCGTAAAAGCTGA | Kaser *et al.* (93) |
| mu_*splicedXbp1* for | 5'- ACACGCTTGGGAATGGACAC | Iwakoshi *et al*. (179) |
| mu_*splicedXbp1* rev | 5'- CCATGGGAAGATGTTCTGGG | Iwakoshi *et al*. (179) |
| mu_*Atf4* for | 5'- ATGGCCGGCTATGGATGAT | Fribley *et al.* (180) |
| mu_*Atf4* rev | 5'- CGAAGTCAAACTCTTTCAGATCCATT | Fribley *et al.* (180) |
| mu_*Grp94* for | 5'- TGGGTCAAGCAGAAAGGAGG | |
| mu_*Grp94* rev | 5'- TCTCTGTTGCTTCCCGACTTT | |
| mu_*Cxcl1* for | 5'- GCTGGGATTCACCTCAAGAA | Ather *et al.* (181) |
| mu_*Cxcl1* rev | 5'- TGGGGACACCTTTTAGCATC | Ather *et al.* (181) |
| mu_*Cxcl10* for | 5'- GCCGTCATTTTCTGCCTCA | Luo *et al.* (182) |
| mu_*Cxcl10* rev | 5'- CGTCCTTGCGAGAGGGATC | Luo *et al.* (182) |
| mu_*Tmem173* for | 5'- AGTAGAGAGCTTTGGGGCCT | |
| mu_*Tmem173* rev | 5'- TTCTGAATGGGGAGACAGCAG | |
| mu_*Ifit1* for | 5'- GAACCCATTGGGGATGCACAACCT | Hasan *et al.* (183) |

| | | |
|---|---|---|
| mu_*Ifit1* rev | 5'- CTTGTCCAGGTAGATCTGGGCTTCT | Hasan *et al.* (183) |
| mu_*Ifit3* for | 5'- TGGCCTACATAAAGCACCTAGATGG | Pokatayev *et al.* (184) |
| mu_*Ifit3* rev | 5'- CGCAAACTTTTGGCAAACTTGTCT | Pokatayev *et al.* (184) |
| mu_*Tnf* for | 5'- TCACACTCAGATCATCTTCTC | Lian *et al.* (185) |
| mu_*Tnf* rev | 5'- AGACTCCTCCCAGGTATATG | Lian *et al.* (185) |
| mu_*Olfm4* for | 5'- CATCAGCGCTCCTTCTGTGA | |
| mu_*Olfm4* rev | 5'- TCCTTGGCCATAGCGAATCC | |
| hu_*ACTB* for | 5'- AGCCTCGCCTTTGCCGATCC | Fan *et al.* (186) |
| hu_*ACTB* rev | 5'- ACATGCCGGAGCCGTTGTCG | Fan *et al.* (186) |
| hu_*GAPDH* for | 5'- GGCATGGCCTTCCGTGTCCC | Niedwziecka *et al.* (187) |
| hu_*GAPDH* rev | 5'- TGCCAGCCCCAGCGTCAAAG | Niedwziecka *et al.* (187) |
| hu_*XBP1* for | 5'- CCTGGTTGCTGAAGAGGAGG | Chen *et al.* (188) |
| hu_*XBP1* rev | 5'- CCATGGGGAGATGTTCTGGAG | Chen *et al.* (188) |
| hu_*splicedXBP1* for | 5'- GCTGAGTCCGCAGCAGGTG | Ma *et al.* (189) |
| hu_*splicedXBP1* rev | 5'- GCTGGCAGGCTCTGGGGAAG | Dery *et al.* (190) |
| hu_*ATF4* for | 5' - AGATGACCTGGAAACCATGC | Wang *et al.* (191) |
| hu_*ATF4* rev | 5'- AGGGATCATGGCAACGTAAG | Wang *et al.* (191) |
| hu_*GRP94* for | 5'- TGCCAAGGAAGGAGTGAAGT | Wang *et al.* (191) |
| hu_*GRP94* rev | 5'- GTTGCCAGACCATCCGTACT | Slepak *et al.* (192) |

Reactions were carried out on the Applied Biosystems 7900HT Fast Real-Time PCR System (Applied Biosystems, Foster City, USA), and relative transcript levels were determined using *ACTB*/*Actb* (TaqMan and SYBR Green) and *GAPDH*/*Gapdh* (SYBR Green) as a housekeeper.

### 3.2.12 Transcriptomics analysis

RNA sequencing (RNAseq) was conducted on small intestinal organoids derived from *Atg16l1*$^{\Delta IEC}$ and *Atg16l1*$^{fl}$ mice (n=4) treated with recombinant murine IL-22 (1 ng/ml) or controls. Samples were sequenced on HiSeq3000 (Illumina, San Diego, United States) using Illumina total RNA stranded TruSeq protocol. An average of ~28 million 150-nt paired-end reads was sequenced for each sample. Raw reads were

pre-processed using cutadapt (193) to remove adapter and low quality sequences. RNAseq reads were aligned to the mm10/Ensemble (GrCm38) reference genome with TopHat2 (194). Gene expression values of the transcripts were computed by HTSeq (195). Differential gene expression levels were analysed and visualised by the Bioconductor package DESeq2(196). The overall effect of IL-22 treatment on organoid cells of *Atg16l1*$^{\Delta IEC}$ and *Atg16l1*$^{fl}$ mice was obtained by multifactorial experimental design of DESeq2. Likelihood ratio test was used to assess the significant differentially expressed genes (DEG) of IL-22 treatment interaction of *Atg16l1*$^{\Delta IEC}$ and *Atg16l1*$^{fl}$ mice ($p < 0.01$). Venn diagrams were drawn using VennDiagram package in R (197). To gain insight into the nature of DEGs uniquely expressed in *Atg16l1*$^{\Delta IEC}$ and *Atg16l1*$^{fl}$ mice upon IL-22 treatment (up- and down-regulated), Gene Ontology (GO) terms obtained within the category of biological processes using the InnateDB database (www.innatedb.com) were identified (198).

### 3.2.13 Transcription factor binding site analysis

Over-represented transcription factor binding sites (TFBS) in the promoter region of DEGs uniquely expressed (up- and down-regulated) in *Atg16l1*$^{\Delta IEC}$ and *Atg16l1*$^{fl/fl}$ mice upon IL-22 treatment were identified by InnateDB (198), integrating predicted TFBS data from the CisRED database (www.cisred.org) (199).

### 3.2.14 Search Tool for the Retrieval of Interacting Genes/Proteins (STRING)

To identify functional clusters and signalling branches within the DEG found in the transcriptomic analyses, results were subjected to gene-gene interaction analysis using web applications of *Search Tool for the Retrieval of Interacting Genes/Proteins* (STRING) (200).

### 3.2.15 Statistical analysis

Statistical analysis was performed using GraphPad Prism (version 5.03) for Windows software (GraphPad Software, San Diego, CA). Statistical significance was evaluated by the Mann–Whitney *U* test for nonparametric data or the Student *t*-test for parametric data unless indicated otherwise. *P* values less than 0.05 were considered statistically significant.

# 4 Results

## 4.1 IL-22 induces ER stress in intestinal epithelial cells

IL-10, a cytokine similar to IL-22 in structure, can potentially suppress epithelial ER stress (162). Therefore, I investigated the role of IL-22 in epithelial ER stress responses. ER stress levels were assessed via gene expression analysis of commonly used ER stress markers encompassing each branch of the UPR using quantitative real-time PCR. 24 h of IL-22 treatment (100 ng/ml) increased expression of *sXBP1*, *ATF4* and *GRP94*, indicating global UPR activation including the IRE1/XBP1 branch, the PERK/ATF4 branch and the ATF6 (GRP94) (figure 4-1).

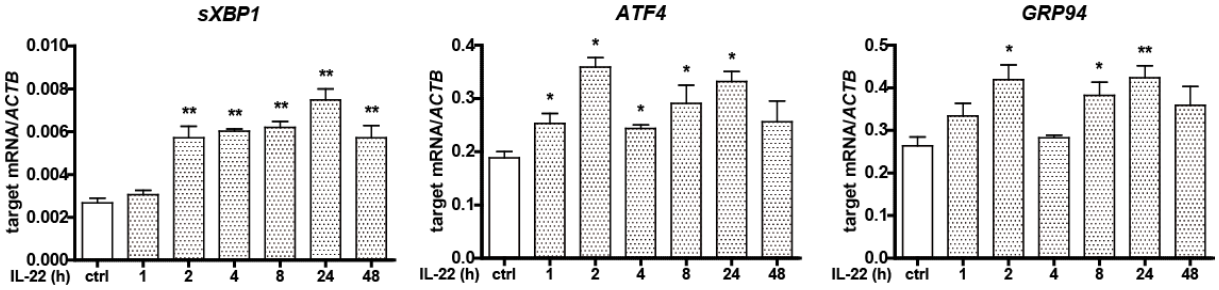


**Figure 4-1: IL-22 induces ER stress in HT-29 cells**

HT-29 cells were treated with either PBS as a control or 100 ng/ml IL-22 for the indicated time in hours (n=3 each). Splicing ratio of *XBP1* and mRNA expression *ATF4* and *GRP94* were analysed by SYBR green qPCR and normalised to *ACTB* expression. Data are shown as mean ± s.e.m. and were tested for statistical significance using unpaired Student's t-test. * $p<0.05$, ** $p<0.01$ vs. ctrl.

To elucidate whether IL-22 augmented chemically induced ER stress in epithelial cells, HT-29 cells were treated with IL-22 (100 ng/ml) 24 or 6 h before or simultaneously with either ER stressing agent tunicamycin (1 µg/ml) or equal volumes of DMSO. Tunicamycin strongly induced all investigated ER stress marker on transcriptional level (figure 4-2a). Pre-treatment of HT-29 cells with IL-22 induced a substantial exacerbation of tunicamycin-induced ER stress, indicating that chemically induced ER stress coincided with physiological ER stress upon cytokine signalling. We validated these findings for murine cells using *Xbp1*$^{fl}$ mice-derived stable long-term organoid cultures. After two passages and a total of 12 days of culture, organoids were treated with IL-22 (100 ng/ml) for 24 h and tunicamycin (0.5

µg/ml) for 6 h (figure 4-2b). Analysis of ER stress markers confirmed IL-22 aggravated tunicamycin-induced ER stress.

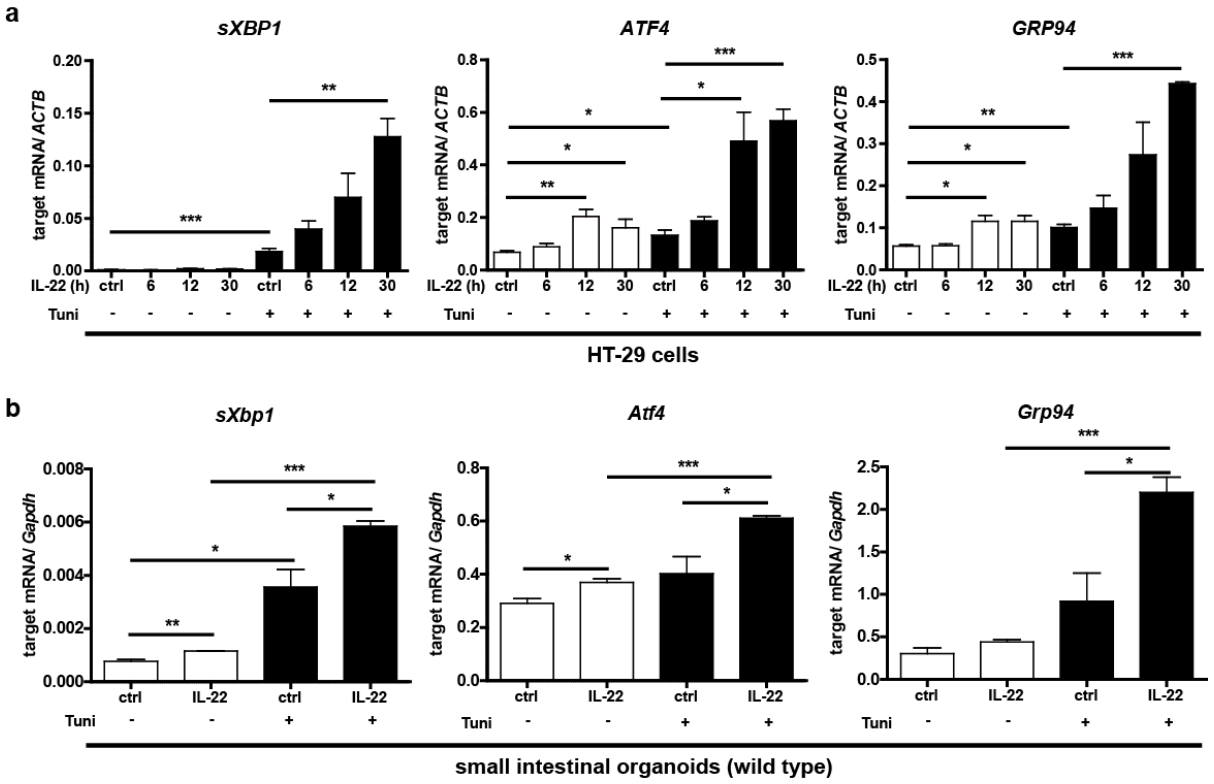


**Figure 4-2: IL-22 augments tunicamycin-induced ER stress in intestinal epithelial cells**
(**a**) HT-29 cells received IL-22 (100 ng/ml) or PBS for the indicated time and tunicamycin (1 µg/ml) or both for 6 h (n=3 each). PBS or DMSO, respectively, served as stimulation controls. Expression levels of *sXBP1*, *ATF4* and *GRP94* were analysed by SYBR green qPCR and normalised to *ACTB* expression. (**b**) Small intestinal organoids were derived from wild type (*Xbp1*$^{fl}$) mice and cultured for 12 days received rmIL-22 (100 ng/ml) for the indicated time and tunicamycin (0.5 µg/ml) or both for 6 h (n=3 each). PBS or DMSO, respectively, served as stimulation controls. Expression levels of *sXbp1*, *Atf4* and *Grp94* were analysed by SYBR green qPCR and normalised to *Gapdh* expression. Data are shown as mean ± s.e.m. and were tested for statistical significance using unpaired Student's t-test. * $p<0.05$, ** $p<0.01$, *** $p<0.001$.

To test whether IL-22 induced epithelial ER stress *in vivo* we stimulated wild type (*Atg16l1*$^{fl}$) mice with IL-22 (2 µg) for 24 h and analysed small intestinal crypt ER stress marker expression. IL-22 upregulated ER stress markers *sXbp1*, *Atf4* and *Grp94* (figure 4-3). However, *Atf4* and *Grp94* mRNA transcript levels were not significantly upregulated by IL-22 treatment.

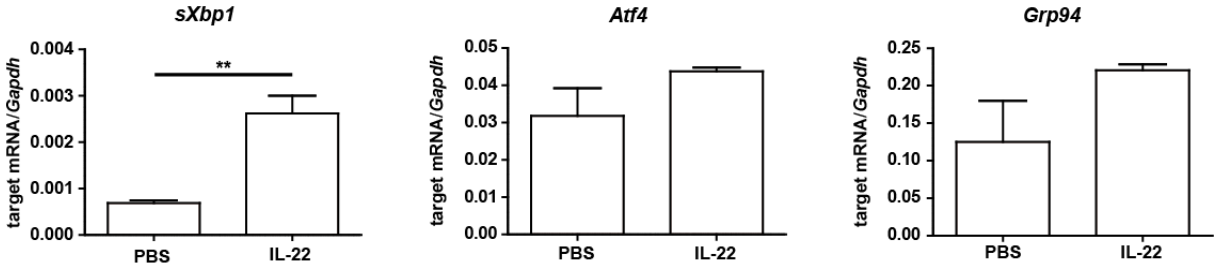


**Figure 4-3: IL-22 induces ER stress in intestinal crypts**

Small intestinal crypts from *Atg16l1*$^{fl}$ mice were collected after treatment with recombinant murine IL-22 (2 µg) 24 hours before sacrifice (n=3 each). Afterwards, mRNA was extracted and transcribed to cDNA before being analysed for gene expression of *sXbp1*, *Atf4* and *Grp94* by SYBR green qPCR and normalised to *Gapdh* expression. Data are shown as mean ± s.e.m. and were tested for statistical significance using unpaired Student's t-test. ** $p<0.01$.

IL-23 is a critical upstream regulator of IL-22 production (75). To test, whether epithelial loss of *Il23r* affects mucosal IL-22 production, crypts from colon and small intestine were crudely isolated (isolates contained lamina propria cells) and treated with IL-23 (50 ng/ml) for 3 hours. Gene expression analysis revealed significant loss of *Il22* expression in *Il23r*$^{\Delta IEC}$ isolates, in particular in the small intestine (figure 4-4a). Therefore, *Il23r*$^{\Delta IEC}$ mice represented a proper model for impaired small intestinal IL-22 signals. To test, whether this affects epithelial ER stress, crypts isolated from small intestine and colon of *Il23r*$^{\Delta IEC}$ mice were subjected to gene expression analysis for *sXbp1*, *Atf4* and *Grp94*. Indeed, epithelial UPR markers were significantly lower expressed in *Il23r*$^{\Delta IEC}$ small intestines compared to their genotype controls (figure 4-4b). Interestingly, colonic crypts displayed similar ER stress levels irrespective of *Il23r* genotype, pointing towards an ER stress-inducing role of IL-22 restricted to the small intestine.

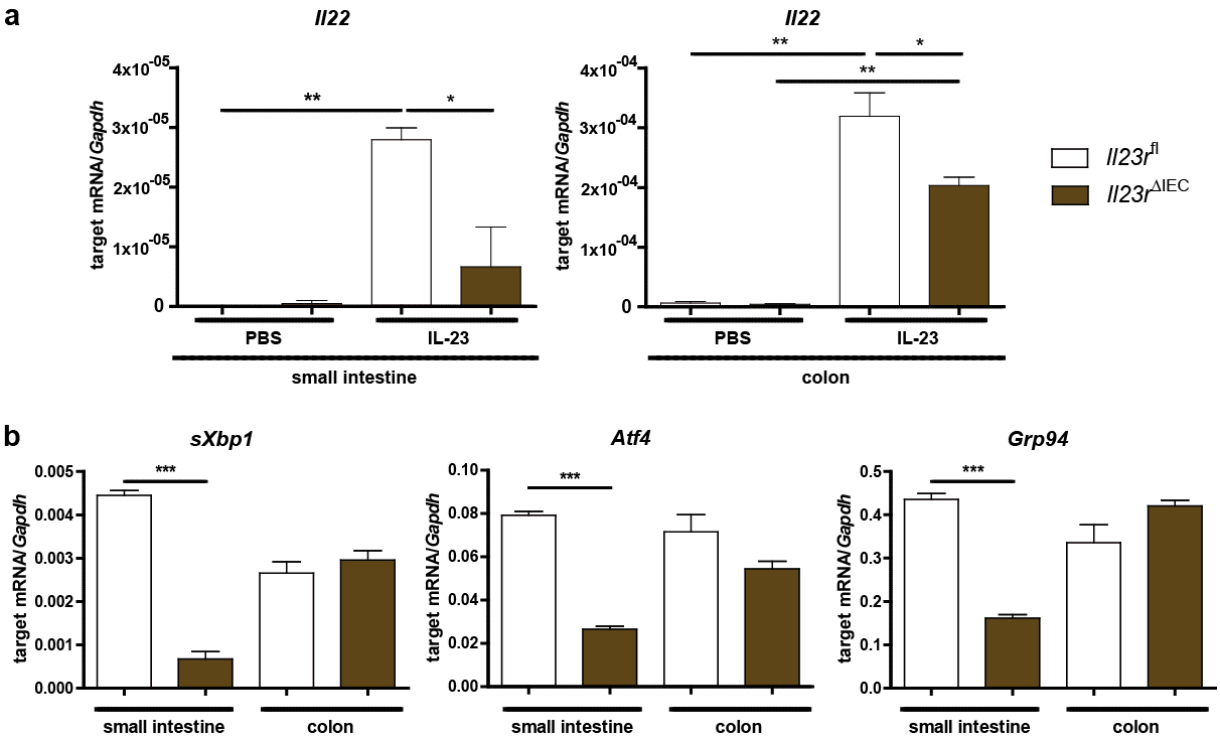


**Figure 4-4: Absence of mucosal IL-22 reduces epithelial UPR in the small intestine**

(**a**) Crude crypt isolates from small intestines and colons from *Il23r*$^{fl}$ and *Il23r*$^{\Delta IEC}$ mice were incubated in RPMI and treated with either PBS or rmIL-23 (50 ng/ml) for 3 h. Gene expression of *Il22* was analysed by SYBR green qPCR and normalised to *Gapdh* expression (n=3 each). (**b**) Intestinal crypts from small intestines and colons from *Il23r*$^{fl}$ and *Il23r*$^{\Delta IEC}$ mice were analysed for gene expression of *sXbp1*, *Atf4* and *Grp94* by SYBR green qPCR and normalised to *Gapdh* expression (n=3 each). Data are shown as mean ± s.e.m. and were tested for statistical significance using unpaired Student's t-test. * p<0.05, ** p<0.01, *** p<0.001.

To test whether the ER stress induction by cytokines is specific to IL-22, HT-29 cells were treated with IL-10 (100 ng/ml) for 24 h and tunicamycin (1 µg/ml) for 6 h. ER stress levels were assessed by gene expression analysis of UPR target genes *sXBP1* and *ATF4*. IL-10 did not prevent ER stress in this setting (figure 4-5), despite the previously proposed protective role of IL-10 (162). Collectively, these data point toward an IL-22 specific role in the adjustment of ER function in the intestinal epithelium.

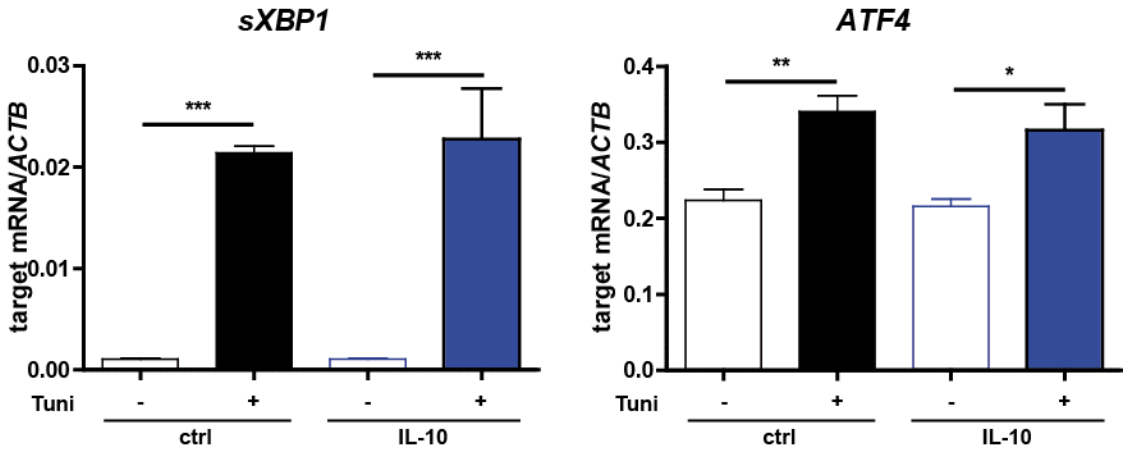


**Figure 4-5: ER stress induction in intestinal epithelial cells is specific for IL-22**

HT-29 cells received recombinant human IL-10 (100 ng/ml) for 24 h (n=3 each) and tunicamycin (1 µg/ml) for 6 h. PBS or DMSO, respectively, served as stimulation controls. Expression levels of *sXBP1* and *ATF4* were analysed by SYBR green qPCR and normalised to *ACTB* expression. Data are shown as mean ± s.e.m. and were tested for statistical significance using unpaired Student's t-test. * $p<0.05$, ** $p<0.01$, *** $p<0.001$.

## 4.2 IL-22 impedes epithelial regeneration in the context of ER stress

Chronic ER stress can impede intestinal proliferation by suppressing intestinal stemness (201). To test the hypothesis that the pro-regenerative response of IL-22 depend on the homeostatic state of the epithelial cell, the epithelial scratch assay as a model of epithelial regeneration was employed. In a first line of evidence, the models were tested whether they are amenable to study the growth-impeding role of ER stress in IEC`s. Directly after wounding, increasing concentrations of tunicamycin or a dimethyl sulfoxide (DMSO) control were added to the medium. After 24 h, tunicamycin suppressed wound closure in a dose-dependent manner (figure 4-6). Doses of 5 µg/ml of tunicamycin even led to further erosion of the epithelial layer.

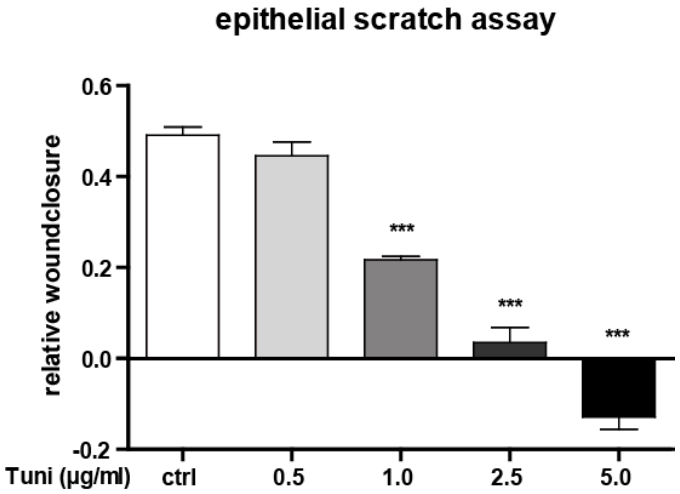


**Figure 4-6: Tunicamycin dose-dependently impedes epithelial wound closure**

(**a**) Scheme of epithelial scratch assays and an example of a wound in a HT-29 cell monolayer at time point 0 h and after 24 h. (**b**) HT-29 cells received indicated concentrations of tunicamycin for 24h (n=3 each). DMSO served as a stimulation control. Wound close relative to the starting wound area was assessed. Data are shown as mean ± s.e.m. and were tested for statistical significance using unpaired Student's t-test. *** $p<0.001$.

Next, effects of IL-22 on epithelial regeneration were assessed. HT-29 cells were treated with IL-22 directly after wounding. EGF or tunicamycin were added to the experiment as positive and negative controls for epithelial growth. IL-22 promoted wound closure until 24 h in line with the pro-regenerative role reported (56) (figure 4-7). However, IL-22-induced wound closure speed declined in the following 24 h. By contrast, EGF treatment maintained epithelial growth for the entire observation period of 48 h. These results suggest a complex, time-dependent role of IL-22 on epithelial regeneration.

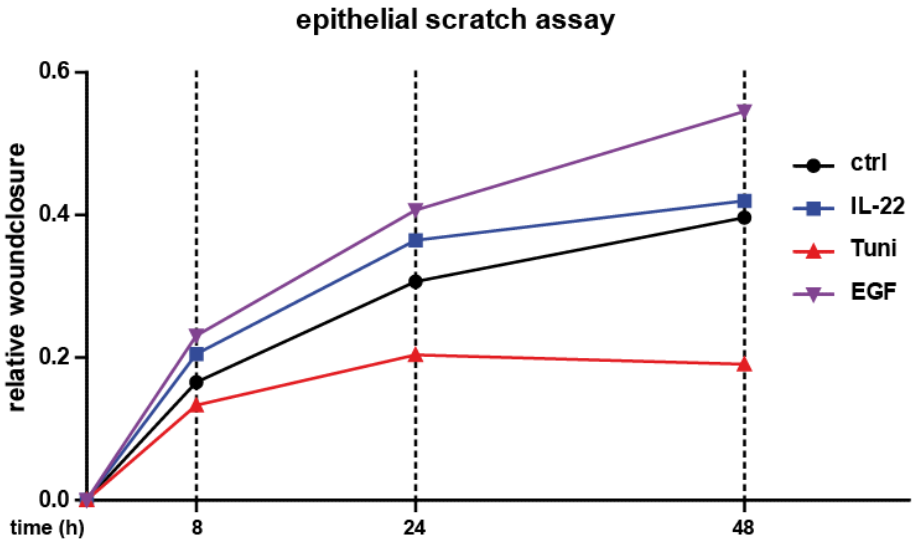


**Figure 4-7: Kinetic of wound closure of HT-29 cells after treatment with IL-22, tunicamycin and EGF**

HT-29 cells received rhIL-22, rhEGF (100 ng/ml each) or tunicamycin (1 µg/ml) directly after wounding, n=6 each. DMSO served as stimulation controls. Wound close relative to the starting wound area was assessed 8, 24 and 48 hours after scratch. Data are shown as mean of 6 replicates.

To further evaluate the effect of IL-22 on ER stress-dependent growth inhibition of wounded epithelial layers, HT-29 cells were treated with IL-22 either for 24h before or simultaneously with epithelial wounding. Tunicamycin was added directly after wounding. In line with the previous finding, pre-treatment with IL-22 did not improve wound healing even if the cells received additional IL-22 after scratching (figure 4-8a). Strikingly, IL-22 exacerbated tunicamycin-dependent wound closure inhibition, in concordance with an ER stress-potentiating role of IL-22 (see figure 4-2). To test whether the described impairment of wound closure is associated with pro-inflammatory cytokine expression, supernatants from this experiment were analysed for human IL-8 levels via ELISA (figure 4-8b). In congruence with the wound healing experiments, IL-22 exacerbated tunicamycin-driven IL-8 expression, indicating an ER stress-dependent pro-inflammatory phenotype upon IL-22 treatment. Hence, IL-22 has a context-dependent effect on epithelial regeneration.

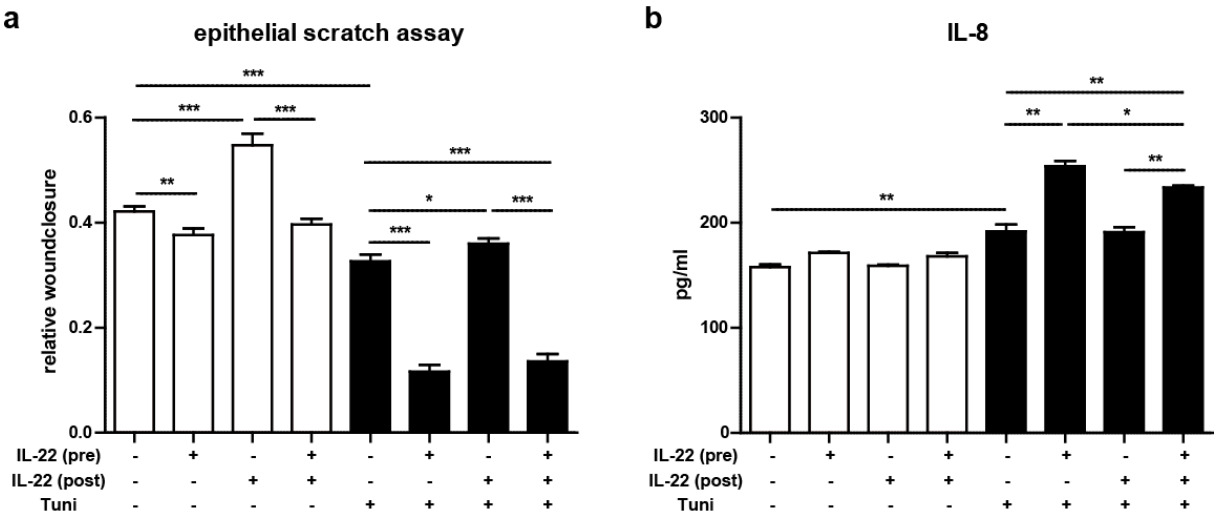


**Figure 4-8: IL-22 exacerbates tunicamycin-driven growth inhibition in HT-29 cells**

(**a**) HT-29 cells received rhIL-22 (100 ng/ml) either 24h before or directly after wounding. Tunicamycin (1 µg/ml) was added directly after wounding. PBS or DMSO served as stimulation controls, respectively. n=18 each. Wound close relative to the starting wound area was assessed 24 hours after scratch. (**b**) Supernatants collected from (a) 24 h after wounding were analysed for hIL-8 levels via ELISA (n=3 each). Data are shown as mean ± s.e.m. and were tested for statistical significance using unpaired Student's t-test. * $p<0.05$, ** $p<0.01$.

## 4.3 ER stress induction by IL-22 is dependent on STAT3 and autophagy

To decipher the underlying mechanisms of IL-22-induced ER stress, we tested whether IL-22-induced ER stress depended on STAT3, the canonical downstream effector of IL-22 (56), HT-29 cells were treated with IL-22 and tunicamycin in the presence or absence of S3I-201, a chemical inhibitor of STAT3 (137). Indeed, STAT3 inhibition reduced ER stress in HT-29 cells treated with IL-22 and tunicamycin (figure 4-9a), indicating that deleterious IL-22 effects are mediated via canonical STAT3 signalling. Homeostatic ER stress is balanced by induction of autophagy, and ER stress and autophagy are essential cross-compensatory mechanisms in IEC`s. Shifts in this balance may contribute to IBD pathogenesis (160). We therefore tested whether inhibition of mTOR, an established mechanism of autophagy induction (202), by rapamycin rescued IL-22-dependent ER stress. HT-29 cells were therefore treated with IL-22 and tunicamycin, with or without concomitant administration of rapamycin.

Rapamycin suppressed synergistically induced ER stress by IL-22 and tunicamycin (figure 4-9b).

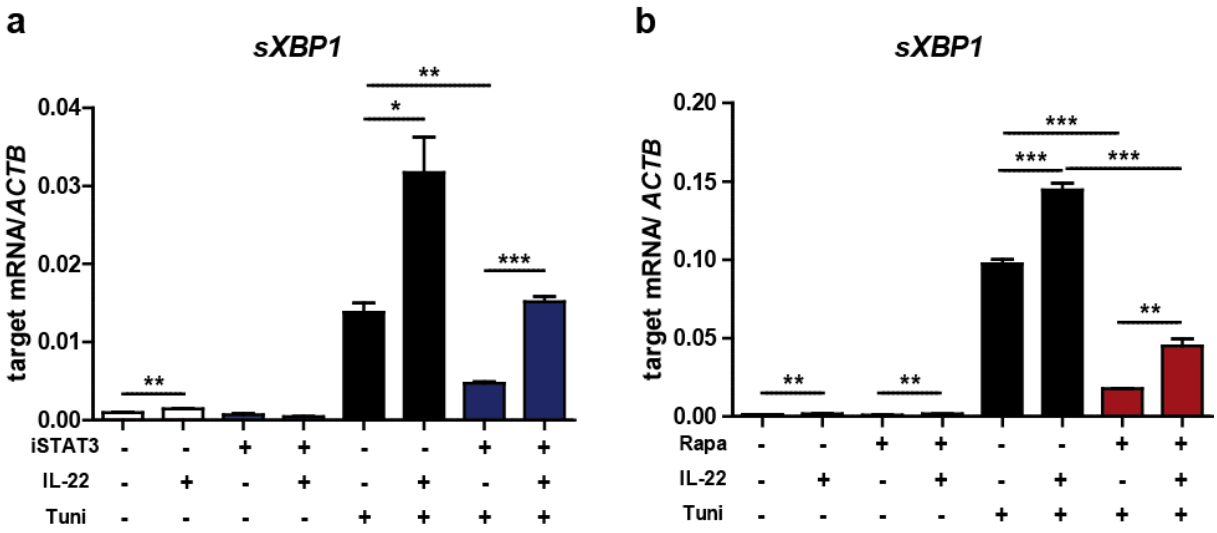


**Figure 4-9: STAT3 and autophagy control IL-22-dependent ER stress**

HT-29 cells received (**a**) S3I-201 (iSTAT3, 5 µM) or (**b**) rapamycin (Rapa, 5 nM) for 48 h, IL-22 (100 ng/ml) for 24 h and tunicamycin (1 µg/ml) for 6h (n=3 each). PBS or DMSO, respectively, served as stimulation controls. Expression levels of *sXBP1* analysed by SYBR green qPCR and normalised to *GAPDH* expression. Data are shown as mean ± s.e.m. and were tested for statistical significance using unpaired Student's t-test. * $p<0.05$, ** $p<0.01$.

To further test, whether STAT3 inhibition or autophagy induction can reverse ER stress-dependent impairment of epithelial regeneration, either iSTAT3 or rapamycin were added prior to IL-22 treatment and epithelial scratch. In line with gene expression data, both iSTAT3 and rapamycin were able to rescue epithelial wound closure after IL-22 and tunicamycin challenge (figure 4-10). Rapamycin treatment also prevented IL-8 expression after IL-22 and tunicamycin challenge. Interestingly, addition of iSTAT3 did not alter IL-8 levels in supernatants of ER stressed HT-29 cells, indicating a STAT3-independent activation of NF-κB signalling in this setting.

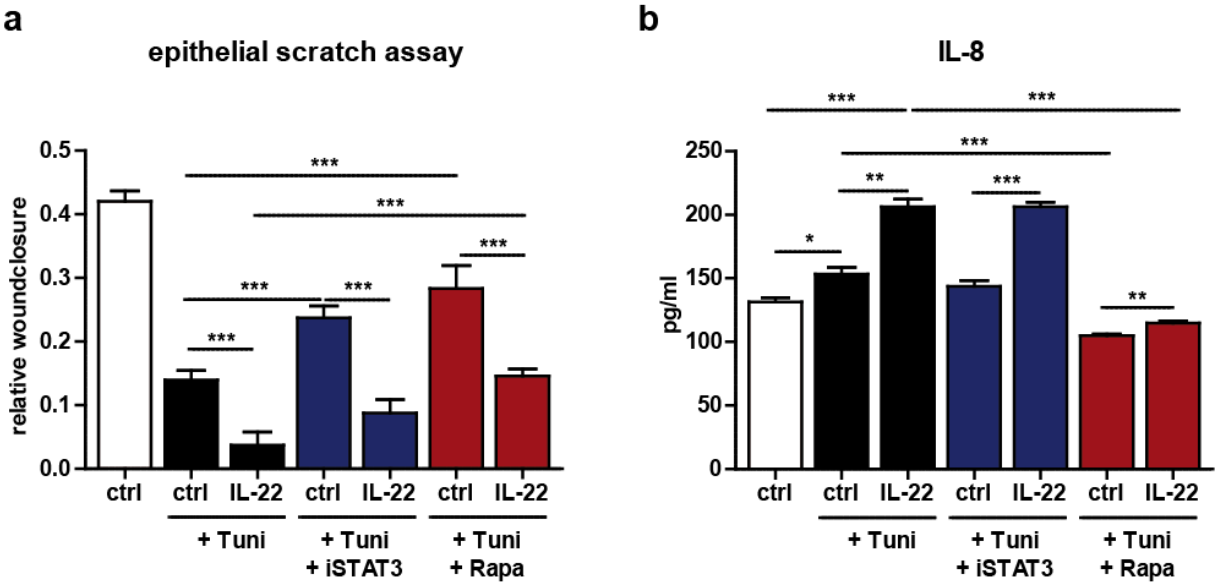


**Figure 4-10: STAT3 inhibition and rapamycin prevent ER stress-dependent inflammatory phenotype**

(**a**) HT-29 cells received S3I-201 (iSTAT3, 5 µM) or rapamycin (Rapa, 5 nM) 48 h and rhIL-22 (100 ng/ml) 24 h before wounding. Tunicamycin (1 µg/ml) was added directly after scratching. PBS or DMSO served as stimulation controls, respectively (n=18 each). Wound close relative to the starting wound area was assessed 24 hours after scratch. (**b**) Supernatants collected (a) 24 h after wounding were analysed for hIL-8 levels via ELISA (n=3 each). Data are shown as mean ± s.e.m. and were tested for statistical significance using unpaired Student's t-test. * $p<0.05$, ** $p<0.01$, *** $p<0.001$.

As previously described, autophagy restrains IRE-1 activity in order to prevent excessive ER stress-dependent NF-κB activation and subsequent inflammation (160). To test whether the ER stress potentiating role of IL-22 is due to inhibition of autophagy, HT-29 cells were treated with IL-22 and tunicamycin as before and an immunoblot against autophagy marker LC3β was performed. IL-22 and tunicamycin unexpectedly both led to increased conversion of LC3β-I to LC3β-II (figure 4-11). In conclusion, IL-22 induces ER stress-dependent autophagy and therefore ER stress potentiation is likely not due to autophagy inhibition.

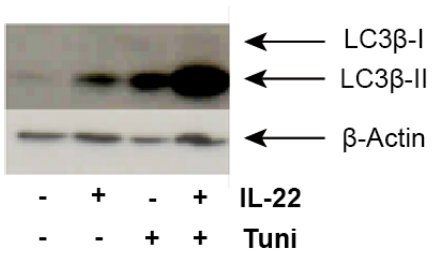


**Figure 4-11: IL-22-dependent ER stress induces autophagy**

HT-29 cells received rhIL-22 (100 ng/ml) for 24 h and tunicamycin (1µg/ml) for 6 h. PBS or DMSO, respectively, served as stimulation controls. Proteins were extracted, immunoblotted and analysed for LC3β. β-Actin served as a loading control. One representative immunoblot out of three independent experiments is shown.

To test whether vice versa inhibition of autophagy mimics the effect of ER stress on epithelial regeneration, HT-29 cells were treated with bafilomycin A1 (BafA), a late stage autophagy inhibitor, in presence or absence of IL-22. Indeed, epithelial layers treated with IL-22 and BafA displayed significantly less wound closure after wounding (figure 4-12). IL-8 levels in the supernatants increased after BafA treatment, which however was not significantly affected by IL-22. Hence, autophagy inhibition mimics the wound closure impairing effect on tunicamycin.

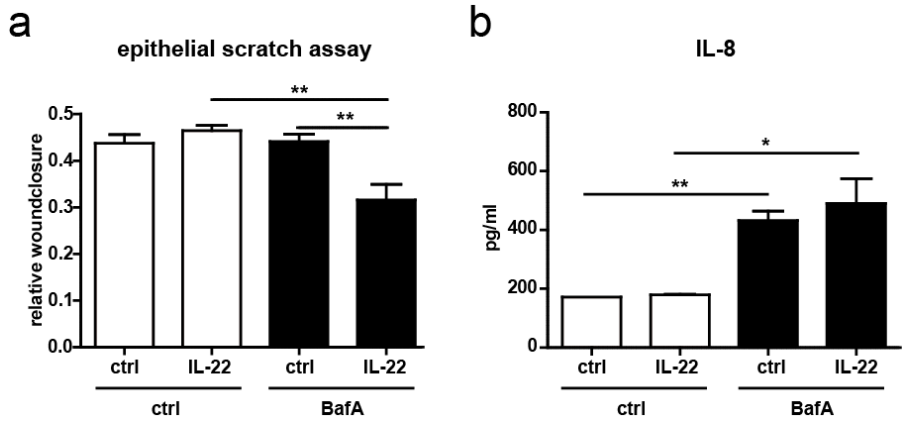


**Figure 4-12: Autophagy inhibition mimics wound repair impairment by tunicamycin**

(**a**) HT-29 cells received bafilomycin A1 (BafA, 5 nM) and rhIL-22 (100 ng/ml) 24 h before wounding. PBS or DMSO, respectively, served as stimulation controls, n=18 each. Relative wound closure was assessed 24 hours after scratch. (**b**) Supernatants collected from (a) 24 h after wounding were analysed for hIL-8 levels via ELISA (n=3 each). Data are shown as mean ± s.e.m. and were tested for statistical significance using unpaired Student's t-test. ** $p<0.01$.

## 4.4 IL-22 induces an inflammatory phenotype in *Xbp1* and *Atg16l1* organoids

IBD risk genes *ATG16L1* and *XBP1* are linked with unresolved ER stress and malfunctioning autophagic machinery (160, 161). To analyse how these risk genes coordinate IL-22 function, I used mice with conditional knockout of *Atg16l1* or *Xbp1* in the intestinal epithelium (*Atg16l1*$^{\Delta IEC}$, *Xbp1*$^{\Delta IEC}$). IL-22 led to marked UPR activation in IL-22 treated compared to control *Xbp1*$^{\Delta IEC}$ mice (figure 4-13). Moreover, *Xbp1*-deficient organoids displayed baseline increased expression levels of *Cxcl1*, the murine homologue of human IL-8. After IL-22 administration, *Cxcl1* expression significantly increased in *Xbp1*$^{\Delta IEC}$ organoids but not in *Xbp1* wild type organoids. Hence, IL-22 induces a pro-inflammatory program in *Xbp1*-deficient organoids.

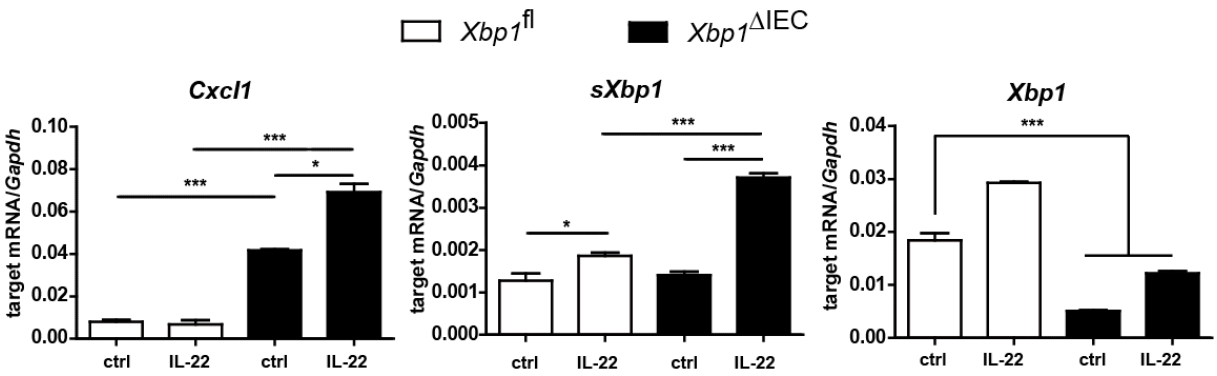


**Figure 4-13: IL-22 induces a pro-inflammatory program in *Xbp1*$^{\Delta IEC}$ organoids**

Organoids derived from *Xbp1*$^{\Delta IEC}$ and *Xbp1*$^{fl}$ mice were treated with either PBS or IL-22 (100 ng/ml) for 24 h (n=3 each). Expression levels of *Cxcl1, sXbp1* and *Xbp1* were analysed by SYBR green qPCR and normalised to *Gapdh*. Data are shown as mean ± s.e.m. and statistical analysis was performed with unpaired Student´s *t*-test. * p<0.05, *** p<0.001.

Since I found that autophagy induction was linked with UPR activation (chapter 4.3), I investigated the role of epithelial *Atg16l1* after IL-22 stimulation. Similar to the results in *Xbp1*$^{\Delta IEC}$ mice, IL-22 potentiated expression of pro-inflammatory cytokines like *Cxcl1* and *Tnf* in *Atg16l1*$^{\Delta IEC}$ mice-derived organoids (figure 4-14). Furthermore, IL-22 induced ER stress markers like *sXbp1*, thus confirming the previously described interplay of autophagy and ER stress. Taken together, IL-22 skews intestinal epithelial cells deficient in *Atg16l1* to a pro-inflammatory state.

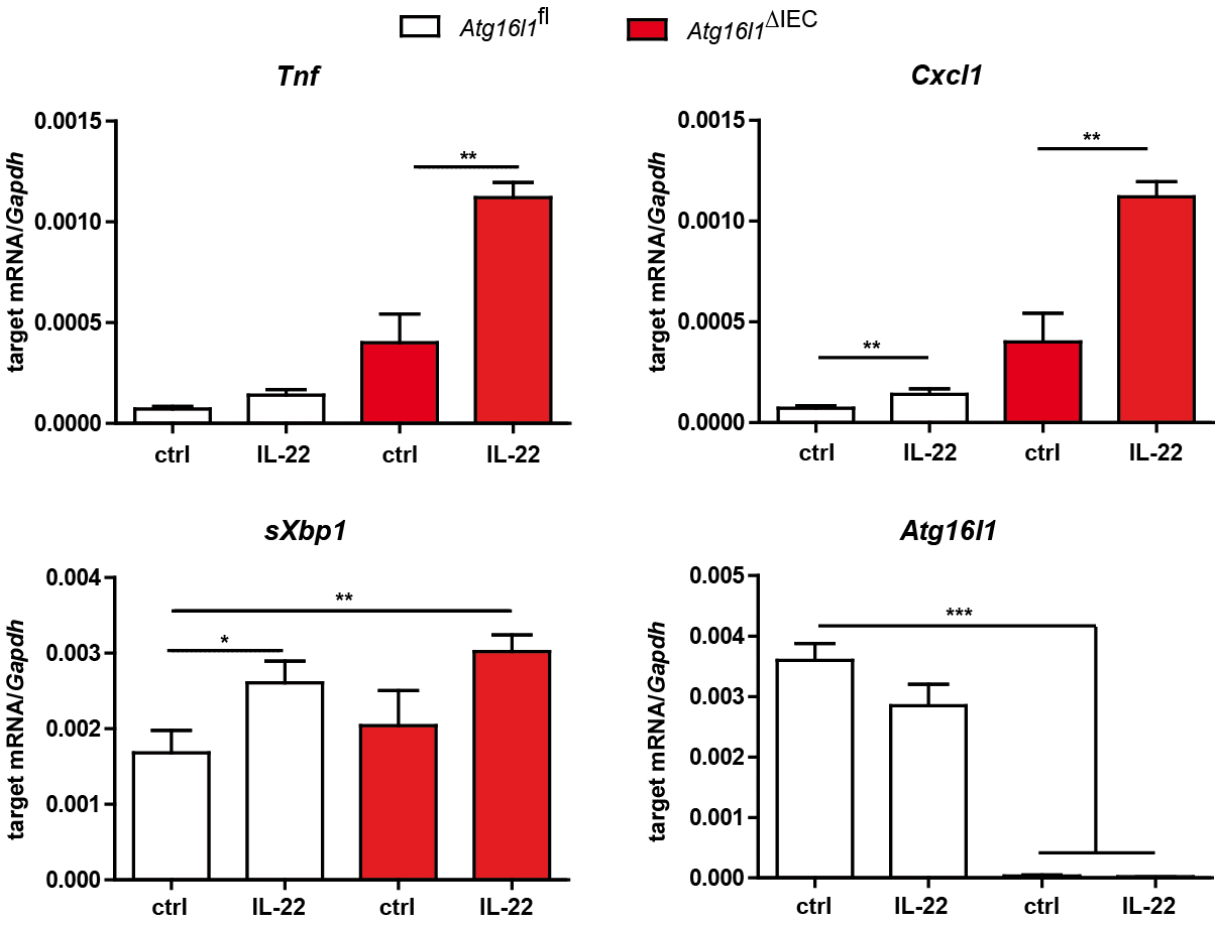


**Figure 4-14: IL-22 drives a pro-inflammatory signature in *Atg16l1*$^{\Delta IEC}$ organoids**
Organoids derived from *Atg16l1*$^{\Delta IEC}$ and *Atg16l1*$^{fl}$ mice were treated with either PBS or IL-22 (100 ng/ml) for 24 h (n=3 each). Expression levels of *Tnf*, *Cxcl1, sXbp1* and *Atg16l1* were measured by SYBR green qPCR and normalised to *Gapdh*. Data are shown as mean ± s.e.m. and statistical analysis was performed with unpaired Student´s *t*-test. * p<0.05, ** p<0.01, *** p<0.001.

Cellular death of intestinal epithelial cells results in defective barrier function of the mucosa, one of the hallmarks of intestinal inflammation. To test whether IL-22-dependent ER stress affected epithelial cell death, I administered IL-22 to *Atg16l1*-deficient organoids. Afterwards, I subjected organoids to a PI-based cell death assay. Indeed, IL-22 significantly induced cell death in *Atg16l1*$^{\Delta IEC}$ organoids but not in their genotype controls in a dose-dependent manner (figure 4-15).

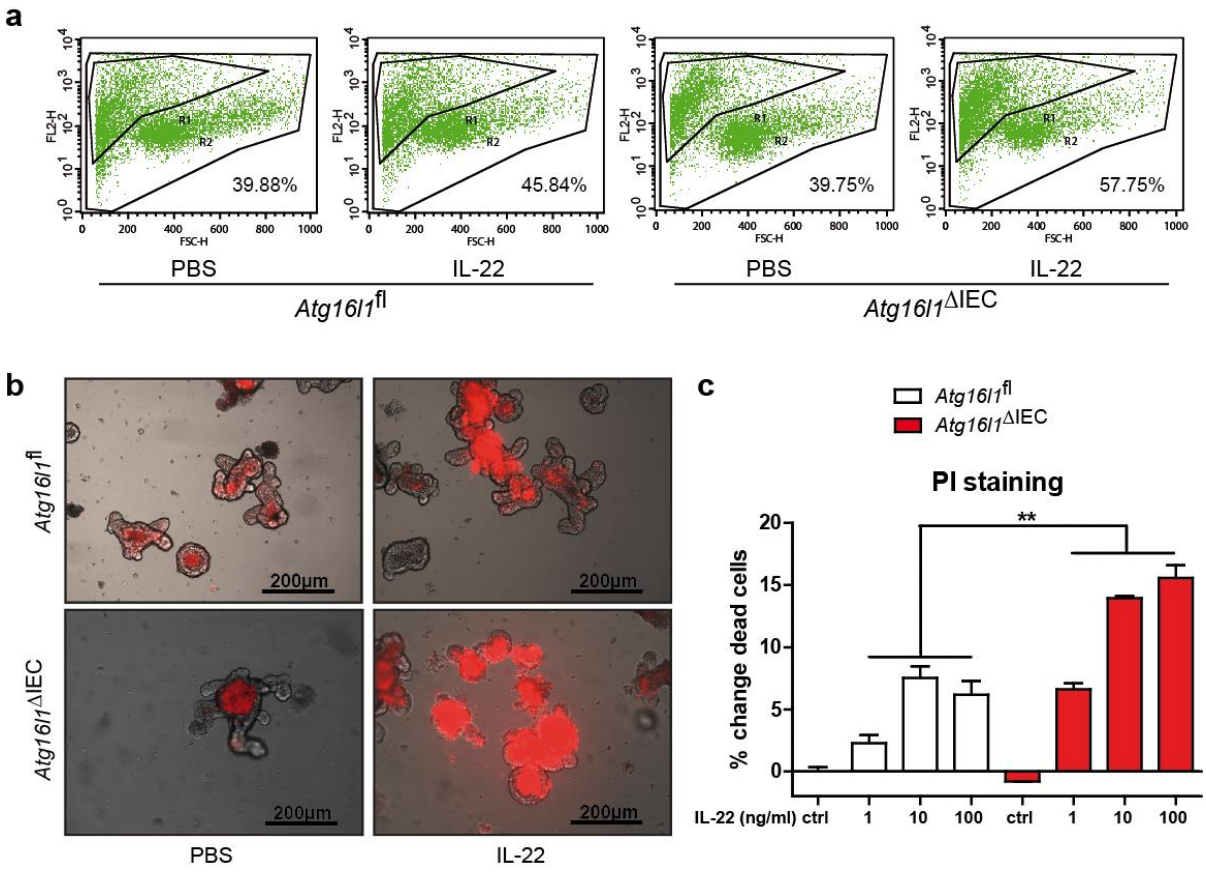


**Figure 4-15: IL-22 induces cell death in a state of disordered autophagy**

Organoids derived *Atg16l1*$^{\Delta IEC}$ and *Atg16l1*$^{fl}$ mice were treated with either PBS or rmIL-22 (1, 10 or 100 ng/ml) for 24 h (n=3 each). Organoids were subjected to PI staining and fluorescence intensities were analysed using flow cytometry. (**a**) Representative FACS plots of dissociated organoid cells derived from *Atg16l1*$^{\Delta IEC}$ and *Atg16l1*$^{fl}$ mice and treated with IL-22 (100 ng/ml). (**b**) Merged images (bright field vs. RFP-filter for PI) from representative organoids incubated with PI (1:1,000 solution in medium) for 24h, 100x magnification, bars indicate 200 µm. (**c**) Statistical analysis of % change dead cells. Data are shown as mean ± s.e.m. and statistical analysis was performed with unpaired Student´s *t*-test. ** p<0.01.

To further determine whether cell death induction is specific for IL-22, I treated *Atg16l1*$^{\Delta IEC}$ organoids with the structurally similar IL-10. Interestingly, *Atg16l1*-deficient organoid cells underwent cellular death to a smaller extent (figure 4-16). Challenge with tunicamycin served as a control. Fitting to the aforementioned inhibitory role of autophagy on ER stress, *Atg16l1*-deficient organoids underwent significantly more cellular death upon ER stress induction as with tunicamycin challenge.

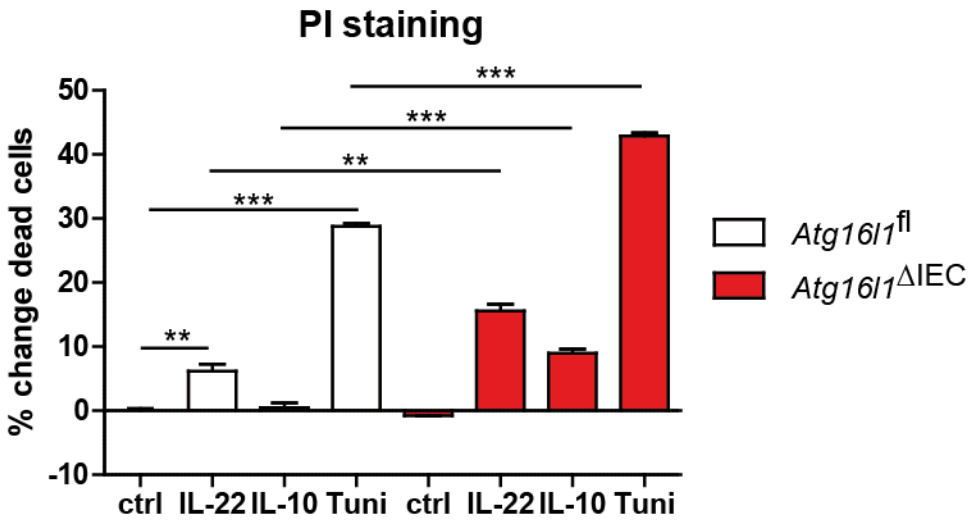


**Figure 4-16: IL-10 is not protective in *Atg16l1* deficiency**

Organoids derived from *Atg16l1*$^{\Delta IEC}$ and *Atg16l1*$^{fl}$ mice were treated with either PBS, rmIL-10 (100 ng/ml), rmIL-22 (100 ng/ml) or tunicamycin (500 ng/ml) for 24 h (n=3 each). Organoids were subjected to PI staining and fluorescence intensities were analysed using flow cytometry. Data are shown as mean ± s.e.m. and statistical analysis was performed with unpaired Student´s *t*-test. ** p<0.01, *** p<0.001.

Thus, *Atg16l1* and *Xbp1* critically control inflammatory signals in the intestinal epithelium upon IL-22, preventing excessive epithelial cell death. Loss of *Atg16l1* reverts tissue protection by IL-10.

## 4.5 ATG16L1 controls IL-22-depedent STING activation and subsequent ISG induction

To delineate the transcriptional program driven by IL-22 in absence or presence of adequate autophagy, **Dr. Raheleh Sheibani-Tezerji kindly performed RNA sequencing** of small intestinal organoids derived from *Atg16l1*$^{\Delta IEC}$ mice or genotype controls treated with rmIL-22 for 24 h. In total, I found 2908 differentially expressed genes (DEGs) in IL-22 treated organoids. IL-22 up-regulated 586 unique genes in *Atg161*$^{fl/fl}$ and 484 in *Atg16l1*$^{\Delta IEC}$ organoids while IL-22 uniquely down-regulated 794 genes in *Atg16l1*$^{fl/fl}$ and 490 genes in*Atg16l1*$^{\Delta IEC}$ organoids (figure 4-17).

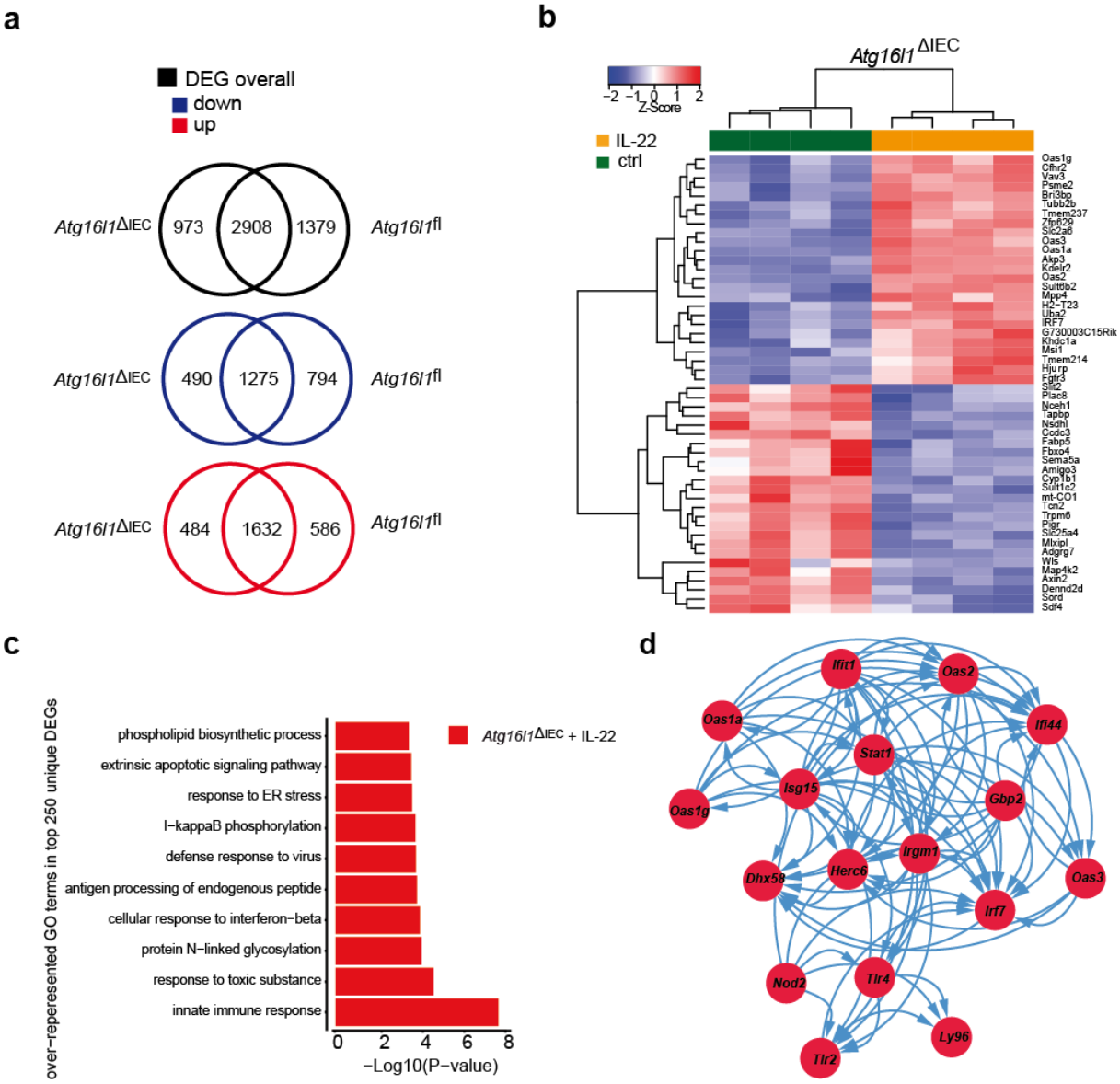


**Figure 4-17: *Atg16l1* orchestrates an IL-22-driven type I interferon expression signature in intestinal organoids**

(**a**) Venn diagram showing overall (top, black) differentially expressed genes and significantly down-regulated (middle, blue) and up-regulated (below, red) genes in *Atg16l1*$^{fl}$ and *Atg16l1*$^{\Delta IEC}$ in response to stimulation with IL-22 (10 ng/ml), n=4 each. (**b**) Heat map showing clustering of top 20 genes differentially expressed in response to IL-22 (10 ng/ml) according to genotype. (**c**) enriched GO terms of top 250 uniquely upregulated genes in IL-22 treated *Atg16l1*$^{\Delta IEC}$ intestinal organoids. (**d**) STRING-based network analysis of all genes contributing to the GO term “innate immune response” detected in (c). **All analyses of this figure were kindly performed by Dr. Raheleh Sheibani-Tezerji.**

To provide a first functional annotation, a gene set enrichment analysis using the gene ontology (GO) term algorithm was performed. Furthermore, DEGs were

clustered using network analysis base on the *Search Tool for the Retrieval of Interacting Genes/Proteins* (STRING) (200). Surprisingly, only IL-22 treated organoids which were deficient for *Atg16l1* showed significant enrichment of genes involved in type I interferon signalling and response (see figure 4-17d). These results imply a strong induction of interferon stimulated genes (ISG) by IL-22 in *Atg16l1*$^{\Delta IEC}$ organoids. To confirm these findings, I treated *Atg16l1*$^{fl}$ and *Atg16l1*$^{\Delta IEC}$ organoids with IL-22 (100 ng/ml) for 24 h. I then analysed gene expression of *Ifit1* and *Ifit3*, which are well-established representatives for ISG (203). *Atg16l1*$^{\Delta IEC}$ organoids displayed increased ISG expression at baseline condition. While administration of IL-22 moderately induced the analysed genes in *Atg16l1*$^{fl}$ organoids, strong induction was observed in *Atg16l1*$^{\Delta IEC}$ tissue (figure 4-18). These data validate the RNA sequencing results, which pointed to a strong ISG induction by IL-22 in *Atg16l1*$^{\Delta IEC}$ organoids.

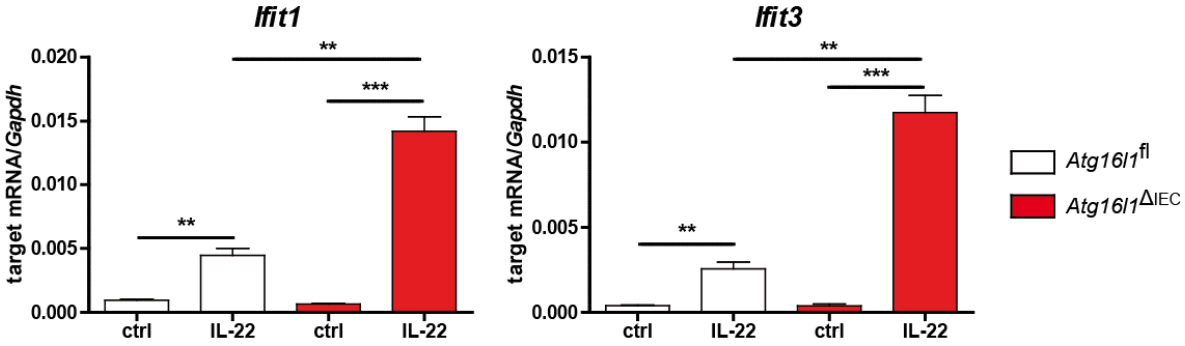


**Figure 4-18: Enhanced ISG induction by IL-22 in *Atg16l1*-deficient organoids**

Organoids derived from *Atg16l1*$^{\Delta IEC}$ and *Atg16l1*$^{fl}$ mice were treated with either PBS or IL-22 (100 ng/ml) for 24 h (n=3 each). Expression levels of *Ifit1* and *Ifit3* were measured by SYBR green qPCR and normalised to *Gapdh*. Data are shown as mean ± s.e.m. and statistical analysis was performed with unpaired Student´s *t*-test. ** p<0.01, *** p<0.001.

Next, we aimed to delineate the molecular origin of increased IFN-I signature in *Atg16l1* deficient organoids. Therefore, I tested whether IL-22-mediated ISG induction depended on canonical IFN-I inducing signalling cascades like cGAS/STING/TBK1 or the RIG-I/MDA5/MAVS axis. I treated organoids derived from *Atg16l1*$^{fl}$, *Atg16l1*$^{\Delta IEC}$, *Mda5*$^{-/-}$ and *Tmem173*$^{gt}$ mice (mice harbouring a golden ticket mutation leading to dysfunction of STING) were treated with IL-22 (1, 10 and 100 ng/ml) for 24 h and analysed gene expression of *Ifit1* and *Ifit3*. In line with results discussed earlier, increased *Atg16l1*-deficient organoids showed higher ISG induction (figure 4-19a). In *Tmem173*$^{gt}$ organoids, expression of ISG was completely

blunted, whereas deficiency of *Mda5* did not affect ISG induction upon IL-22 treatment. To further elucidate the STING-dependent signals upon IL-22, protein lysates were generated from IL-22 treated *Atg16l1*$^{\Delta IEC}$ organoids. IL-22 increased TBK1 phosphorylation in *Atg16l1*$^{\Delta IEC}$ organoids as revealed by immunoblot analysis (figure 4-19b). To validate these findings in another cellular system, I treated Caco-2 cells deficient for *ATG16L1* with IL-22 (100 ng/ml) for 24, 48 and 72h (figure 4-20c). Again, TBK1 was phosphorylated in IL-22-treated cells deficient for *ATG16L1*. In conclusion, *Atg16l1* deficiency intensifies IL-22-dependent activation of STING signalling.

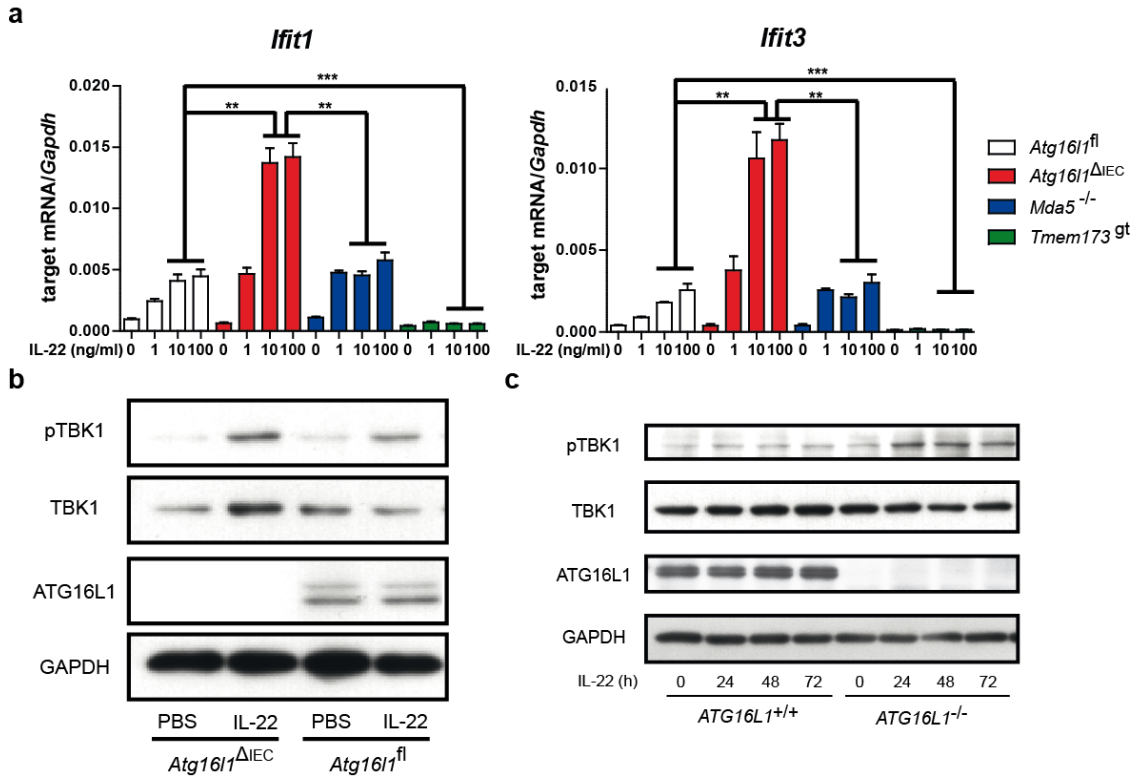


**Figure 4-19: STING regulates induction of ISG by IL-22 signals**

(**a**) Organoids derived from *Atg16l1*$^{fl}$, *Atg16l1*$^{\Delta IEC}$, *Mda5*$^{-/-}$ and *Tmem173*$^{-/-}$ mice were treated with either PBS or IL-22 (1, 10 or 100 ng/ml) for 24 h (n=3 each). Gene expression level of *Ifit1* and *Ifit3* was measured by SYBR green qPCR and normalised to *Gapdh*. Data are shown as mean ± s.e.m. and statistical analysis was performed with unpaired Student´s *t*-test. ** p<0.01, *** p<0.001. (**b**) Organoids derived from *Atg16l1*$^{fl}$ and *Atg16l1*$^{\Delta IEC}$ mice were treated with either PBS or IL-22 (100 ng/ml) for 24 h. Proteins were extracted, immunoblotted and analysed for pTBK1, TBK1 and ATG16L1. GAPDH served as a loading control. (**c**) *ATG16L1*$^{+/+}$ and *ATG16L1*$^{-/-}$ Caco-2 cells were treated with IL-22 (100 ng/ml) for the indicated time. Proteins were extracted, immunoblotted and analysed for pTBK1, TBK1 and ATG16L1. GAPDH served as a loading control. One representative immunoblot out of two independent experiments is shown.

Based on the previous finding of STING activation in Atg16l1 deficiency, I hypothesised that cytosolic dsDNA was involved in IL-22-dependent ISG induction in *Atg16l1* deficiency. Using CRISPR/Cas9 technology, Caco-2 cells (a human intestinal carcinoma cell line) deficient for *ATG16L1* were generated and stimulated with IL-22 (100 ng/ml) for 24 h. I then performed immunofluorescence staining against dsDNA. Indeed, *ATG16L1*$^{-/-}$ deficiency in Caco-2 cells led to accumulation of cytosolic/extranuclear dsDNA which was further induced by IL-22 stimulation (figure 4-20, **analysis kindly performed by Dr. Kareen Bartsch**).

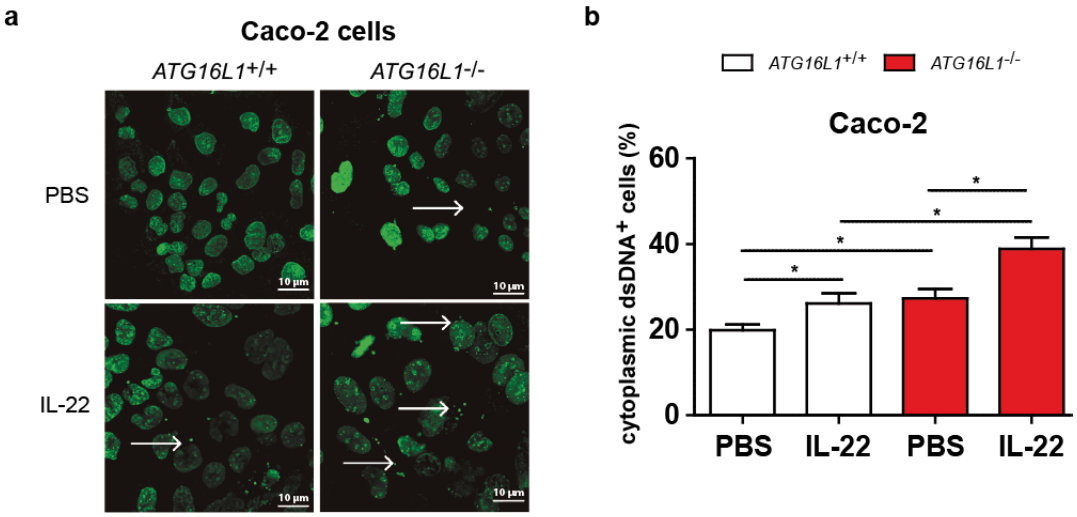


**Figure 4-20: IL-22 releases cytosolic dsDNA in *ATG16L1* deficiency**

(**a**) Caco-2 cells proficient (*ATG16L1*$^{+/+}$) or deficient (*ATG16L1*$^{-/-}$) for *ATG16L1* were treated with either PBS or IL-22 (100 ng/ml) for 24 h (n=3 each) before fixation and immunofluorescence staining against dsDNA. White arrows indicate extranuclear dsDNA punctae. White bars indicate 10 µm. (**b**) Quantification of cells positive for cytoplasmic dsDNA. Data are shown as mean ± s.e.m. and statistical analysis was performed with unpaired Student´s *t*-test. * p<0.05. **The analysis was kindly performed by Dr. Kareen Bartsch.**

To exclude that upregulation of STING signalling was due to increased availability of STING protein or altered post-translational modification or impaired cellular trafficking, *Atg16l1*$^{fl}$ and *Atg16l1*$^{\Delta IEC}$ organoids were generated and treated with IL-22 (1, 10 or 100 ng/ml) for 24 h. IL-22 dose-dependently induced gene expression of *Tmem173*, which encodes for STING (figure 4-21), an effect not affected by *Atg16l1* status. In line with this, immunoblot analysis revealed an undistinguishable IL-22-dependent induction of STING in *Atg16l1*$^{\Delta IEC}$ mice compared to the wild-type control. Stimulation with hydroxyurea, a DNA double strand break-inducing agent, served as

a control. Thus, STING is not regulated by *Atg16l1* on transcript and total protein level.

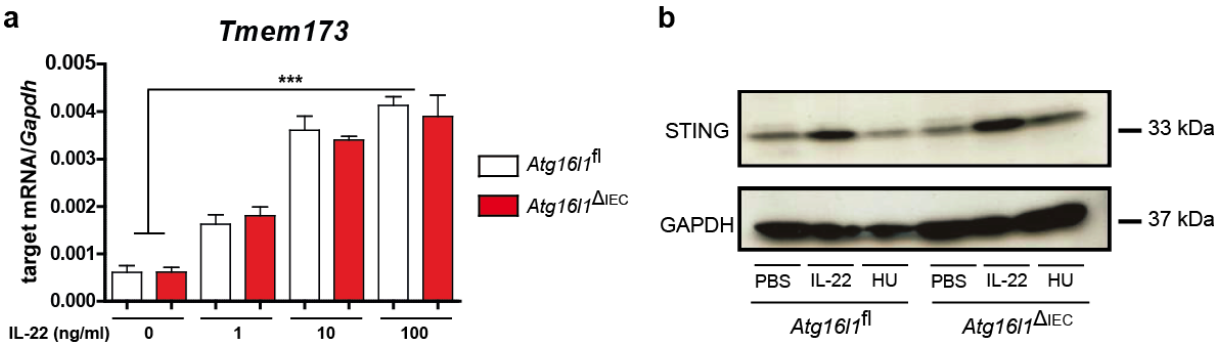


**Figure 4-21: Induction of *Tmem173*/STING by IL-22 is not altered in *Atg16l1*-deficient organoids**

(**a**) Organoids derived from *Atg16l1*$^{\Delta IEC}$ and *Atg16l1*$^{fl}$ mice were treated with either PBS or IL-22 (1, 10 or 100 ng/ml) for 24 h (n=3 each). Gene expression level of *Tmem173* was measured by SYBR® green qPCR and normalised to *Gapdh*. Data are shown as mean ± s.e.m. and statistical analysis was performed with unpaired Student´s *t*-test. *** p<0.001. (**b**) Organoids derived from *Atg16l1*$^{\Delta IEC}$ and *Atg16l1*$^{fl}$ mice were treated with either PBS, IL-22 (100 ng/ml) or hydroxyurea (HU, 1 µM) for 24 h. Proteins were extracted, immunoblotted and analysed for STING expression. GAPDH served as a loading control. One representative immunoblot out of two independent experiments is shown.

To investigate whether control of ISG induction by *Atg16l1* relied on canonical autophagy, I treated *Atg16l1*$^{fl}$ organoids with IL-22 (100 ng/ml) for 24h along with bafilomycin A1 (BafA, 5nM), a late phase autophagy inhibitor which blocks fusion of autophagosomes with lysosomes. Bafilomycin co-treatment of organoids mimicked the effect of *Atg16l1* deletion on ISG induction as shown by induction of *Ifit1* and *Ifit3* expression after IL-22 stimulation (figure 4-22). This finding suggests autophagy dysfunction as a result of *Atg16l1* deletion responsible for uncontrolled ISG induction.

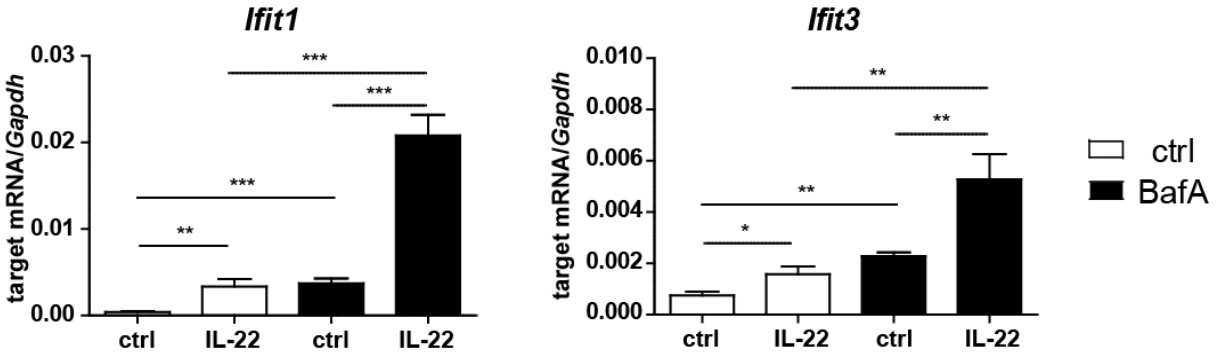


**Figure 4-22: Bafilomycin treatment mimics *Atg16l1*$^{\Delta IEC}$ phenotype of potentiation of IL-22-dependent ISG expression**

Organoids derived from small intestine of wild type mice were treated with IL-22 (100 ng/ml) and bafilomycin A1 (BafA, 5nM) for 24 h, n=3 each. PBS or DMSO served as stimulation controls, respectively. Expression levels of *Ifit1* and *Ifit3* were analysed by SYBR green qPCR and normalised to *Gapdh* expression. Data are shown as mean ± s.e.m. and were tested for statistical significance using unpaired Student's t-test. * $p<0.05$, ** $p<0.01$, *** $p<0.001$.

The WD40 repeat domain of the ATG16L1 protein is believed to form a platform without enzymatic activity for protein-protein interactions, as it is thought to fold into β-propellers. Truncated variants of ATG16L1 lacking the WD40 repeat domain displayed impaired autophagy function and was associated with cellular phenotypes in mice reminiscing *Atg16l1* knockouts (166). Similarly, the protein encoded by the common IBD risk variant *ATG16L1*$^{T300A}$ is cleaved by caspase-3 at the stalk of the WD40 domain, ultimately resulting in loss of functional ATG16L1 protein (204). To test whether ATG16L1-dependent control of ISG induction was affected by absence of WD40 repeat domain, small intestinal organoids were generated from mice ubiquitously harbouring the WD40 truncated variant of ATG16L1 (*Atg16l1*$^{\Delta WD40}$) and analysed for ISG expression after challenge with IL-22 (100 ng/ml) for 24 h. Expression levels of *Cxcl10*, *Ifit1* and *Ifit3* showed slight, albeit not significant reduction in response to IL-22, implying a non-essential role of the WD40 repeat domain in controlling ISG induction (figure 4-23).

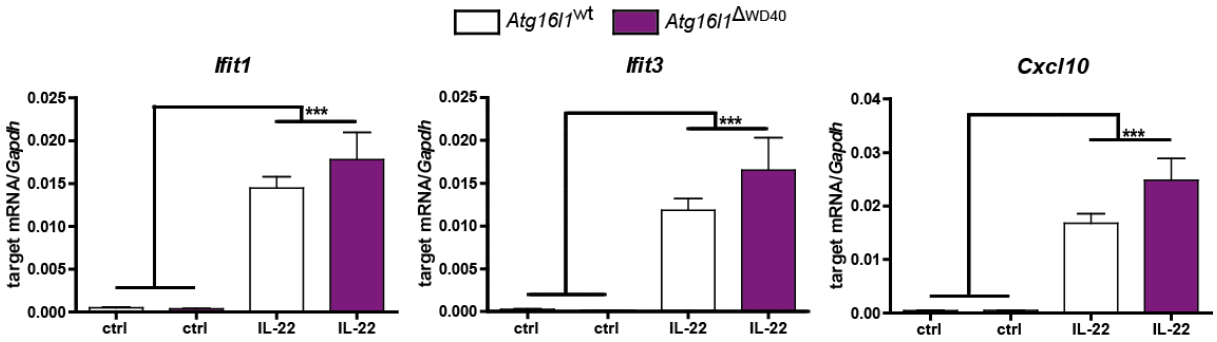


**Figure 4-23: Absence of the WD40 repeat domain in ATG16L1 did not alter induction of ISG by IL-22**

Organoids derived from *Atg16l1*$^{\Delta WD40}$ and *Atg16l1*$^{wt}$ mice were treated with either PBS or IL-22 (100 ng/ml) for 24 h (n=3 each). Expression levels of *Ifit1*, *Ifit3* and *Cxcl10* were measured by SYBR® green qPCR and normalised to *Gapdh*. Data are shown as mean ± s.e.m. and statistical analysis was performed with unpaired Student´s *t*-test. *** p<0.001.

Taken together, ATG16L1 controls ISG induction by IL-22, an effect dependent on the cGAS/STING/TBK1 pathway. This role of ATG16L1 depends on the autophagy supporting properties of the protein but not on the WD40 repeat domain.

## 4.6 IL-22 and downstream type I interferons synergistically induce TNFα-dependent necroptosis

Having shown that IL-22 induces a type I interferon response in a STING-dependent fashion particularly in absence of *Atg16l1*, I unravelled the role of this signalling on cell death and mucosa inflammation. Gene expression analysis of intestinal organoids for *Tnf* and *Cxcl1* revealed strong upregulation of these NF-κB target genes in absence of *Atg16l1*, which was potentiated by IL-22 administration (figure 4-14). On the flipside, *Tmem173* repressed *Tnf* induction by IL-22 while *Cxcl1* gene expression was unaffected (figure 4-24). Importantly, IL-22-dependent induction of ISG was completely abolished in *Tmem173* knockout organoids. These findings indicate a type I interferon-dependent regulation of epithelial *Tnf* expression, with STING signalling enhancing IL-22-dependent *Tnf* induction.

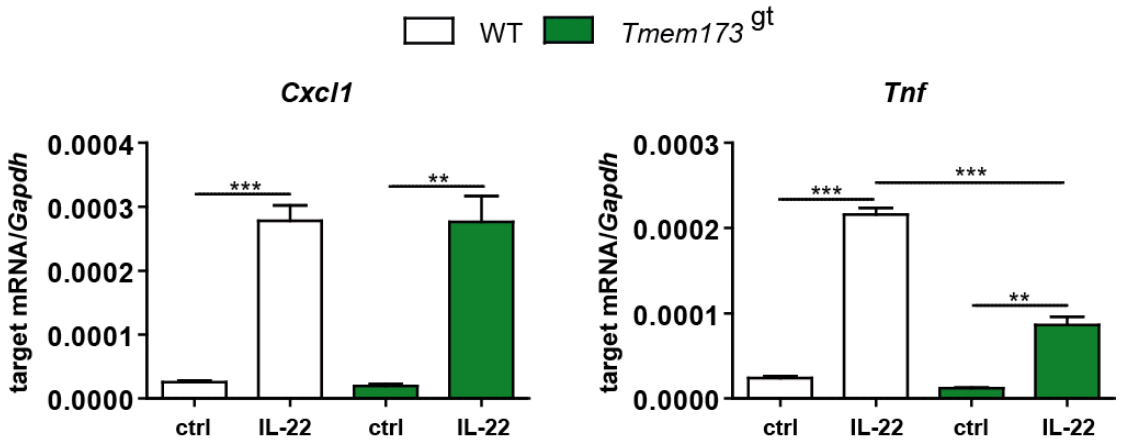


**Figure 4-24: *Tnf* expression is dependent on STING-signalling**

Organoids derived from wild type and *Tmem173*$^{gt}$ mice were treated with IL-22 (100 ng/ml) for 24 h (n=3 each). Expression levels of *Cxcl1* and *Tnf* were measured by SYBR® green qPCR and normalised to *Gapdh*. Data are shown as mean ± s.e.m. and statistical analysis was performed with unpaired Student´s *t*-test. ** p<0.01, *** p<0.001

To further investigate the role of type I interferons in *Tnf* induction, organoids harbouring a defective *Tmem173* variant (golden ticket mutation) were generated and treated with IL-22 and IFN-β. Strikingly, IL-22 and IFN-β synergistically induced *Tnf* in *Tmem173*$^{gt}$ (figure 4-25, **stimulation kindly performed by Dr. Go Ito**).

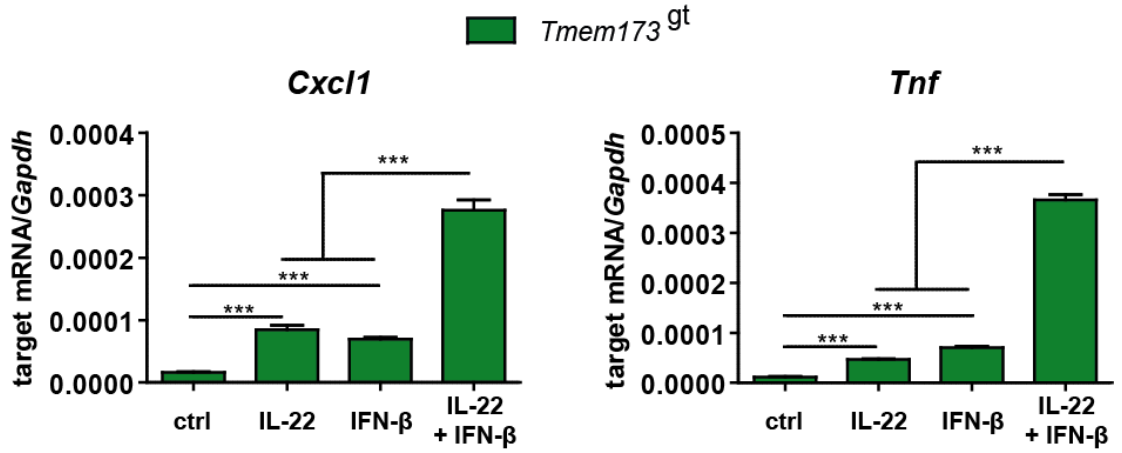


**Figure 4-25: IL-22 and type I interferons synergistically induce *Tnf***

Organoids derived from *Tmem173*$^{gt}$ mice and their genotype controls were treated with rmIL-22 and rmIFN-β (100 ng/ml each) for 24 h (n=3 each). Expression levels of *Cxcl1* and *Tnf* were measured by SYBR® green qPCR and normalised to *Gapdh*. Data are shown as mean ± s.e.m. and statistical analysis was performed with unpaired Student´s *t*-test. *** p<0.001. **Stimulation kindly performed by Dr. Go Ito.**

Having established that type I interferons act as signal enhancer for IL-22-dependent induction of *Tnf*, I investigated the role of epithelial tumor necrosis factor alpha (TNFα). TNFα is a cell death inducing cytokine, while the modus of cell death context-dependently varies between apoptosis via canonical membrane-bound death receptors like FADD and necroptosis in a RIPK1, RIPK3 and MLKL1-dependent fashion (205) (206). Necroptosis is of particular interest as it has been implicated in pathogenesis of IBD (91, 207).

To test whether necroptosis was a relevant cell death mode in the context of IL-22 in autophagy deficiency, intestinal organoids were generated from *Ripk3* knockout (*Ripk3*$^{-/-}$) mice, from mice having a mutated variant of Ripk1 with a loss of function of the kinase domain (*Ripk1*$^{D138N}$) (205) and from *Mlkl* knockout (*Mlkl*$^{-/-}$) mice. Administration of IL-22 and bafilomycin induced significant cell death in organoids of each genotypes, but *Mlkl*$^{-/-}$ organoids were significantly protected from cellular death while *Ripk3*$^{-/-}$ organoids behaved similar to the wild type (figure 4-26). Organoids derived from *Ripk1*$^{D138N}$ mice were albeit slightly protected from BafA + IL-22-induced cellular death.

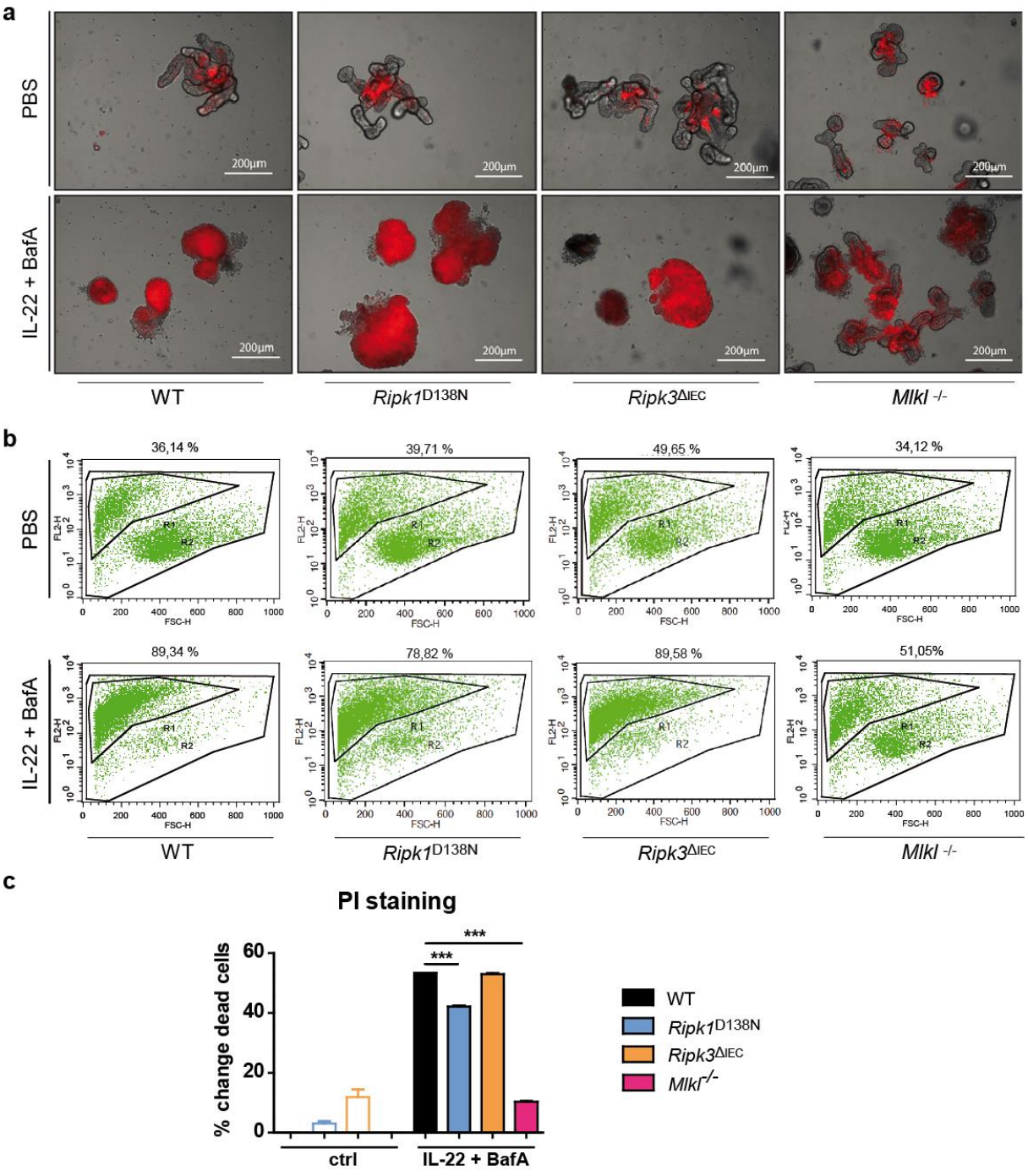


**Figure 4-26: ISG induction by IL-22 and defective autophagy induces necroptosis**

Organoids derived from *Ripk3*$^{-/-}$, *Ripk1*$^{D138N}$ and *Mlkl*$^{-/-}$ mice and their genotype controls were treated with rmIL-22 (100 ng/ml) and BafA (5 nM) for 24 h (n=3 each). (**a**) Merged images (bright field vs. RFP-filter for PI) from representative organoids incubated with PI (1:1,000 solution in medium) for 24h, 100x magnification, bars indicate 200 µm. (**b**) Organoids were subjected to PI and fluorescence intensities were quantified using flow cytometry. (**c**) Statistical analysis of PI$^{+}$ cells from (b). Data are shown as mean ± s.e.m. and statistical analysis was performed with unpaired Student´s *t*-test. *** p<0.001.

Based on these data, I hypothesised that excessive STING signalling contributes to necroptotic cell death in autophagy deficient epithelial cells, via IFN-I-dependent downstream engagement of TNFα. To test this, I stimulated *Tmem173*$^{gt}$ and wild type organoids with IL-22 and BafA. As presumed, *Tmem173*$^{gt}$ organoids succumbed less after IL-22+BafA challenge compared to the wild type controls (figure 4-27).

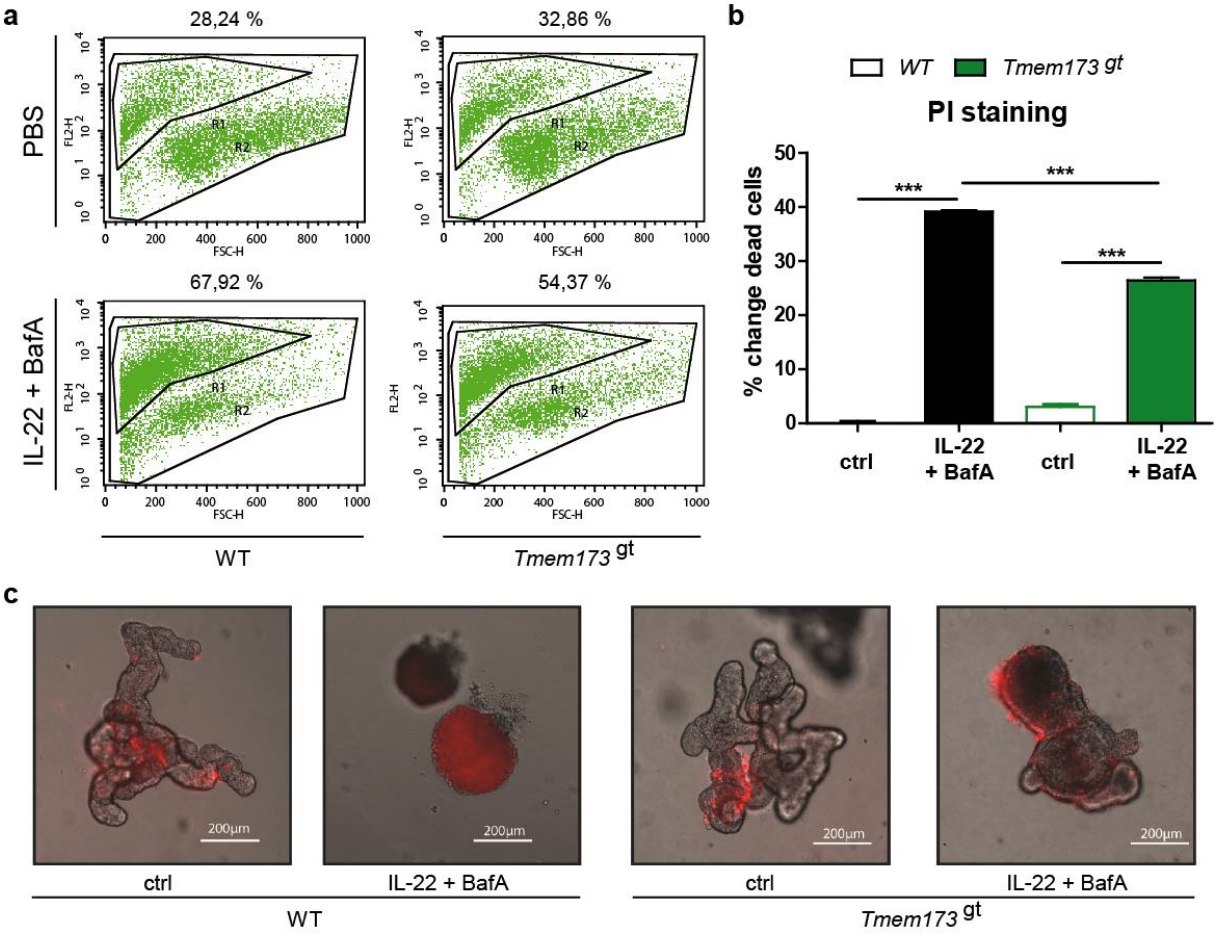


**Figure 4-27: Loss of STING protects against IL-22 induced necroptosis**

Organoids derived from *Tmem173*$^{gt}$ mice and their genotype controls were treated with rmIL-22 (100 ng/ml) and BafA (5 nM) for 24 h (n=3 each). Organoids were subjected to PI and fluorescence intensities were quantified using flow cytometry. (a) representative FACS plots. (b) Statistical analysis of $PI^+$ cells. (c) Merged images (bright field vs. RFP-filter for PI) from representative organoids incubated with PI (1:1,000 solution in medium) for 24 h, 100x magnification, bars indicate 200 µm.. Data are shown as mean ± s.e.m. and statistical analysis was performed with unpaired Student´s *t*-test. *** p<0.001.

Hence, RIPK1/RIPK3-independent necroptosis is a critical mode of cell death resulting from signalling via the IL-22/STING/ISG/TNFα axis.

## 4.7 IL-22 drives a local, small intestinal inflammatory phenotype in the absence of epithelial *Atg16l1* and *Xbp1*

I have shown that absence of *Xbp1* or *Atg16l1* renders IL-22 receptive intestinal organoids to a more cell death prone phenotype. I therefore meant to investigate whether the failed epithelial interplay contributes to the manifestation of small intestinal inflammation in mice or not.

To further confirm a biologically meaningful pro-inflammatory role of IL-22 in the context of epithelial *Atg16l1* deficiency, *Atg16l1*$^{\Delta IEC}$ and *Atg16l1*$^{fl/fl}$ mice were treated with either 2 µg IL-22 or PBS via intraperitoneal injection for 6 consecutive days (figure 4-28a). Colitis was induced by 2% DSS in drinking water from day 2 until days 6 of the IL-22 treatment. Daily assessment of body weight change revealed significant weight loss in the group of IL-22-treated *Atg16l1*$^{\Delta IEC}$ mice, which was accompanied by significant increase of the Disease Activity Index score (figure 4-28b, composed of weight loss, stool consistency and rectal bleeding). However, liver, spleen and caecum weight, markers for systemic inflammatory burden, were similar in both genotypes (figure 4-28c).

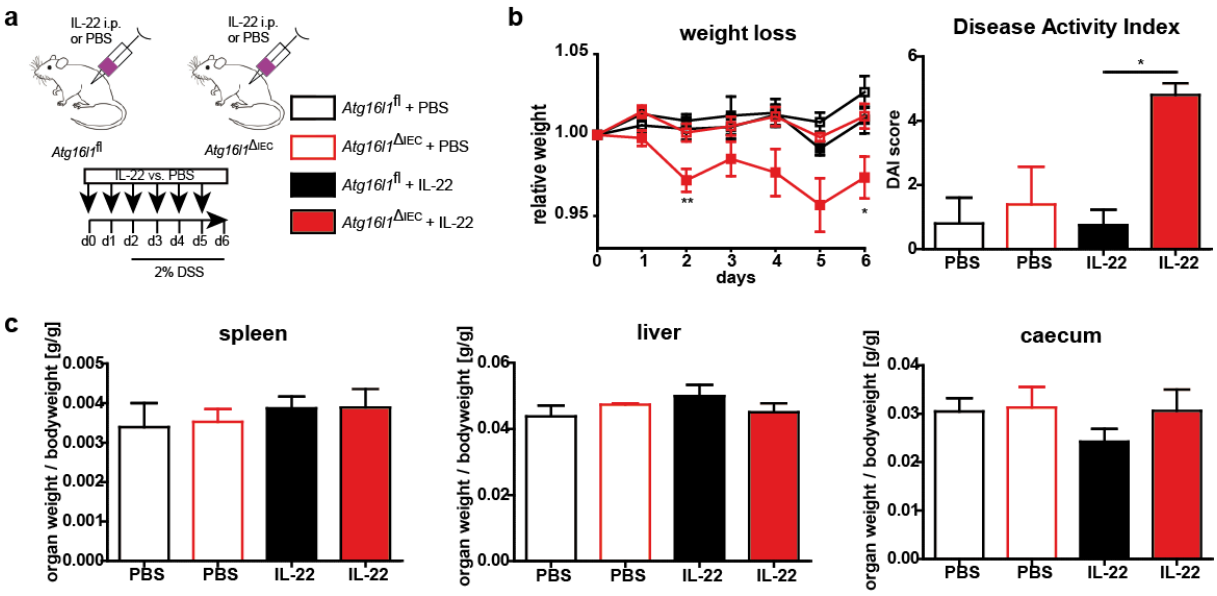


**Figure 4-28: Assessment of the disease course of *Atg16l1*$^{\Delta IEC}$ mice after 6 days of IL-22 treatment**

(a) Treatment scheme of IL-22 administration and DSS challenge. (b) Body weight relative to day 0 value of *Atg16l1*$^{\Delta IEC}$ and *Atg16l1*$^{fl}$ mice treated with either PBS or IL-22 (2 µg) i.p. every day for 6 days (n=5 each). 2% DSS were administrated from day 2 until day 6. Disease Activity Index at day 6 is shown in a separate plot. (c) Assessment of spleen, liver and caecum weight relative to bodyweight. Data are shown as mean ± s.e.m. and statistical analysis was performed with nonparametric Mann-Whitney *U* test. * p<0.05, ** p<0.01.

Next, intestinal inflammation levels were investigated by histological assessment. H&E staining revealed slightly elevated inflammation scores in the ileal mucosa of *Atg16l1*$^{\Delta IEC}$ mice compared to their wild-type controls which increased significantly upon IL-22 treatment (figure 4-29). To evaluate epithelial cell death in the mucosa, I performed TUNEL staining. TUNEL$^{+}$ cells accumulated in epithelial crypts of *Atg16l1*$^{\Delta IEC}$ mice but not in *Atg16l1*$^{fl}$ mice. IL-22 treatment had no effect on TUNEL$^{+}$ cell number in *Atg16l1*$^{fl}$ mice but increased number of dead epithelial cells in absence of *Atg16l1*. In line with this, γH2AX$^{+}$ cells were also enriched in *Atg16l1*$^{\Delta IEC}$ small intestinal crypts, especially with IL-22 treatment, underscoring the hypothesis of DNA damage accumulation in autophagy-deficient conditions. This finding was underpinned by accumulation of pTBK1$^{+}$ punctae in the crypts of IL-22-treated *Atg16l1*$^{\Delta IEC}$ mice but not of *Atg16l1*$^{fl}$ mice, suggesting activation of the cGAS/STING/pTBK1 pathway downstream of DNA damage.

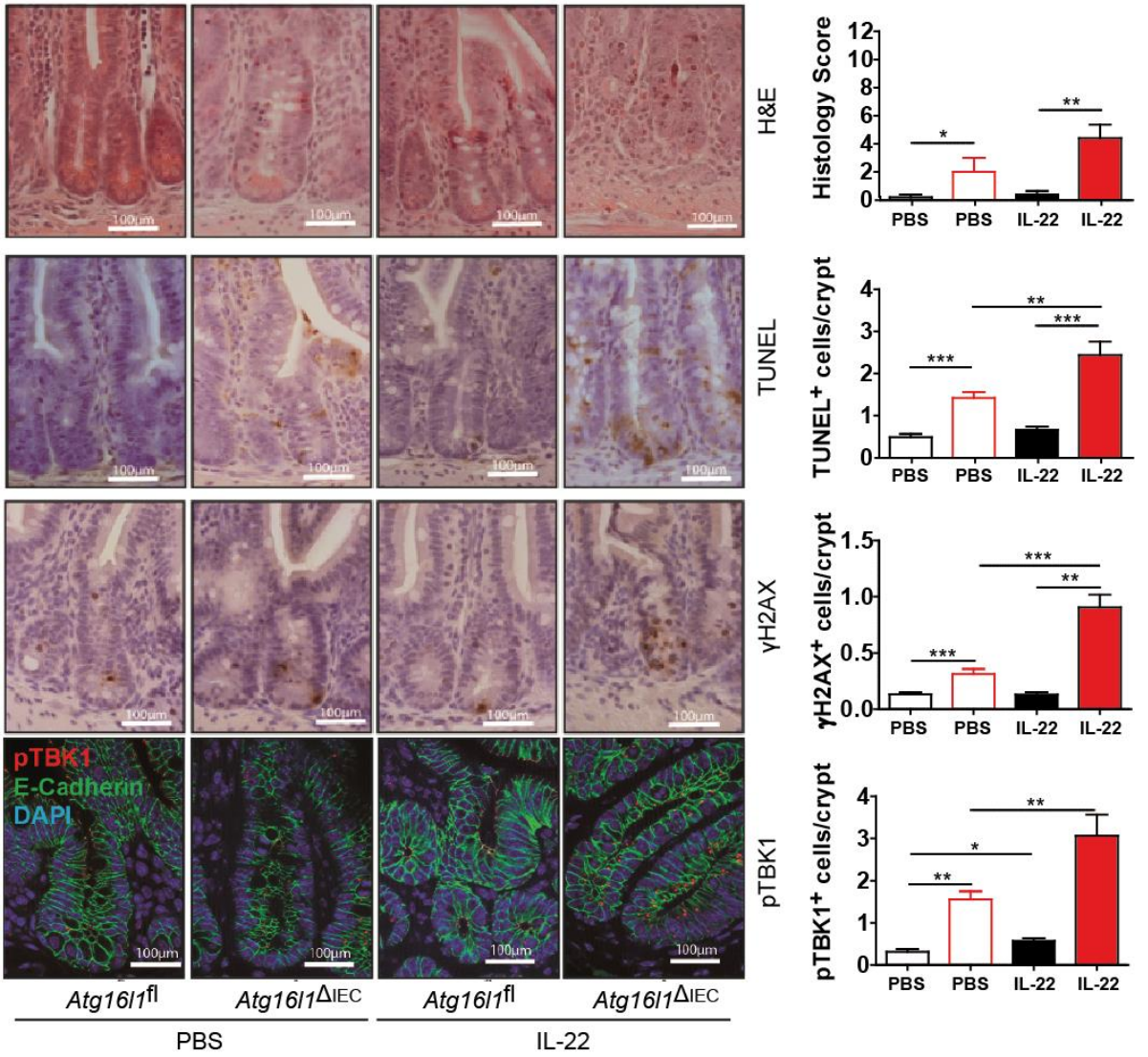


**Figure 4-29: Histological assessment of small intestinal tissue of *Atg16l1*$^{\Delta IEC}$ mice treated with IL-22 and 2% DSS**

Histological assessment of ileal tissue obtained from the experiment of figure 4-28. H&E staining including assessment of ileal inflammation score as well as TUNEL, anti-γH2AX IHC and anti-pTBK1 (2$^{nd}$ antibody: anti-rabbit Alexa Fluor 555, red) / anti-E-cadherin (2$^{nd}$ antibody: anti-mouse Alexa Fluor 488, green) / DAPI (blue) IF staining were performed (colour code as in figure 4-28). White bars indicate 100 µm. Data are shown as mean ± s.e.m. and statistical analysis was performed using nonparametric Mann-Whitney *U* test. * p<0.05, ** p<0.01, *** p<0.001.

Next, small intestinal crypts from the same experiment were collected and mRNA was isolated for gene expression analysis. In line with results from *ex vivo* organoid cultures, solely crypts derived from IL-22-treated *Atg16l1*$^{\Delta IEC}$ mice displayed an increased type I interferon (IFN-I) signature, ultimately resulting in *Tnf* expression (figure 4-30).

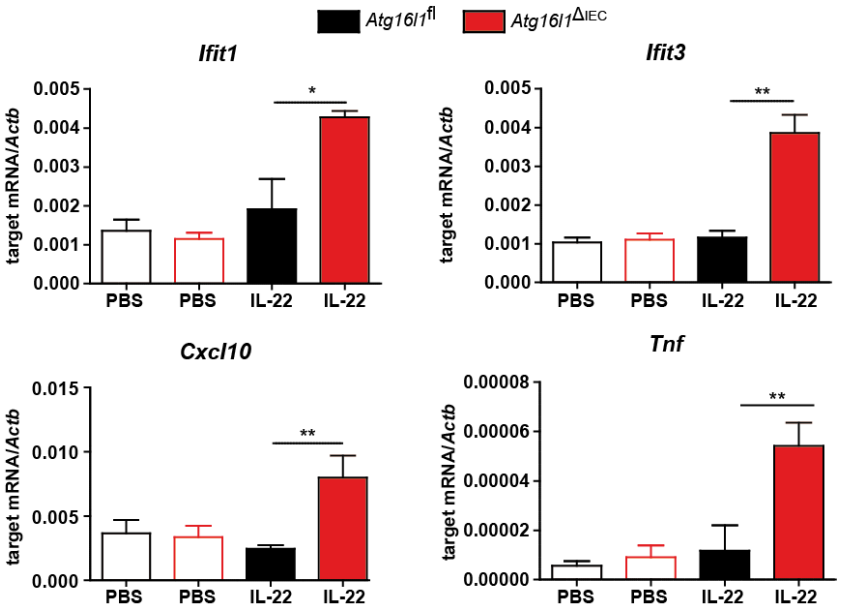


**Figure 4-30: IFN-I signature in small intestinal crypts derived from *Atg16l1*$^{\Delta IEC}$ mice treated with IL-22 and 2% DSS**

Gene expression analysis of small intestinal crypts obtained from the mice used in the experiment of figure 4-28. Expression levels of *Cxcl10*, *Ifit1*, *Ifit3* and *Tnf* were measured by SYBR® green qPCR and normalised to *Actb*. Data are shown as mean ± s.e.m. and statistical analysis was performed using nonparametric Mann-Whitney test. * $p<0.05$, ** $p<0.01$.

These results validated the role of IFN-I in IL-22-induced cell death in highly proliferating epithelial cells deficient for *Atg16l1*. To integrate the previous established role of ER stress resolution in IL-22 biology, *Atg16l1*$^{\Delta IEC}$/*Xbp1*$^{\Delta IEC}$ mice at the age of 8-10 weeks were subjected to i.p. rmIL-22 treatment for 13 days every other day before sacrifice (figure 4-31a, ***in vivo* treatment and sacrifice kindly performed by Dr. Markus Tschurtschenthaler and Dr. Joya Bhattacharyya, Cambridge**). This age was chosen as *Atg16l1*$^{\Delta IEC}$/*Xbp1*$^{\Delta IEC}$ mice develop spontaneous inflammation at the age of 8 to 12 weeks. H&E staining revealed spontaneous transmural ileal inflammation in *Atg16l1*$^{\Delta IEC}$/*Xbp1*$^{\Delta IEC}$ mice in line with previous reports (208). Administration of IL-22 aggravated spontaneous inflammation in *Atg16l1*$^{\Delta IEC}$/*Xbp1*$^{\Delta IEC}$ mice but not wild type controls, an effect predominantly localised in crypts (figure 4-31b). This was accompanied by increased focal anti-γH2AX staining and extranuclear anti-dsDNA punctae, indicating an accumulation of extranuclear damaged DNA in the epithelial crypts of *Atg16l1*$^{\Delta IEC}$/*Xbp1*$^{\Delta IEC}$ mice especially after IL-22 treatment (figure 4-31c). In line with finding from my organoid model, IL-22 induced accumulation of pTBK1 in absence of epithelial *Xbp1* and *Atg16l1 in vivo*.

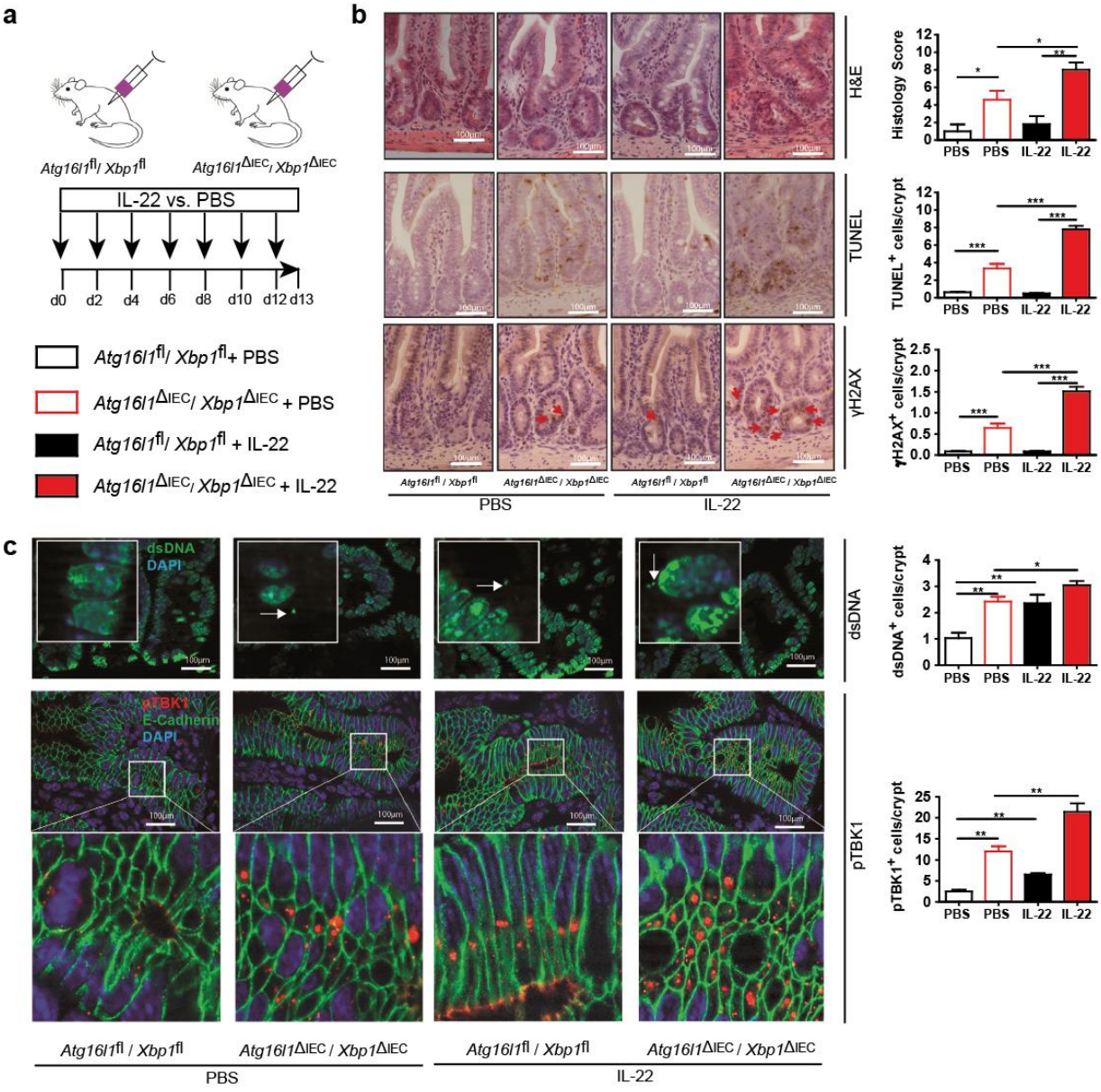


**Figure 4-31: IL-22 exacerbates spontaneous ileal inflammation in *Atg16l1*$^{\Delta IEC}$*/Xbp1*$^{\Delta IEC}$ mice**

(**a**) Treatment scheme of IL-22 i.p. injections over the course of 13 days. (**b**) Histological assessment of ileal tissues from the experiment in (a). H&E staining and assessment of ileal inflammation score, TUNEL staining and statistical analysis of TUNEL$^+$ cells. Anti-γH2AX immunohistochemistry staining and statistical analysis of γH2AX$^+$ cells. (**c**) Anti-dsDNA (2$^{nd}$ antibody: anti-mouse Alexa Fluor 488, green) / DAPI (blue) and anti-pTBK1 (2$^{nd}$ antibody: anti-rabbit Alexa Fluor 555, red) / anti-E-cadherin (2$^{nd}$ antibody: anti-mouse Alexa Fluor 488, green) / DAPI (blue) immunofluorescence staining with the statistical analyses of pTBK1$^+$ and dsDNA$^+$ punctae (white arrow indicate dsDNA$^+$ punctae) per crypt. White bars indicate 100 µm. Data are shown as mean ± s.e.m. and statistical analysis was performed using tnonparametric Mann-Whitney *U* test. * p<0.05, ** p<0.01, *** p<0.001.

I have shown that systemic IL-22 treatment renders aggravated small intestinal inflammation in *Atg16l1*$^{\Delta IEC}$ and *Atg16l1*$^{\Delta IEC}$/*Xbp1*$^{\Delta IEC}$ mice. We further delineated in *in vitro* experiments that excessive STING/IFN-I contributes to cell death phenotype in *Atg16l1*$^{\Delta IEC}$ organoids. We therefore postulated that IL-22-dependent exacerbation of small intestinal cell death and inflammation depends on IFN-I signalling. To test this I conducted another *in vivo* colitis study using *Atg16l1*$^{\Delta IEC}$ mice including an additionally treatment group which received neutralising antibodies that block the common downstream receptor interferon-α/β-receptor (IFNAR). Mice were treated with 2% DSS for the first 5 days of 10 days i.p. treatment with IL-22. Anti-IFNAR antibodies were administrated on day 0, 2, 4 and 6 (figure 4-32a), which partially reverted ileal inflammation on histological level in *Atg16l1*$^{\Delta IEC}$ mice challenged with IL-22, reflected by a significant lower histology score and significantly fewer TUNEL$^+$ cells (figure 4-32b).

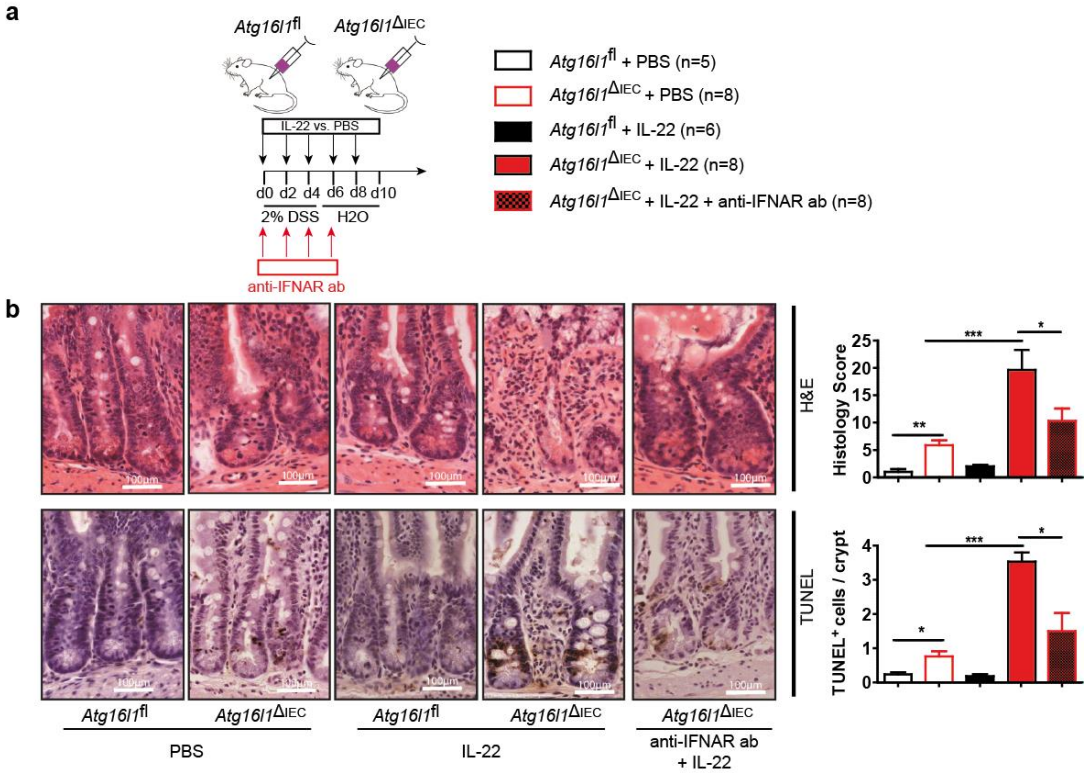


**Figure 4-32: Histological assessment of small intestinal tissue of *Atg16l1*$^{\Delta IEC}$ mice treated with IL-22, anti-IFNAR ab and 2% DSS**

(**a**) Treatment scheme of experimental colitis with 2% DSS, IL-22 i.p. injections and anti-IFNAR ab treatment over the course of 10 days. (**b**) H&E staining and assessment of ileal inflammation score, as well as TUNEL staining and statistical analysis of TUNEL$^+$ cells. White bars indicate 100 µm. Data are shown as mean ± s.e.m. and statistical analysis was performed using nonparametric Mann-Whitney *U* test. * p<0.05, *** p<0.001.

This suggests a pro-inflammatory role for IFN-I in the small intestine as downstream effectors of IL-22. As chronic inflammation in human IBD often affects colonic sites, especially in UC, I analysed colonic tissues obtained from the above-mentioned animal experiment for inflammatory phenotypes. *Atg16l1*$^{\Delta IEC}$ mice displayed a higher histological level of inflammation compared to their wild type controls. However, this was not affected by IL-22 administration (figure 4-33). Additional neutralisation of IFNAR did not rescue the genotype-dependent inflammatory phenotype in *Atg16l1*$^{\Delta IEC}$ mice. Therefore, the IL-22/STING/IFN-I axis is not critical for colonic mucosal homeostasis.

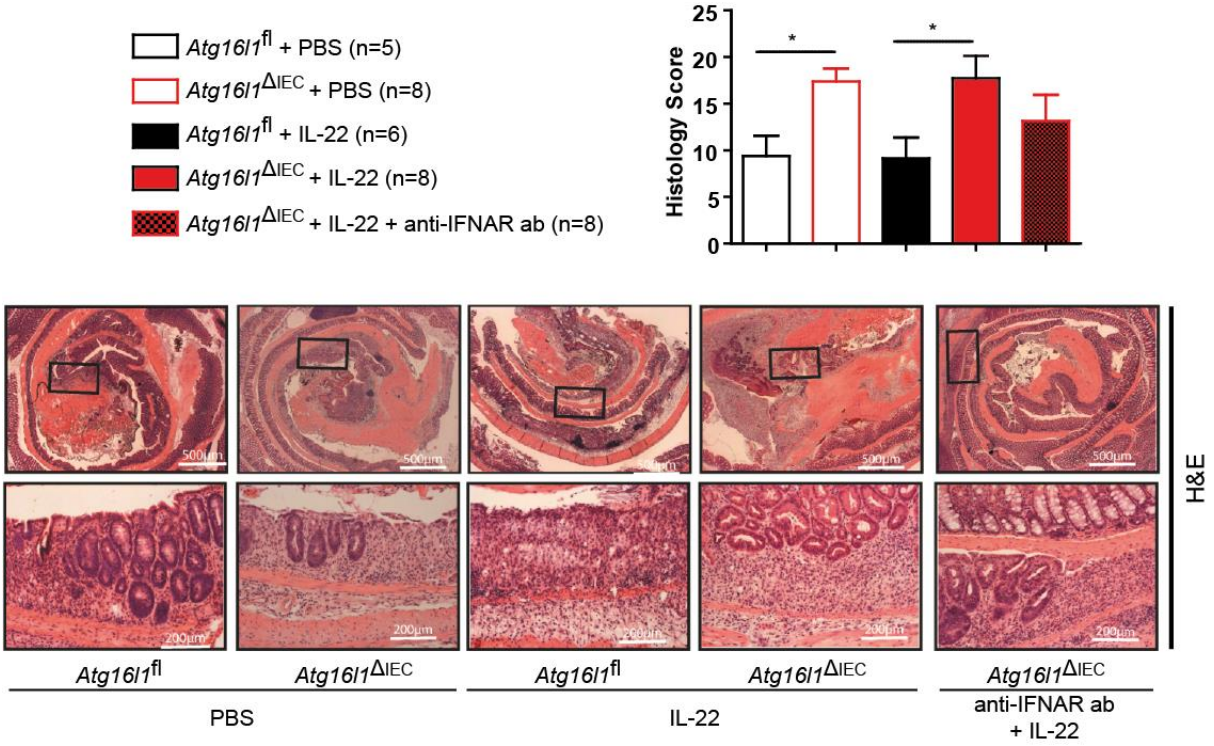


**Figure 4-33: Histological assessment of colonic tissue of *Atg16l1*$^{\Delta IEC}$ mice treated with IL-22, anti-IFNAR ab and 2% DSS**

H&E staining and assessment of colonic inflammation score from samples obtained from the experiment in figure 4-32. White bars indicate 500 µm or 200 µm, respectively. Data are shown as mean ± s.e.m. and statistical analysis was performed using nonparametric Mann-Whitney *U* test. * $p<0.05$.

In sum, these results establish a key role of *Atg16l1* and *Xbp1* in coordinating the dignity of IL-22 in the context of intestinal inflammation *in vivo*.

# 5 Discussion

In this study, I demonstrated that two IBD risk genes *ATG16L1* and *XBP1*, representing fundamental disease pathomechanisms autophagy and ER stress, direct the dignity of IL-22 exposure of the intestinal epithelium. In *in vitro* models, I showed that IL-22 surprisingly induced ER stress, which counters the initial hypothesis of an ER stress-ameliorating role of the IL-10 superfamily based on prior studies (162, 163). Furthermore, my results pointed towards a detrimental role of IL-22 in the context of *Atg16l1* deficiency, namely by necroptosis induction. Using a systemic approach, I identified the type I interferon axis as one of the distinct critical molecular signals in *Atg16l1* deficiency. Next, the cGAS/STING system was pinpointed down to facilitate IFN-I signals in response to cytosolic dsDNA after IL-22 treatment in our model. I discovered that IL-22 and IFN-I synergistically promote necroptosis. Lastly, I confirmed the *in vitro* results *in viv*o by demonstrating aggravated cell death and widespread ileal inflammation in *Atg16l1*$^{\Delta IEC}$ and *Atg16l1*$^{\Delta IEC}$/*Xbp1*$^{\Delta IEC}$ mice treated with IL-22, which was rescued by additional blocking of IFN-I signalling.

This work demonstrates a surprising link between pathophysiological principles of intestinal inflammation. As chronically impaired states of ER stress, autophagy and IL-22 have been implicated in a variety of human disorders including metabolic syndrome and cancer, the study has important consequences for a broad spectrum of human diseases beyond IBD. IL-22 plays as an essential role in orchestrating intestinal homeostasis. It is secreted from circulating immune cells and acts on intestinal epithelial cells to mount effective regenerative as well as antibacterial and antiviral cellular programs. With IL-22 currently under development by several companies in such indications (prominently by Genentech as IL-22Fc in IBD, metabolic syndrome and skin ulcer disease) the novel dichotomy of IL-22 biology shown in this thesis may have profound clinical implications. The critical findings of this work are as followed and addressed in this chapter:

(i) Proficient autophagy and ER stress resolution are critical prerequisites for IL-22 induced epithelial regeneration
(ii) IL-22 is an inducer of the cGAS/STING/IFN-I signalling loop, a process controlled by ATG16L1 and XBP1

(iii) Excessive IL-22-dependent STING activation due to deletion of *Atg16l1* and *Xbp1* results in necroptotic cell death via TNFα induction

## 5.1 Friend or foe? Exploring the dark side of IL-22

IL-22 is a pleiotropic cytokine, which exerts an important protective role on epithelial homeostasis by controlling proliferative capacity, but also acts on antimicrobial and antiviral gene expression (209). However, it has been shown that under certain conditions unrestrained IL-22 signalling may evoke tissue damage (210), impeding epithelial expansion *in vitro* (98) and may thus aggravate inflammatory responses (211).

### 5.1.1 IL-22/STAT3 induces ER stress

In this study, IL-22 indeed increased ER stress levels in both chemical (by tunicamycin, figures 4-1 to 4-3) and genetic (*Atg16l1*$^{\Delta IEC}$, *Xbp1*$^{\Delta IEC}$, figures 4-13 & 4-14) setting and thereby impeded epithelial regeneration as demonstrated by wound healing assays (figure 4-8). This was associated with increased expression of pro-inflammatory cytokines (figure 4-8). In a murine model of diminished mucosal IL-22 expression (*Il23r*$^{\Delta IEC}$), ER stress markers were inversely decreased (figure 4-4). Impaired autophagy led to uncontrolled UPR induction upon ER stress and therefore autophagy blockade mimicked the described phenomena of IL-22 (figure 4-12). Vice versa induction of autophagy by rapamycin dampened IL-22-dependent ER stress and reverted the inflammatory, anti-regenerative phenotype (figures 4-9 & 4-10). Interestingly, STAT3 activation was required for ER stress induction as chemical inhibition of STAT3 also repressed UPR induction and improved wound healing of IL-22 and tunicamycin challenged *in vitro* scratch wounds (figures 4-9 & 4-10). These findings evoked two hypotheses: First, secretory burden and replication pressure are the main drivers of IL-22 promoted ER stress as expression of antimicrobial peptides and cellular replication has been shown to be STAT3-dependent (56). Second, STAT3 is crucial in maintaining homeostasis of autophagy as phosphorylation of STAT3 (downstream of IL-22) has been implicated to be both inhibitory and activating on the autophagy machinery (165, 212, 213). Imbalanced autophagy homeostasis might lead to disinhibited ER stress after IL-22 challenge in the scenario of intestinal inflammation, though this aspect was not in this work's focus. However, STAT3

inhibition was not sufficient to repress ER stress-dependent induction of IL-8 (figure 4-9), one of the most known targets of NF-κB signalling, indicating that STAT3 is dispensable for this signalling branch.

Absence of ER stress and autophagy regulators like *Xbp1* or *Atg16l1* altered IL-22 signalling. These conditions exacerbated IL-22-induced pro-inflammatory cytokine signatures and signalling, alongside with cellular death induction (figures 4-13 to 4-15). In line this that, we challenged mice deficient for *Atg16l1* and *Xbp1* with systemic IL-22, leading to aggravated DSS induced (*Atg16l1*$^{\Delta IEC}$, figure 4-29) or spontaneous (*Atg16l1*$^{\Delta IEC}$/*Xbp1*$^{\Delta IEC}$, figure 4-31) ileal inflammation as evidenced by accumulation of TUNEL$^{+}$ dead epithelial cells. Interestingly, IL-22 selectively exacerbated small intestinal inflammation but not colitis in these settings (figures 4-28 & 4-33), which suggested a role for IL-22 in Crohn's-like phenotypes.

Importantly, IL-22Fc is under evaluation as a therapeutic drug in IBD due to its pro-regenerative role in general. This work, however, suggests a careful selection of IBD patients before treatment with IL-22Fc as genetic footprints of these patients are often associated with increased ER stress and defective autophagy, exemplified by the high frequency of the *ATG16L1*$^{T300A}$ variant (rs2241880) of around 55% in the European population (24). Under these circumstances, the results of the ongoing phase Ib trial of IL-22Fc in IBD should be carefully evaluated for safety.

Hence, I revealed novel interdependency between cellular stress characteristic for IBD and IL-22 signalling. IL-22 induced a pro-inflammatory signalling that synergistically enhanced and was driven by ER stress in intestinal epithelial cells. This effect was controlled by autophagy function and downstream STAT3. Vice versa, the outcome of IL-22 signalling in the intestinal epithelium depended on a functioning autophagic machinery and proper resolution of ER stress, adding new dimensions of so far described dichotomies in IL-22 biology (214).

### 5.1.2 Target specificity of the IL-10 superfamily?

Contrasting the role of IL-10 on epithelial ER stress in goblet cells (162), I did not observe induction of ER stress and cellular death in *Atg16l1* deficient organoids after IL-10 treatment (figure 4-5 & figure 4-16) although the experimental setups were identical. This discrepancy can be explained by the different site of inflammation (colon vs. small intestine). However, our working group demonstrated that IL-10

along with IL-19, another member of the IL-10 superfamily, failed to induce IFN-I signature as well as *Tnf* in colorectal adenocarcinoma cell lines and small intestinal organoids (data not shown). Hence, the activation of the STING axis was specific for IL-22 within the IL-10 superfamily. Additionally, IL-10 and IL-19 failed to phosphorylate STAT3 in equivalent doses to IL-22, underscoring the abovementioned role of STAT3 in this context (data not shown). These *in vitro* findings were confirmed in intestinal organoid models, which resemble the *in vivo* epithelium in morphological hallmarks like cellular polarity, crypt-villus architecture, cell type differentiation and cellular function (105). The specific can be explained by the unique downstream STAT3 of IL-22R1, one subunit of the receptor for IL-22, while the other subunit IL-10R2 is shared with other cytokines of the IL-10 superfamily like IL-10.

## 5.2 ATG16L1 and XBP1 orchestrate cGAS/STING-dependent induction of IFN-I

### 5.2.1 IFN-I in chronic inflammatory disease

Type I interferons (IFN-I) like interferon α (IFNα) or IFNβ are cytokines involved in anti-infective defence, in particular in antiviral response, and possess immunoregulatory functions like establishing the $T_h1/T_h2$ balance. Overall, type I interferons possess rather pro-inflammatory properties, which paradoxically are protective in specific diseases like viral hepatitis, multiple sclerosis and melanoma. In the intestinal epithelium, deletion of a central receptor of IFN-I signalling called interferon alpha/beta receptor (IFNAR) caused microbial changes which facilitate hyperproliferation of IECs and expansion of the Paneth cell niche (215). Hence, IFN-I signalling clearly contributes to the intestinal homeostasis.

Previous studies already attributed IFN-I as modulators of IL-22 signalling, switching the main downstream target from protective STAT3 to pro-inflammatory STAT1 activation (62). Moreover, *ATG16L1* has been linked to IFN-I signalling as *ATG16L1*-deficient cells exert RIG-I/melanoma differentiation antigen 5 (MDA5)/mitochondrial antiviral-signaling protein (MAVS)- or TRIF-dependent interferon induction (150, 216). This was associated with an improved survival in colorectal cancer as IFN-I upregulation promotes anti-tumour responses. In this work, we used a systemic approach using full mRNA transcriptome sequencing of organoids to determine

differentially regulated genes and signals upon IL-22 treatment in defective autophagy. Genes involved in innate immunity are amongst the top differentially expressed genes, with a big cluster around a type-I interferon signature (see figure 4-17). Indeed, IL-22 is a potent inducer of IFN-I in IECs as indicated by dose-dependent upregulation of downstream targets like *Ifit1*, *Ifit3* and *Cxcl10* in further *in vitro* experiments (figure 4-19). In line with this, canonical markers for IFN-I signalling (*Ifit1*, *Ifit3* and *Cxcl10*) were found up-regulated in *Atg16l1*-deficient IECs, particularly after IL-22 challenge (figure 4-18 & 4-19). Chemical inhibition of autophagy by bafilomycin mimicking this finding (figure 4-22). Interestingly, the WD40 domain was dispensable for *Atg16l1* to control ISG induction by IL-22 (figure 4-23). Type I interferons might therefore play a role in IL-22 driven inflammation in the context of autophagy defects. *In vivo* rescue of DSS-challenged and IL-22-treated *Atg16l1*$^{\Delta IEC}$ mice using recombinant antibodies against IFNAR supported this hypothesis (see figure 4-32). Together with the previous described findings on epithelial *Ifnar* (215), the increased levels of IFN-I in *Atg16l1* deficiency might contribute to the phenotype of *Atg16l1*$^{\Delta IEC}$ mice (less and hypomorphic Paneth cells, impaired epithelial regeneration) (153). To prove this, generation of *Atg16l1*$^{\Delta IEC}$/*Ifnar*$^{\Delta IEC}$ mice is required to evaluate the proposed phenotypical rescue. The experiment in figure 4-32, however, did not exclude that IFNAR neutralisation ameliorated colitis IL-22-independently, though epithelial deletion of *Ifnar* had no effect on colitis severity (215). Therefore, another control experiment including anti-IFNAR without IL-22 administration is necessary.

Other differentially regulated signalling pathways involve ER related functions and signals like response to ER stress and toxic substances, protein N-linked glycosylation and phospholipid biosynthetic processes as well as antigen processing of endogenous peptides (see figure 4-17).

### 5.2.2 Autophagy as a central regulator of STING signalling

One of the main questions raised from these findings addressed the intracellular signalling which linked IL-22 stimulation with IFN-I production. Two canonical signalling pathways were found interesting in this scenario: (i) the RIG-I/MDA5/MAVS pathway and (ii) the cGAS/STING/TBK1 cascade. Both intracellular systems converge in IFN-I production upon sensing of intracellular nucleic acids by RIG-I

(ssRNA and dsRNA) and cGAS (dsDNA), respectively. Recently, a newly established autophagy/ATG16L1-governed axis involving TLR4/TIR-domain-containing adapter-inducing interferon-β (TRIF) was found to be a critical contributor of IFN-I response in an IBD setting (150).

STING is the central integrator of cytoplasmic dsDNA mediated immune response which has been genetically and mechanistically implicated in anti-infective defence (217, 218) and in the pathophysiology of systemic lupus erythematosus (SLE) and diseases with lupus-like phenotypes (219). Indeed, excess of dsDNA contribute to the development of autoantibodies against dsDNA, one of the hallmarks and diagnostic criteria for SLE. Moreover, a few rare conditions like the Aicardi-Goutières syndrome associated with accumulation of dsDNA fragments due to massive DNA double strand breaks display excessive STING activation, ultimately leading to a type I interferonopathy (184) and immunosenescence of tissues (220). The mechanisms of STING-dependent IFN-I induction is currently under review as potential target in immunotherapy in cancer settings, as several studies infer critical roles of STING in coordinating innate immune response (121, 203).

Human cells harbouring hypomorphic ATG16L1 variants support induction of type I interferon response upon dsRNA challenge in a mitochondrial antiviral signalling (MAVS)-dependent fashion (216). Similarly, cytosolic dsDNA is an established inducer of ISG (115). Proteins involved in autophagy are crucial for removal of cytosolic dsDNA as deficiency in several autophagy related genes resulted in exacerbated dsDNA-mediated activation of stimulator of interferon genes (STING)-dependent ISG induction (221). Here, *Mda5* knock-out did not affect ISG induction by IL-22 whereas *Tmem173* depletion in organoids completely diminished ISG induction (figure 4-19). Interestingly, IL-22 induces *Tmem173*/STING to enhance ISG induction (figure 4-21), which is in line with results reported in colonic organoids (58). IL-22 treatment enhanced downstream phosphorylation of TBK1 by STING in *Atg16l1*-deficient organoids and epithelial cells *in vitro* and *in vivo*. These results point towards the cGAS/STING system as the critical link between IL-22 signalling and IFN-I production. Another IFN-I activating signalling branch in context of defective autophagy has been described for the interdependency of STING and Atg9a in fibroblast models (222). To ultimately prove the role of STING in *Atg16l1* deficiency, the generation of *Atg16l1*$^{\Delta IEC}$/*Tmem173*$^{\Delta IEC}$ mice to intensively study the signalling in

organoids and demonstrate a blunted IFN-I signature would be necessary. Surprisingly, the RIG-I/MDA5/MAVS cascade does not play a major role in the context of inflammation, contrasting the described *ATG16L1*$^{T300A}$-dependent role in colorectal cancer (216).

The excessive increase of cGAS/STING response may be important for either removal of active STING signalling-complexes (222) or involved in the generation of the endogenous activation principle by aggravating the ER stress-mitochondria axis, which in turn leads to the induction of ROS- dependent nuclear DNA damage, as described previously (210). Indeed, STING signalling has been linked to ER stress and selective autophagy of stressed ER membrane (ER-phagy/reticulophagy) as a compensatory mechanism (120). For instance, Prabakaran *et al* showed that p62-dependent autophagy restrains overt STING/TBK1/IRF3-dependent IFN-I signals be p62-mediated autophagic degradation of STING (223). STING activation also promotes a kind of cell death referred to as lysosomal cell death upon translocation to lysosomal membrane (224), indicating that trafficking of STING is crucial for cellular fate. Impairment of this lysosomal trafficking linked to insufficient autophagy might also affect STING signalling under this aspect. In our model, loss of autophagic capacity could be causative for uncontrolled STING-dependent ER stress due to insufficient degradation of STING. Surprisingly, *Xbp1* deficiency led to a completely blunted ISG signal upon IL-22 and bafilomycin treatment (data not shown), indicating that either XBP1 specifically controls the STING/IFN-I cascade, that STING-dependent signals wear out under chronic ER stress conditions or that compensatory autophagy/reticulophagy lead to degradation of ER resident STING. This autophagy-STING axis will hence be explored more densely due to new insights into the role of selective autophagy in the IBD context. Furthermore, the role of the STING axis is under extensive investigation as potential therapeutic target in the context of immunotherapy in cancer settings (122, 225).

dsDNA is the canonical activator of cGAS, which in turn produces cyclic guanosine monophosphate-adenosine monophosphate (cGAMP) as second messenger to activate STING (118). This pathway plays a critical role against viral invasion like HSV infections (218), leading to intracellular release of viral dsDNA. In this setting, the IFN-I production acts as a tissue-protective feedback mechanism to induce cell death in order to restrain viral replication. Indeed, IL-22 treatment leads to increased

accumulation of cytosolic dsDNA in *ATG16L1*-deficient cells (figure 4-20). The potential origin of fragmented dsDNA in the cytosol is either the nucleus or the mitochondrion. Release of dsDNA from the nucleus has been described upon massive DNA damage induction, e.g. via irradiation or genetic defect in DNA repair genes (114). Here, IL-22 treatment increased γH2AX as a DNA damage marker in *Atg16l1*/*ATG16L1*-knockout cells *in vivo* and *in vitro* (figures 4-19 & 4-29). Increased proliferation and thus increased speed of DNA replication, making amplifying cells prone to replication errors, could explain increase of DNA double strand breaks by IL-22 treatment. Recently, autophagy has been reported to be crucial in removing accumulated DNA fragments (221), which suggest that loss of *Atg16l1*/*ATG16L1* resulted in increased γH2AX signals. Beyond this, ER stress also affect DNA quality as shown in this work (figure 4-31). These findings point towards a possible rendezvous between genomic integrity and ER stress resolution and autophagic flux, respectively.

A role for mitochondrial DNA in STING activation needs to be discussed as well. Insufficient removal of dysfunctional mitochondria by mitophagy is a critical contributor to several neurodegenerative and inflammatory conditions. In the context of intestinal inflammation, previous studies described an accumulation of damaged mitochondria in *Atg16l1*-deficiency IECs (154), which makes the possibility of relevant leakage of dsDNA to stimulate STING conceivable. To address this, ethidium bromide-dependent methods (226) or viral transfection of restriction endonucleases (227) to deplete mitochondrial DNA (mtDNA) in *ATG16L1*-deficient vs. proficient cells are necessary.

## 5.3 STING drives TNFα induction and necroptosis in *Atg16l1* deficiency

In this work, IL-22 induced TNFα (figure 4-25), one of the most central cytokine and therapeutic target in intestinal inflammation (228). This induction was dependent on STING as *Tmem173*$^{-/-}$ organoids displayed diminished TNFα induction after IL-22 treatment (figure 4-24) while IFN-β administration restored *Tnf* expression (figure 4-25). One effect of TNFα is the induction of cellular death in inflammatory and neoplastic settings (228). While apoptosis was firstly described as the main cell death mode and implicated as critical contributor to several inflammatory conditions,

growing evidence point towards a more subtle regulation and differentiation of cell death involving other modes like necroptosis and their implications for inflammatory diseases (229). Necroptosis, “programmed necrosis” of cells, is characterised by receptor-mediated signalling, leading to leakage and rupture of the cellular membrane and reminiscing a necrotic process. Receptor interacting protein kinase 1 and 3 (RIPK1, RIPK3) and mixed lineage kinase domain-like (MLKL) are the canonical regulators of necroptosis:

RIPK1 is a serine/threonine kinase which associates to transmembrane death receptor complexes including tumour necrosis factor receptor 1 (TNFR1) (230), Fas-associated protein with death domain (FADD) (231) and tumour necrosis factor receptor type 1-associated DEATH domain protein (TRADD) (230) and phosphorylates downstream RIPK3 to assemble the so-called necrosome to achieve necroptosis induction by TNFα (232). Deficiency of *Ripk1* in mice is lethal, whereas transgenic mice carrying a Ripk1 D138N variant leading to diminished activity of the kinase domain (“kinase dead Ripk1”) were viable and protected from TNFα- and poly(I:C)-induced necroptosis *in vitro* and *in vivo* (168). In contrast, *Ripk3* deficiency prevents necroptosis associated cellular and embryonic death in mice deficient for FADD (233), FLIP (234) or caspase 8 (235). MLKL, the downstream master regulator of necroptosis, works as the indispensable downstream target of the necrosome to form cellular pore complexes, which permeabilise the cell after translocation to the cellular membrane (236, 237). Dysregulated necroptosis is an important driver of epithelial cell death in the gut and -as such- is an emerging pathophysiological principle of chronic inflammatory states including human IBD (238-240). However, *Tnf* deletion in mice did not lead to complete resolution of the necroptotic phenotype in *FADD*-deficient animals, particularly in the small intestinal epithelium (240). Thus, additional co-stimulatory pathways besides presence of TNFα are necessary for necroptosis induction. Interestingly, in macrophages type I interferons are critical for induction of RIPK1/RIPK3-dependent necroptosis after bacterial infection (241). In this work, treatment of *Ripk3*-deficient or *Ripk1*$^{D138N}$ organoids with IL-22 and bafilomycin led to unaltered cell death induction versus wild-type controls but significantly reduced cell death induction in *Mlkl* knockout organoids (figure 4-26). *Tmem173*$^{gt}$ organoids were protected from IL-22 and bafilomycin induced cell death (figure 4-27). Thus, the IL-22-dependent STING/IFN-I/TNFα loop induces RIPK1/RIPK3-independent necroptosis in the context of impaired autophagy. To

prove that necroptosis induction in this scenario is dependent on TNFα, administration of neutralising anti-TNFα antibodies to IL-22-treated *Atg16l1*-deficient organoids is required. The expected outcome would be cell death prevention by TNFα neutralisation. Based on these findings, excessive cell death in the ileal intestinal crypts in *Atg16l1*$^{\Delta IEC}$ mice by IL-22 treatment is presumably necroptosis, while the absolute proof, e.g. by rescue using necroptosis inhibitors *in vivo* or generation of *Atg16l1*$^{\Delta IEC}$/*Mlkl*$^{\Delta IEC}$ mice, is still pending.

It is conceivable that a switch to excessive IFN-I and TNFα induction and subsequent programmed cell death may be protective in viral infections, conditions in which autophagy and resolution of ER stress are often impaired (242-244). These results therefore add to recent findings about the role of autophagy proteins acting as critical switches for cellular death modalities (245). Most significantly, the role of *Atg16l1* in preventing epithelial necroptosis was confirmed in the context of intestinal viral infections and graft versus host disease (GvHD) very recently using similar biomedical approaches like studying *Atg16l1*$^{\Delta IEC}$ mice and organoids (94). In detail, mice with IEC-specific *Atg16l1* deletion succumbed to allogenic hematopoietic stem cell transplant as well as to DSS colitis after murine norovirus (an ssRNA virus) infection (94). This goes along with Paneth cell loss and TNFα-dependent cell death, which was rescued with neutralising anti-TNFα antibodies (94). The viability of organoids was rescued by necrostatin-1 or knockdown of *Ripk3* and *Mlkl* in *Atg16l1* deficiency while administration of the pan-caspase inhibitor Z-VAD-FMK skewed cellular fate towards cell death, indicating that necroptosis is the critical cell death mode in these scenarios (94). Mitochondrial dysfunction in autophagy defective cells are assumed to be causative for necroptotic death, adding to the theory that *Atg16l1* governs mitochondrial quality by mitophagy in order to prevent mitochondria associated cellular damage, e.g. through ROS production (154). Other programmed cellular death modes include pyroptosis (246) (inflammasome/caspase 1-mediated cell death), ferroptosis (247) (iron-dependent cell death, characterised by the accumulation of lipid peroxides), paraptosis (248) (insulin-like growth factor 1 receptor (IGF-1R)-inducible cell death) and parthanatos (249) (PAR-mediated cell death) were not addressed in this work. However, their role in intestinal inflammation is enigmatic and therefore would be interesting to study. In particular, inflammasome activation and associated cell death has been proposed to be dependent on

autophagy (250), however robust evidence towards the role of IBD risk genes like *ATG16L1* on pyroptosis in IEC are still lacking.

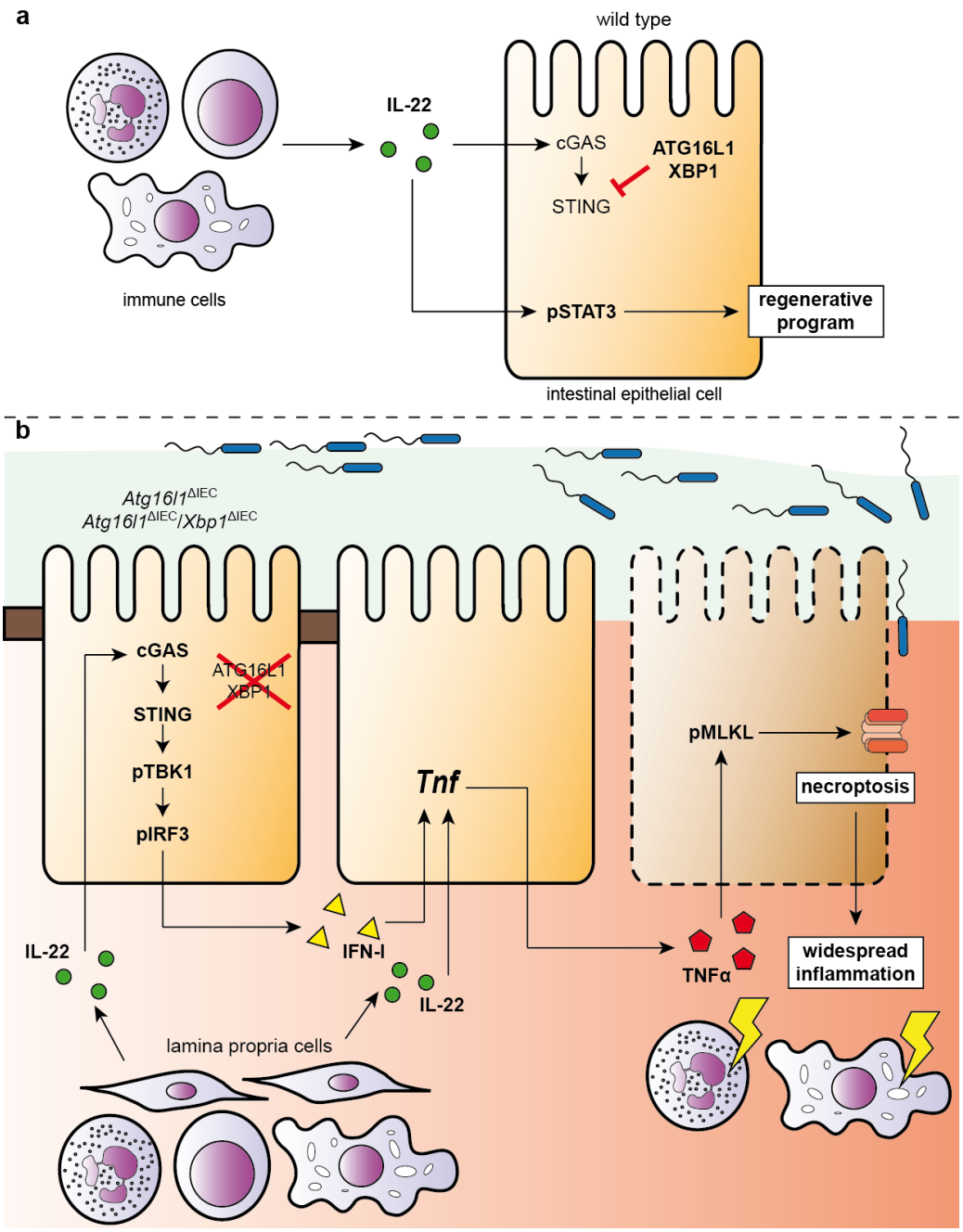


**Figure 5-1: Proposed model based on this work**

(**a**) Immune cell-derived IL-22 activates a regenerative program in wild type IEC. The cGAS/STING axis is addressed as well; however, ATG16L1 and XBP1 are protectively controlling excessive downstream signalling. (**b**) Genetic disruption of autophagy or ER stress in the intestinal epithelium as in *Atg16l1*$^{\Delta IEC}$ and *Atg16l1*$^{\Delta IEC}$ /*Xbp1*$^{\Delta IEC}$ mice disinhibited IL-22-dependent IFN-I induction, which synergistically with IL-22 promote TNFα production. This ultimately leads to MLKL-dependent necroptosis, loss of barrier integrity and subsequent widespread inflammation.

In sum, *Atg16l1* controls IL-22-dependent STING signalling to prevent TNFα-induced epithelial necroptosis.

## 5.4 In the end: New insights into IBD biology or just another mouse study?

In this thesis work, most of the experiments shown were *in vivo* studies in mice or *ex vivo* investigations conducted in murine intestinal organoids. The findings were consistent in the chosen models and suggestive for the transferability into IBD, however I did not show studies on primary human (inflamed) material like biopsies or organoids in this work. Hence, I will discuss the relevance of this work for human IBD in the following.

The availability of organoids cultures provides a new tool for *in vitro* research of epithelial biology with hallmarks of *in vivo* tissue (105). Indeed, the feasibility of long-term culture and storage of organoids reduced the number of sacrificed mice for tissue collection purposes. Despite the relatively high costs for organoid cultures at the current stage, this will help performing more sustainable science. Another advantage is the elegant translation into human IBD settings, as organoids can be derived from human samples (like endoscopic biopsies or surgical specimens) (108) to study human biology in general or personalised disease signatures in particular. However, despite the similarities to the *in vivo* tissues, organoids are still highly artificial systems depending on extrinsic stimuli and growth factors. The culture lacks the interplay with luminal microflora and basolateral crosstalk with lamina propria cells like immune cells, fibroblasts/fibrocytes and neuronal cells. Co-cultures with different cellular types may provide scenarios closer to the *in vivo* situation but, however, will not replace the scientific proof for the *in vivo* biology. Due to ethical aspects, this can only be pursued by animal experiments, e.g. using genetically modified mice.

In this work, the *in vivo* experiments delivered settings of intestinal inflammation, by either genotype-driven spontaneous ileal inflammation (*Atg16l1*$^{\Delta IEC}$/*Xbp1*$^{\Delta IEC}$) reminiscing CD biology (figure 4-31) or experimental enterocolitis using DSS in drinking water (figure 4-28). DSS is a commonly used agent for induction of colitis in rodent models (251), which is not absorbed by mucosa. Hence, concentration

gradient of DSS along the gastrointestinal tract were found (252), which explains the (distal) colon as the major affected site of inflammation, reminiscing UC disease pattern. Though, the small intestine has been shown to be more subtly but significantly affected by DSS (252). Hence, the purpose of the induction of DSS enterocolitis was to enhance disease burden rather than to specifically provoke inflammation in the small intestine. Still, DSS models are very artificial and only partially reflect human IBD.

Genetic knockout of disease-related genes is a commonly used strategy to approximate human diseases in animal models. In this work, I used conditional knockouts to study the role of IBD risk genes in the intestinal epithelium. Using the Cre-Lox recombination (253), an essential exon of the gene of interest is removed, resulting in loss of the full protein. Here, the villin promotor was chosen to target the intestinal epithelium as IECs highly express villin (254). However, renal tube cells display villin expression as well (254). This needs to be considered as potential off-target effect for *in vivo* studies in this system. To investigate whether the human risk variant *ATG16L1*$^{T300A}$ is responsible for the same phenotype as *Atg16l1* deletion in mice or not, mice with the CD-associated T300A variant knock-in were generated (153). Indeed, these mice displayed a similar phenotype with distorted Paneth cell morphology and function in comparison to *Atg16l1*$^{\Delta IEC}$, which is explained by caspase-3-dependent degradation of mutated ATG16L1 (204). Similarly, *Xbp1* depletion in mice approximate the rare IBD risk polymorphisms of *XBP1* (e.g. rs35873774) which result in hypomorphic XBP1 function (93).

The deleterious role of IL-22 in the context of defective autophagy and ER stress needs to be shown in human samples, e.g. in patient biopsy-derived organoids. Stratification of these ileal or colonic organoids for *ATG16L1* and *XBP1* genotype could provide optimal settings for studying IL-22-dependent responses. The potential drug IL-22Fc/UTTR1147A needs to be tested for pharmacokinetics/-dynamics and potential off-target effects in humans. Furthermore, application of UTTR1147A in comparison to recombinant murine IL-22 in the used animal models of this work would be interesting. If these results can confirm the murine findings of IL-22 signalling, genotyping for IBD risk genes will be a prediction tool for response to IL-22Fc/UTTR1147A.

Overall, this study allows new insights in to the biology of intestinal inflammation in mice, with a high degree of transferability into chronic inflammation in humans as in IBD. Indeed, our working group demonstrated high concordant correlations of *IL22*, *TNF*, *MLKL* and ISG mRNA expression and inverse correlation to positive therapy response in sigmoid biopsies from IBD patients (cite Paper). Still, more studies are necessary to confirm the definite role of the proposed mechanisms in IBD patients.

## 5.5 Future prospects

In this study, I put forward a model whereby under conditions of intestinal injury, genetic disease susceptibility in the integrated autophagy/UPR pathway turns a regenerative IL-22-dependent response into a vicious circle of tissue damage and inflammation. The experiments shown raise another plethora of yet unsolved questions towards the biology of this link. As mentioned before, the creation of *Atg16l1*$^{\Delta IEC}$/*Tmem173*$^{\Delta IEC}$, *Atg16l1*$^{\Delta IEC}$/*Ifnar*$^{\Delta IEC}$ and *Atg16l1*$^{\Delta IEC}$/*Mlkl*$^{\Delta IEC}$ mice are useful to ultimately prove the proposed link between autophagy and STING/ISG-dependent necroptosis induction in synergy with IL-22.

In colorectal cancer patients, the *ATG16L1*$^{T300A}$ variants is associated with increased IFN-I signalling and improved survival (216). On the contrary, the IL-22 is a strong driver of carcinogenesis (78). Thus, the role of IL-22 in *Atg16l1* deficiency on inflammatory-driven carcinogenesis would be interesting to study. Intraperitoneal administration is not feasible due to the duration of classical carcinogenesis models using azoxymethane (AOM) and DSS (255) and the high costs of recombinant murine IL-22. Therefore, the *Atg16l1*$^{\Delta IEC}$ mice need to be crossed with either IL-22 overexpressing transgenic mice or mice deficient for *Il22bp* (resulting in disinhibited IL-22 signalling) before undergoing AOM/DSS regimens.

As described above, immunogenic cell death modes like necroptosis and pyroptosis play important roles in IBD pathophysiology. After providing evidence of autophagy controlled necroptosis in the intestinal epithelium, the role of autophagy in inflammasome activation in intestinal epithelial cells needs to be addressed in further studies. For instance, the IBD risk gene *LRRK2* encodes for the autophagy-related protein LRRK2 interacting with NLRC4 (256). STING and AIM2, a sensor for cytosolic dsDNA involved in inflammasome formation, are reciprocally regulated (257). Thus, we will study the role of different inflammasome proteins in *Atg16l1* deficient IEC.

Another point of interest is the hitherto underestimated role of DNA damage in the pathogenesis of intestinal inflammation. In a genetic mouse model of massive accumulation of DNA damage in the intestinal epithelium and subsequent upregulation of the STING/IFN-I axis, *Rnaseh2b* controls excessive inflammation by modulating STING signalling in a p53-dependent fashion in preliminary results. Interestingly, increased intestinal inflammation level was associated with p53-dependent tumour suppression in cancerogenesis models, whereas additional depletion of p53 in the intestinal epithelium resulted in spontaneous tumour formation. In this context, *Atg16l1* and *Xbp1* control p53-related cellular responses in ongoing experiments in *Atg16l1*$^{\Delta IEC}$/*Rnaseh2b*$^{\Delta IEC}$ and *Xbp1*$^{\Delta IEC}$/*Rnaseh2b*$^{\Delta IEC}$ mice and organoids. These finding give rise to several follow-up experiments addressing the molecular mechanism of ATG16L1/XBP1/STING interactions in inflammatory and neoplastic conditions.

# 6 Summary

Inflammatory bowel diseases (IBD) are playing a more and more important socioeconomic role due to increasing incidences. However, the detailed pathophysiology is not fully understood, yet. This is reflected by the yet unsatisfactory treatment efficiency of even the most modern drugs under development. Genetic factors, environmental triggers, lifestyle and microbial signals are interactively contributing to the development of IBD.

Coding variants of the IBD risk genes *ATG16L1* and *XBP1* have been associated with defective autophagy, deregulation of endoplasmic reticulum (ER) function and impaired pathogen clearance. IL-22 is a barrier protective cytokine by inducing regeneration and antimicrobial responses in the intestinal mucosa.

Here, we show that *XBP1* and *ATG16L1* critically orchestrates beneficial IL-22 signalling in intestinal epithelium. IL-22 stimulation physiologically leads to transient ER stress, intracellular release of dsDNA and subsequent activation of the cGAS-STING pathway. Loss of *ATG16L1* exacerbates IL-22-induced ER stress and augments STING-dependent IFN-I responses in IECs. IFN-I amplifies epithelial TNFα production downstream of IL-22 and leads to necroptotic cell death. *In vivo,* IL-22 treatment in *Atg16l1*$^{\Delta IEC}$ mono- and *Atg16l1*$^{\Delta IEC}$/*Xbp1*$^{\Delta IEC}$ double knockout mice potentiates endogenous ileal inflammation and causes widespread necroptotic epithelial cell death, which can be partially rescued by neutralising the IFN-I signalling using anti-IFNAR antibodies. Under conditions of chronic intestinal inflammation and with clear genetic “hits” to the autophagic and ER stress machinery like in human IBD, however, such a fate of IL-22 signals may crucially contribute to a vicious circle of tissue damage and inflammation.

# 7 Zusammenfassung

Chronisch-entzündliche Darmerkrankungen (CED) spielen auf Grund einer steigenden Inzidenz eine zunehmende sozioökonomische Rolle mit einer wachsenden Belastung für das Gesundheitssystem. Dennoch ist die Pathophysiologie bislang noch nicht vollständig verstanden, was sich in der aktuell insgesamt noch unzufrieden-stellenden medikamentösen Therapie widerspiegelt. Zur Entwicklung einer CED spielen interaktiv sowohl genetische Faktoren als auch Umweltfaktoren, der Lebensstil und mikrobielle Signale eine bedeutende Rolle.

Verschiedene kodierende Varianten der CED-Risikogene *ATG16L1* und *XBP1* sind assoziiert mit defekter Autophagie, einer Dysregulation der Funktion des Endoplasmatischen Retikulums (ER) sowie einer gestörten Abwehr gegen Pathogene. Demgegenüber wird das Interleukin (IL)-22 in der intestinalen Mukosa als Barriere-schützendes Zytokin, welches die epitheliale Regeneration und die antimikrobielle Antwort in der intestinalen Mukosa vermittelt, gebildet.

In dieser Arbeit wurde gezeigt, dass *ATG16L1* und *XBP1* kritische Regulatoren dieses protektiven IL-22-Signals sind. IL-22-Stimulation führt zu physiologischem, transientem ER-Stress, einer intrazellulären Freisetzung von doppelsträngiger Desoxyribonukleinsäure und nachfolgender Aktivierung des cGAS-STING-Signalweges. Eine Depletion von *ATG16L1* führt zu einer Exazerbation des IL-22-induzierten ER-Stress und verstärkt die STING-abhängige Typ-I-Interferon-Antwort in intestinalen Epithelzellen. Typ-I-Interferone amplifizieren die IL-22-abhängige epitheliale Produktion von Tumornekrosefaktor-α (TNF-α), welche schließlich zu nekroptotischem epithelialen Zelltod führt. *In vivo* potenziert eine IL-22-Behandlung von *Atg16l1*$^{\Delta IEC}$- und *Atg16l1*$^{\Delta IEC}$/*Xbp1*$^{\Delta IEC}$-Mäusen deren endogene Inflammation im Ileum, welche mit einer massenhaften Nekroptose von intestinalen Epithelzellen verbunden ist. Neutralisierung des Typ-I-Interferon-Signals durch einen anti-IFNAR-Antikörper kann diese Inflammation teilweise eindämmen. Im Kontext von chronischen intestinalen Entzündungen und einer klaren genetischen Affektion der Autophagie-ER-Stress-Achse wie bei einer CED ist eine solche Effektumkehr des IL-22-Signals ein potenzieller Faktor, welcher den Teufelskreislauf von Gewebsschäden und Inflammation unterhält.

# 8 Appendix

## 8.1 Buffers and Media

**Table 7: Table of used buffers**

| Devices | Composition | Company |
|---|---|---|
| 10 x TBS | 200 mM Tris (pH 7.6)<br>1,37 M NaCl | - |
| 10 x TGS buffer | 25 mM Tris (pH 8.3)<br>92 mM glycine<br>0.1 % SDS | BioRad (Munich, Germany) |
| 2 x DLB buffer | 20 mM Tris (pH 7.4)<br>2 % SDS | - |
| 5 x SDS loading dye | 250 mM Tris (pH 6.8)<br>10 % SDS<br>50 % glycerol<br>500 mM DTT | - |
| anode buffer 1 | 30 mM Tris<br>20 % methanol | - |
| anode buffer 2 | 300 mM Tris<br>20 % methanol | - |
| cathode buffer | 25 mM Tris<br>40 mM 6-aminocaproic acid<br>20 % methanol | - |
| citrate buffer | 11 mM Citric acid (pH 6.0) | - |
| phosphate-buffered saline (PBS) | 1 mM KH2PO4<br>155 mM NaCl<br>3 mM Na2HPO4-7H2O | Gibco (Darmstadt, Germany) |
| separation buffer | 1.5 M Tris (pH 8.8)<br>0.4 % SDS | - |
| stacking buffer | 0.5 M Tris (pH 6.8)<br>0.4 % SDS | - |
| stripping buffer | 2 % SDS<br>62.5 mM Tris (pH 6.8) | - |
| T/TBS | 1 x TBS<br>0.1 %Tween20 | - |

**Table 8: Table of used media**

| Media | Company |
|---|---|
| Advanced DMEM/F12 medium | Gibco (Darmstadt, Germany) |
| CryoStor™ CS10 | StemCell Technologies (Cologne, Germany) |
| DMEM cell culture medium | Gibco (Darmstadt, Germany) |
| Hank´s Balanced Salt Solution (HBSS) | Gibco (Darmstadt, Germany) |
| IntestiCult™ Organoid Growth Medium (Mouse) | StemCell Technologies (Cologne, Germany) |
| MEM cell culture medium | Gibco (Darmstadt, Germany) |
| RPMI cell culture medium | Gibco (Darmstadt, Germany) |

## 8.2 Kits

**Table 9: Table of used kits**

| Kit | Company |
|---|---|
| ApopTag® Plus Peroxidase *In Situ* Apoptosis Detection Kit | Merck Millipore (Darmstadt, Germany) |
| DC™ Protein Assay | Bio-Rad (Munich, Germany) |
| IL-8 Human ELISA Kit | ThermoFischer Scientific (Darmstadt, Germany) |
| Maxima H Minus First Strand cDNA Synthesis kit | ThermoFischer Scientific (Darmstadt, Germany) |
| HiSeq Reagent Kit v4 (2 x 150 bp) | Illumina (San Diego, USA) |
| RNeasy kit | Qiagen (Hilden, Germany) |
| Vectastain Elite ABC Kit Rabbit IgG | Vector Labs (Peterborough, United Kingdom) |

## 8.3 Reagents and chemicals

**Table 10: Table of used reagents and chemicals**

| Reagent/chemical | Company |
|---|---|
| 1 % Eosin solution | Roth (Karlsruhe, Germany) |
| 10 % Formalin | Sigma Aldrich (Munich, Germany) |
| 10 x SYBR® Safe DNA gel stain | Life Technologies (Darmstadt, Germany) |
| 30 % Bis-acrylamide (37.5:1) | Bio-Rad (Munich, Germany) |
| 4-(2-hydoxyethyl)-1-piperazineethanesulfonic acid (HEPES) | Sigma Aldrich (Munich, Germany) |
| 5 x Green GoTaq® Reaction Buffer | Promega (Mannheim, Germany) |
| 6-aminocaproic acid | Sigma Aldrich (Munich, Germany) |
| agarose | Biozym (Hessisch Oldendorf, Germany) |
| ammonium persulfate (APS) | Sigma Aldrich (Munich, Germany) |
| bafilomycin A | Enzo Life Sciences GmbH (Lörrach, Germany) |
| blotting grade blocker (non-fat dry milk) | Bio-Rad (Munich, Germany) |

| | |
|---|---|
| bovine serum albumin (BSA) | Roth (Karlsruhe, Germany) |
| citric acid | Roth (Karlsruhe, Germany) |
| deoxynucleotide triphosphates (dNTPs) | ThermoFischer Scientific (Darmstadt, Germany) |
| dimethyl sulfoxide (DMSO) | Sigma Aldrich (Munich, Germany) |
| dithiothreitol (DTT) | Sigma Aldrich (Munich, Germany) |
| DreamTaq DNA Polymerase | ThermoFischer Scientific (Darmstadt, Germany) |
| ECL™ Western Blotting Detection Reagents | GE Healthcare (Hamburg, Germany) |
| epidermal growth factor (EGF) (recombinant human) | Peprotech (Hamburg, Germany) |
| ethanol | Roth (Karlsruhe, Germany) |
| ethylenediaminetetraacetic acid (EDTA) | Sigma Aldrich (Munich, Germany) |
| foetal bovine serum (FBS) | Merck Millipore (Darmstadt, Germany) |
| glycerol | Roth (Karlsruhe, Germany) |
| hematoxylin solution | Th Geyer (Renningen, Germany) |
| hydroxyurea | Sigma Aldrich (Munich, Germany) |
| interferon-β (IFN-β) (recombinant mouse) | Peprotech (Hamburg, Germany) |
| interleukin-10 (IL-10) (recombinant mouse) | Peprotech (Hamburg, Germany) |
| interleukin-22 (IL-22) (recombinant mouse) | Peprotech (Hamburg, Germany) |
| interleukin-22 (IL-22) (recombinant human) | Peprotech (Hamburg, Germany) |
| interleukin-23 (IL-22) (recombinant mouse) | Peprotech (Hamburg, Germany) |
| Matrigel | BD Biosciences (Heidelberg, Germany) |
| methanol | Roth (Karlsruhe, Germany) |
| N,N,N',N'-tetramethylethylendiamin (TEMED) | Sigma Aldrich (Munich, Germany) |
| nuclease-free water | Qiagen (Hilden, Germany) |
| paraffin | ThermoFischer Scientific (Darmstadt, Germany) |
| penicillin/streptomycin (10,000 U/mL) | Life Technologies (Darmstadt, Germany) |
| Phusion HotStart Flex 2 Master Mix | New England Biolanbs GmbH (Frankfurt a.M., Germany) |
| Pierce ECLTM Plus Western Blotting Substrate | ThermoFischer Scientific (Darmstadt, Germany) |
| propidium iodide (PI) | Sigma Aldrich (Munich, Germany) |
| protease and phosphatase inhibitor | ThermoFischer Scientific (Darmstadt, Germany) |
| proteinase K | ThermoFischer Scientific (Darmstadt, Germany) |
| rapamycin (Streptomyces hygroscopicus) | Sigma Aldrich (Munich, Germany) |
| Roti-Histokitt mounting medium | Roth (Karlsruhe, Germany) |
| S3I-201 | EMD Millipore (Darmstadt, Germany) |
| sodium chloride (NaCl) | Merck Millipore (Darmstadt, Germany) |
| sodium dodecyl sulfate (SDS) | Roth (Karlsruhe, Germany) |
| SYBR® Select Master Mix | Applied Biosystems (Darmstadt, Germany) |
| TaqMan Gene Expression Master | Applied Biosystems (Darmstadt, Germany) |
| Tris | Merck Millipore (Darmstadt, Germany) |

| | |
|---|---|
| TrypLE Express | ThermoFischer Scientific (Darmstadt, Germany) |
| tunicamycin | Calbiochem (Darmstadt, Germany) |
| Tween 20 | Roth (Karlsruhe, Germany) |
| xylene | ThermoFischer Scientific (Darmstadt, Germany) |

## 8.4 Devices

**Table 11: Table of used devices**

| Devices | Company |
|---|---|
| 100-1000 µl pipette | Eppendorf (Hamburg, Germany) |
| 10-100 µl pipette | Eppendorf (Hamburg, Germany) |
| 10-200 µl multi-channel pipette | Eppendorf (Hamburg, Germany) |
| 1-10 µl pipette | Eppendorf (Hamburg, Germany) |
| 7900HT Fast Real Time PCR System | Applied Biosystems (Darmstadt, Germany) |
| agarose gel chamber wide mini sub-cell GT | Bio-Rad (Munich, Germany) |
| automatic developer machine Curix 60 | Agfa (Mortsel, Belgium) |
| Axio Imager Z1 | ZEISS (Oberkochen, Germany) |
| balance | PeqLab (Erlangen, Germany) |
| cell counter (Cellometer Auto T4 Plus) | Heraeus (Hanau, Germany) |
| centrifuge Fresco21 Centrifuge | Heraeus (Hanau, Germany) |
| centrifuge Megafuge 16 | Bio-Rad (Munich, Germany) |
| ChemiDoc XRS | Biometra (Göttingen, Germany) |
| electrophoresis chamber Multigel G44 | Tecan (Männedorf, Switzerland) |
| ELISA plate shaker | ThermoFischer Scientific (Darmstadt, Germany) |
| ELISA washer Columbus plus | BD Biosciences (Heidelberg, Germany) |
| embedding station STP120 | Applied Biosystems (Darmstadt, Germany) |
| FACSCaliburTM | BD Biosciences (Heidelberg, Germany) |
| GeneAmp PCR System 9700 | Sartorius (Göttingen, Germany) |
| incubator | Tecan (Männedorf, Switzerland) |
| magnetic stirring plate | Severin (Sundern, Germany) |
| microplate reader Infinite M200 Pro | Illumina (San Diego, USA) |
| microwave | PeqLab (Erlangen, Germany) |
| HiSeq 3000 sequencer | Illumina (San Diego, USA) |
| NanoDrop spectrometer ND1000 | Biometra (Göttingen, Germany) |

| | |
|---|---|
| power Supply PP 3000 | Bandelin (Berlin, Germany) |
| RM2255 microtome | Heraeus (Hanau, Germany) |
| sonificator Sonopuls | Eppendorf (Hamburg, Germany) |
| sterile bench Herasafe KS12 | Bio-Rad (Munich, Germany) |
| Thermomixer compact | ZEISS (Oberkochen, Germany) |
| TransBlot Turbo Transfer System | Stuart Scientific (Chelmsford, United Kingdom) |
| tube rotator SRT6 | GFL (Burgwedel, Germany) |
| Vortex Genie 2 | Scientific Industries (New York, USA) |
| Water Bath 1013 | GFL (Burgwedel, Germany |

## 8.5 Consumables

**Table 12: Table of used consumables**

| Consumables | Company |
|---|---|
| 0.5 ml/1.5 ml/2.0 ml tubes | Sarstedt (Nümbrecht, Germany) |
| 1.5 ml/2.0 ml safe seal tubes | Sarstedt (Nümbrecht, Germany) |
| 10 ml syringe | BD Biosciences (Heidelberg, Germany) |
| 1-10 µl/10-100 µl/100-1000 µl pipette (filter) tips | Sarstedt (Nümbrecht, Germany) |
| 15 cm/10 ml petri dish | Sarstedt (Nümbrecht, Germany) |
| 15 ml/50 ml tubes | Sarstedt (Nümbrecht, Germany) |
| 18G/20G/26G needles | BD Biosciences (Heidelberg, Germany) |
| 1 ml syringe | BD Biosciences (Heidelberg, Germany) |
| 384-well plates | Life Technologies (Darmstadt, Germany) |
| 100 µm cell strainer | BD Biosciences (Heidelberg, Germany) |
| 5 ml/10 ml/25 ml pipettes | Sarstedt (Nümbrecht, Germany) |
| 6-well/12-well/24-well/96-well plate (flat bottom) | Sarstedt (Nümbrecht, Germany) |
| Amersham Hyperfilm ECL | GE Healthcare (Hamburg, Germany) |
| cell scraper | Sarstedt (Nümbrecht, Germany) |
| coversplips (24x50mm) | Geyer (Renningen, Germany) |
| FACS tubes | Greiner (Frickenhausen, Germany) |

# 9 References


1. Schreiber S, Rosenstiel P, Albrecht M, Hampe J, Krawczak M. Genetics of Crohn disease, an archetypal inflammatory barrier disease. Nat Rev Genet. 2005;6(5):376-88.
2. Podolsky DK. Inflammatory bowel disease. N Engl J Med. 2002;347(6):417-29.
3. Freeman HJ. Colorectal cancer risk in Crohn's disease. World J Gastroenterol. 2008;14(12):1810-1.
4. Zheng JJ, Zhu XS, Huangfu Z, Gao ZX, Guo ZR, Wang Z. Crohn's disease in mainland China: a systematic analysis of 50 years of research. Chin J Dig Dis. 2005;6(4):175-81.
5. Desai HG, Gupte PA. Increasing incidence of Crohn's disease in India: is it related to improved sanitation? Indian J Gastroenterol. 2005;24(1):23-4.
6. Bernstein CN, Shanahan F. Disorders of a modern lifestyle: reconciling the epidemiology of inflammatory bowel diseases. Gut. 2008;57(9):1185-91.
7. Calkins BM. A meta-analysis of the role of smoking in inflammatory bowel disease. Dig Dis Sci. 1989;34(12):1841-54.
8. Jones DT, Osterman MT, Bewtra M, Lewis JD. Passive smoking and inflammatory bowel disease: a meta-analysis. Am J Gastroenterol. 2008;103(9):2382-93.
9. Yadav P, Ellinghaus D, Remy G, Freitag-Wolf S, Cesaro A, Degenhardt F, et al. Genetic Factors Interact With Tobacco Smoke to Modify Risk for Inflammatory Bowel Disease in Humans and Mice. Gastroenterology. 2017;153(2):550-65.
10. Wild GE, Drozdowski L, Tartaglia C, Clandinin MT, Thomson AB. Nutritional modulation of the inflammatory response in inflammatory bowel disease--from the molecular to the integrative to the clinical. World J Gastroenterol. 2007;13(1):1-7.
11. Sakamoto N, Kono S, Wakai K, Fukuda Y, Satomi M, Shimoyama T, et al. Dietary risk factors for inflammatory bowel disease: a multicenter case-control study in Japan. Inflamm Bowel Dis. 2005;11(2):154-63.
12. Amre DK, D'Souza S, Morgan K, Seidman G, Lambrette P, Grimard G, et al. Imbalances in dietary consumption of fatty acids, vegetables, and fruits are associated with risk for Crohn's disease in children. Am J Gastroenterol. 2007;102(9):2016-25.
13. Chassaing B, Koren O, Goodrich JK, Poole AC, Srinivasan S, Ley RE, et al. Dietary emulsifiers impact the mouse gut microbiota promoting colitis and metabolic syndrome. Nature. 2015;519(7541):92-6.
14. Frank DN, St Amand AL, Feldman RA, Boedeker EC, Harpaz N, Pace NR. Molecular-phylogenetic characterization of microbial community imbalances in human inflammatory bowel diseases. Proc Natl Acad Sci U S A. 2007;104(34):13780-5.
15. Gophna U, Sommerfeld K, Gophna S, Doolittle WF, Veldhuyzen van Zanten SJ. Differences between tissue-associated intestinal microfloras of patients with Crohn's disease and ulcerative colitis. J Clin Microbiol. 2006;44(11):4136-41.

16. Hildebrand H, Malmborg P, Askling J, Ekbom A, Montgomery SM. Early-life exposures associated with antibiotic use and risk of subsequent Crohn's disease. Scand J Gastroenterol. 2008;43(8):961-6.

17. Lupp C, Robertson ML, Wickham ME, Sekirov I, Champion OL, Gaynor EC, et al. Host-mediated inflammation disrupts the intestinal microbiota and promotes the overgrowth of Enterobacteriaceae. Cell Host Microbe. 2007;2(3):204.

18. Rossen NG, Fuentes S, van der Spek MJ, Tijssen JG, Hartman JH, Duflou A, et al. Findings From a Randomized Controlled Trial of Fecal Transplantation for Patients With Ulcerative Colitis. Gastroenterology. 2015;149(1):110-8 e4.

19. Paramsothy S, Kamm MA, Kaakoush NO, Walsh AJ, van den Bogaerde J, Samuel D, et al. Multidonor intensive faecal microbiota transplantation for active ulcerative colitis: a randomised placebo-controlled trial. Lancet. 2017;389(10075):1218-28.

20. Liu JZ, van Sommeren S, Huang H, Ng SC, Alberts R, Takahashi A, et al. Association analyses identify 38 susceptibility loci for inflammatory bowel disease and highlight shared genetic risk across populations. Nat Genet. 2015;47(9):979-86.

21. Ji SG, Juran BD, Mucha S, Folseraas T, Jostins L, Melum E, et al. Genome-wide association study of primary sclerosing cholangitis identifies new risk loci and quantifies the genetic relationship with inflammatory bowel disease. Nat Genet. 2017;49(2):269-73.

22. Jostins L, Ripke S, Weersma RK, Duerr RH, McGovern DP, Hui KY, et al. Host-microbe interactions have shaped the genetic architecture of inflammatory bowel disease. Nature. 2012;491(7422):119-24.

23. Hampe J, Cuthbert A, Croucher PJ, Mirza MM, Mascheretti S, Fisher S, et al. Association between insertion mutation in NOD2 gene and Crohn's disease in German and British populations. Lancet. 2001;357(9272):1925-8.

24. Hampe J, Franke A, Rosenstiel P, Till A, Teuber M, Huse K, et al. A genome-wide association scan of nonsynonymous SNPs identifies a susceptibility variant for Crohn disease in ATG16L1. Nat Genet. 2007;39(2):207-11.

25. Mokry M, Middendorp S, Wiegerinck CL, Witte M, Teunissen H, Meddens CA, et al. Many inflammatory bowel disease risk loci include regions that regulate gene expression in immune cells and the intestinal epithelium. Gastroenterology. 2014;146(4):1040-7.

26. Russell RK, Satsangi J. IBD: a family affair. Best Pract Res Clin Gastroenterol. 2004;18(3):525-39.

27. Satsangi J, Grootscholten C, Holt H, Jewell DP. Clinical patterns of familial inflammatory bowel disease. Gut. 1996;38(5):738-41.

28. Tysk C, Lindberg E, Jarnerot G, Floderus-Myrhed B. Ulcerative colitis and Crohn's disease in an unselected population of monozygotic and dizygotic twins. A study of heritability and the influence of smoking. Gut. 1988;29(7):990-6.

29. Spehlmann ME, Begun AZ, Burghardt J, Lepage P, Raedler A, Schreiber S. Epidemiology of inflammatory bowel disease in a German twin cohort: results of a nationwide study. Inflamm Bowel Dis. 2008;14(7):968-76.

30. Zeissig Y, Petersen BS, Milutinovic S, Bosse E, Mayr G, Peuker K, et al. XIAP variants in male Crohn's disease. Gut. 2015;64(1):66-76.

31. Kotlarz D, Beier R, Murugan D, Diestelhorst J, Jensen O, Boztug K, et al. Loss of interleukin-10 signaling and infantile inflammatory bowel disease: implications for diagnosis and therapy. Gastroenterology. 2012;143(2):347-55.

32. Glocker EO, Kotlarz D, Boztug K, Gertz EM, Schaffer AA, Noyan F, et al. Inflammatory bowel disease and mutations affecting the interleukin-10 receptor. N Engl J Med. 2009;361(21):2033-45.

33. Uhlig HH, Schwerd T, Koletzko S, Shah N, Kammermeier J, Elkadri A, et al. The diagnostic approach to monogenic very early onset inflammatory bowel disease. Gastroenterology. 2014;147(5):990-1007 e3.

34. Zeissig S, Petersen BS, Tomczak M, Melum E, Huc-Claustre E, Dougan SK, et al. Early-onset Crohn's disease and autoimmunity associated with a variant in CTLA-4. Gut. 2015;64(12):1889-97.

35. Yang SK. Personalizing IBD Therapy: The Asian Perspective. Dig Dis. 2016;34(1-2):165-74.

36. Girardin M, Manz M, Manser C, Biedermann L, Wanner R, Frei P, et al. First-line therapies in inflammatory bowel disease. Digestion. 2012;86 Suppl 1:6-10.

37. Mantzaris GJ. Thiopurines and Methotrexate Use in IBD Patients in a Biologic Era. Curr Treat Options Gastroenterol. 2017;15(1):84-104.

38. Begos DG, Rappaport R, Jain D. Cytomegalovirus infection masquerading as an ulcerative colitis flare-up: case report and review of the literature. Yale J Biol Med. 1996;69(4):323-8.

39. Lofberg R. New steroids for inflammatory bowel disease. Inflamm Bowel Dis. 1995;1(2):135-41.

40. van der Valk ME, Mangen MJ, Leenders M, Dijkstra G, van Bodegraven AA, Fidder HH, et al. Healthcare costs of inflammatory bowel disease have shifted from hospitalisation and surgery towards anti-TNFalpha therapy: results from the COIN study. Gut. 2014;63(1):72-9.

41. Sandborn WJ, Hanauer SB. Antitumor necrosis factor therapy for inflammatory bowel disease: a review of agents, pharmacology, clinical results, and safety. Inflamm Bowel Dis. 1999;5(2):119-33.

42. Danese S, Vuitton L, Peyrin-Biroulet L. Biologic agents for IBD: practical insights. Nat Rev Gastroenterol Hepatol. 2015;12(9):537-45.

43. Schreiber S, Khaliq-Kareemi M, Lawrance IC, Thomsen OO, Hanauer SB, McColm J, et al. Maintenance therapy with certolizumab pegol for Crohn's disease. N Engl J Med. 2007;357(3):239-50.

44. Sandborn WJ, Feagan BG, Stoinov S, Honiball PJ, Rutgeerts P, Mason D, et al. Certolizumab pegol for the treatment of Crohn's disease. N Engl J Med. 2007;357(3):228-38.

45. Sandborn WJ, Feagan BG, Rutgeerts P, Hanauer S, Colombel JF, Sands BE, et al. Vedolizumab as induction and maintenance therapy for Crohn's disease. N Engl J Med. 2013;369(8):711-21.

46. Dickson I. IBD: Ustekinumab therapy for Crohn's disease. Nat Rev Gastroenterol Hepatol. 2017;14(1):4.

47. Sandborn WJ, Su C, Sands BE, D'Haens GR, Vermeire S, Schreiber S, et al. Tofacitinib as Induction and Maintenance Therapy for Ulcerative Colitis. N Engl J Med. 2017;376(18):1723-36.

48. Fiorino G, Gilardi D, Danese S. The clinical potential of etrolizumab in ulcerative colitis: hypes and hopes. Therap Adv Gastroenterol. 2016;9(4):503-12.

49. Sandborn WJ, Feagan BG. Ozanimod Treatment for Ulcerative Colitis. N Engl J Med. 2016;375(8):e17.

50. Dumoutier L, Louahed J, Renauld JC. Cloning and characterization of IL-10-related T cell-derived inducible factor (IL-TIF), a novel cytokine structurally related to IL-10 and inducible by IL-9. J Immunol. 2000;164(4):1814-9.

51. Eyerich S, Eyerich K, Pennino D, Carbone T, Nasorri F, Pallotta S, et al. Th22 cells represent a distinct human T cell subset involved in epidermal immunity and remodeling. J Clin Invest. 2009;119(12):3573-85.

52. Zenewicz LA, Yancopoulos GD, Valenzuela DM, Murphy AJ, Karow M, Flavell RA. Interleukin-22 but not interleukin-17 provides protection to hepatocytes during acute liver inflammation. Immunity. 2007;27(4):647-59.

53. Xue J, Zhao Q, Sharma V, Nguyen LP, Lee YN, Pham KL, et al. Aryl Hydrocarbon Receptor Ligands in Cigarette Smoke Induce Production of Interleukin-22 to Promote Pancreatic Fibrosis in Models of Chronic Pancreatitis. Gastroenterology. 2016;151(6):1206-17.

54. Hirose K, Takahashi K, Nakajima H. Roles of IL-22 in Allergic Airway Inflammation. J Allergy (Cairo). 2013;2013:260518.

55. Ikeuchi H, Kuroiwa T, Hiramatsu N, Kaneko Y, Hiromura K, Ueki K, et al. Expression of interleukin-22 in rheumatoid arthritis: potential role as a proinflammatory cytokine. Arthritis Rheum. 2005;52(4):1037-46.

56. Pickert G, Neufert C, Leppkes M, Zheng Y, Wittkopf N, Warntjen M, et al. STAT3 links IL-22 signaling in intestinal epithelial cells to mucosal wound healing. J Exp Med. 2009;206(7):1465-72.

57. Zheng Y, Valdez PA, Danilenko DM, Hu Y, Sa SM, Gong Q, et al. Interleukin-22 mediates early host defense against attaching and effacing bacterial pathogens. Nat Med. 2008;14(3):282-9.

58. Pham TA, Clare S, Goulding D, Arasteh JM, Stares MD, Browne HP, et al. Epithelial IL-22RA1-mediated fucosylation promotes intestinal colonization resistance to an opportunistic pathogen. Cell Host Microbe. 2014;16(4):504-16.

59. Stefanich EG, Rae J, Sukumaran S, Lutman J, Lekkerkerker A, Ouyang W, et al. Pre-clinical and translational pharmacology of a human interleukin-22 IgG fusion protein for potential treatment of infectious or inflammatory diseases. Biochem Pharmacol. 2018;152:224-35.

60. Lamarthee B, Malard F, Gamonet C, Bossard C, Couturier M, Renauld JC, et al. Donor interleukin-22 and host type I interferon signaling pathway participate in intestinal graft-versus-host disease via STAT1 activation and CXCL10. Mucosal Immunol. 2016;9(2):309-21.

61. Lejeune D, Dumoutier L, Constantinescu S, Kruijer W, Schuringa JJ, Renauld JC. Interleukin-22 (IL-22) activates the JAK/STAT, ERK, JNK, and p38 MAP kinase pathways in a rat hepatoma cell line. Pathways that are shared with and distinct from IL-10. J Biol Chem. 2002;277(37):33676-82.

62. Bachmann M, Ulziibat S, Hardle L, Pfeilschifter J, Muhl H. IFNalpha converts IL-22 into a cytokine efficiently activating STAT1 and its downstream targets. Biochem Pharmacol. 2013;85(3):396-403.

63. Mitra A, Raychaudhuri SK, Raychaudhuri SP. IL-22 induced cell proliferation is regulated by PI3K/Akt/mTOR signaling cascade. Cytokine. 2012;60(1):38-42.

64. Liang SC, Tan XY, Luxenberg DP, Karim R, Dunussi-Joannopoulos K, Collins M, et al. Interleukin (IL)-22 and IL-17 are coexpressed by Th17 cells and cooperatively enhance expression of antimicrobial peptides. J Exp Med. 2006;203(10):2271-9.

65. Chung Y, Yang X, Chang SH, Ma L, Tian Q, Dong C. Expression and regulation of IL-22 in the IL-17-producing CD4+ T lymphocytes. Cell Res. 2006;16(11):902-7.

66. Duhen T, Geiger R, Jarrossay D, Lanzavecchia A, Sallusto F. Production of interleukin 22 but not interleukin 17 by a subset of human skin-homing memory T cells. Nat Immunol. 2009;10(8):857-63.

67. Trifari S, Kaplan CD, Tran EH, Crellin NK, Spits H. Identification of a human helper T cell population that has abundant production of interleukin 22 and is distinct from T(H)-17, T(H)1 and T(H)2 cells. Nat Immunol. 2009;10(8):864-71.

68. Witte E, Witte K, Warszawska K, Sabat R, Wolk K. Interleukin-22: a cytokine produced by T, NK and NKT cell subsets, with importance in the innate immune defense and tissue protection. Cytokine Growth Factor Rev. 2010;21(5):365-79.

69. Zindl CL, Lai JF, Lee YK, Maynard CL, Harbour SN, Ouyang W, et al. IL-22-producing neutrophils contribute to antimicrobial defense and restitution of colonic epithelial integrity during colitis. Proc Natl Acad Sci U S A. 2013;110(31):12768-73.

70. Satoh-Takayama N, Vosshenrich CA, Lesjean-Pottier S, Sawa S, Lochner M, Rattis F, et al. Microbial flora drives interleukin 22 production in intestinal NKp46+ cells that provide innate mucosal immune defense. Immunity. 2008;29(6):958-70.

71. Sonnenberg GF, Monticelli LA, Elloso MM, Fouser LA, Artis D. CD4(+) lymphoid tissue-inducer cells promote innate immunity in the gut. Immunity. 2011;34(1):122-34.

72. Alam MS, Maekawa Y, Kitamura A, Tanigaki K, Yoshimoto T, Kishihara K, et al. Notch signaling drives IL-22 secretion in CD4+ T cells by stimulating the aryl hydrocarbon receptor. Proc Natl Acad Sci U S A. 2010;107(13):5943-8.

73. Lee JS, Cella M, McDonald KG, Garlanda C, Kennedy GD, Nukaya M, et al. AHR drives the development of gut ILC22 cells and postnatal lymphoid tissues via pathways dependent on and independent of Notch. Nat Immunol. 2011;13(2):144-51.

74. Kinnebrew MA, Buffie CG, Diehl GE, Zenewicz LA, Leiner I, Hohl TM, et al. Interleukin 23 production by intestinal CD103(+)CD11b(+) dendritic cells in response to bacterial flagellin enhances mucosal innate immune defense. Immunity. 2012;36(2):276-87.

75. Aden K, Rehman A, Falk-Paulsen M, Secher T, Kuiper J, Tran F, et al. Epithelial IL-23R Signaling Licenses Protective IL-22 Responses in Intestinal Inflammation. Cell Rep. 2016;16(8):2208-18.

76. Andoh A, Zhang Z, Inatomi O, Fujino S, Deguchi Y, Araki Y, et al. Interleukin-22, a member of the IL-10 subfamily, induces inflammatory responses in colonic subepithelial myofibroblasts. Gastroenterology. 2005;129(3):969-84.

77. Wolk K, Witte E, Hoffmann U, Doecke WD, Endesfelder S, Asadullah K, et al. IL-22 induces lipopolysaccharide-binding protein in hepatocytes: a potential systemic role of IL-22 in Crohn's disease. J Immunol. 2007;178(9):5973-81.

78. Huber S, Gagliani N, Zenewicz LA, Huber FJ, Bosurgi L, Hu B, et al. IL-22BP is regulated by the inflammasome and modulates tumorigenesis in the intestine. Nature. 2012;491(7423):259-63.

79. Dumoutier L, Lejeune D, Colau D, Renauld JC. Cloning and characterization of IL-22 binding protein, a natural antagonist of IL-10-related T cell-derived inducible factor/IL-22. J Immunol. 2001;166(12):7090-5.

80. Jiang R, Tan Z, Deng L, Chen Y, Xia Y, Gao Y, et al. Interleukin-22 promotes human hepatocellular carcinoma by activation of STAT3. Hepatology. 2011;54(3):900-9.

81. Wang Z, Yang L, Jiang Y, Ling ZQ, Li Z, Cheng Y, et al. High fat diet induces formation of spontaneous liposarcoma in mouse adipose tissue with overexpression of interleukin 22. PLoS One. 2011;6(8):e23737.

82. Lüllmann-Rauch R. Taschenbuch Histologie. 5., vollst. überarb. Auflage ed. Stuttgart u.a.: Thieme; 2015. XVIII, 726 S. p.

83. Van der Sluis M, De Koning BA, De Bruijn AC, Velcich A, Meijerink JP, Van Goudoever JB, et al. Muc2-deficient mice spontaneously develop colitis, indicating that MUC2 is critical for colonic protection. Gastroenterology. 2006;131(1):117-29.

84. Gibbons MA, Bowdish DM, Davidson DJ, Sallenave JM, Simpson AJ. Endogenous pulmonary antibiotics. Scott Med J. 2006;51(2):37-42.

85. Koslowski MJ, Kubler I, Chamaillard M, Schaeffeler E, Reinisch W, Wang G, et al. Genetic variants of Wnt transcription factor TCF-4 (TCF7L2) putative promoter region are associated with small intestinal Crohn's disease. PLoS One. 2009;4(2):e4496.

86. Wehkamp J, Fellermann K, Herrlinger KR, Baxmann S, Schmidt K, Schwind B, et al. Human beta-defensin 2 but not beta-defensin 1 is expressed preferentially in colonic mucosa of inflammatory bowel disease. Eur J Gastroenterol Hepatol. 2002;14(7):745-52.

87. Ferguson A, Murray D. Quantitation of intraepithelial lymphocytes in human jejunum. Gut. 1971;12(12):988-94.

88. Kucharzik T, Walsh SV, Chen J, Parkos CA, Nusrat A. Neutrophil transmigration in inflammatory bowel disease is associated with differential expression of epithelial intercellular junction proteins. Am J Pathol. 2001;159(6):2001-9.

89. Zeissig S, Burgel N, Gunzel D, Richter J, Mankertz J, Wahnschaffe U, et al. Changes in expression and distribution of claudin 2, 5 and 8 lead to discontinuous tight junctions and barrier dysfunction in active Crohn's disease. Gut. 2007;56(1):61-72.

90. Waldschmitt N, Berger E, Rath E, Sartor RB, Weigmann B, Heikenwalder M, et al. C/EBP homologous protein inhibits tissue repair in response to gut injury and is inversely regulated with chronic inflammation. Mucosal Immunol. 2014;7(6):1452-66.

91. Gunther C, Martini E, Wittkopf N, Amann K, Weigmann B, Neumann H, et al. Caspase-8 regulates TNF-alpha-induced epithelial necroptosis and terminal ileitis. Nature. 2011;477(7364):335-9.

92. Nava P, Koch S, Laukoetter MG, Lee WY, Kolegraff K, Capaldo CT, et al. Interferon-gamma regulates intestinal epithelial homeostasis through converging beta-catenin signaling pathways. Immunity. 2010;32(3):392-402.

93. Kaser A, Lee AH, Franke A, Glickman JN, Zeissig S, Tilg H, et al. XBP1 links ER stress to intestinal inflammation and confers genetic risk for human inflammatory bowel disease. Cell. 2008;134(5):743-56.

94. Matsuzawa-Ishimoto Y, Shono Y, Gomez LE, Hubbard-Lucey VM, Cammer M, Neil J, et al. Autophagy protein ATG16L1 prevents necroptosis in the intestinal epithelium. J Exp Med. 2017.

95. Lei-Leston AC, Murphy AG, Maloy KJ. Epithelial Cell Inflammasomes in Intestinal Immunity and Inflammation. Front Immunol. 2017;8:1168.

96. Yilmaz OH, Katajisto P, Lamming DW, Gultekin Y, Bauer-Rowe KE, Sengupta S, et al. mTORC1 in the Paneth cell niche couples intestinal stem-cell function to calorie intake. Nature. 2012;486(7404):490-5.

97. McCabe LR, Parameswaran N. Recent Advances in Intestinal Stem Cells. Curr Mol Biol Rep. 2017;3(3):143-8.

98. Lindemans CA, Calafiore M, Mertelsmann AM, O'Connor MH, Dudakov JA, Jenq RR, et al. Interleukin-22 promotes intestinal-stem-cell-mediated epithelial regeneration. Nature. 2015;528(7583):560-4.

99. Hao JQ. Targeting interleukin-22 in psoriasis. Inflammation. 2014;37(1):94-9.

100. Barker N, van Es JH, Kuipers J, Kujala P, van den Born M, Cozijnsen M, et al. Identification of stem cells in small intestine and colon by marker gene Lgr5. Nature. 2007;449(7165):1003-7.

101. Ruffner H, Sprunger J, Charlat O, Leighton-Davies J, Grosshans B, Salathe A, et al. R-Spondin potentiates Wnt/beta-catenin signaling through orphan receptors LGR4 and LGR5. PLoS One. 2012;7(7):e40976.

102. Haramis AP, Begthel H, van den Born M, van Es J, Jonkheer S, Offerhaus GJ, et al. De novo crypt formation and juvenile polyposis on BMP inhibition in mouse intestine. Science. 2004;303(5664):1684-6.

103. Dignass AU, Sturm A. Peptide growth factors in the intestine. Eur J Gastroenterol Hepatol. 2001;13(7):763-70.

104. Gregorieff A, Liu Y, Inanlou MR, Khomchuk Y, Wrana JL. Yap-dependent reprogramming of Lgr5(+) stem cells drives intestinal regeneration and cancer. Nature. 2015;526(7575):715-8.

105. Sato T, Vries RG, Snippert HJ, van de Wetering M, Barker N, Stange DE, et al. Single Lgr5 stem cells build crypt-villus structures in vitro without a mesenchymal niche. Nature. 2009;459(7244):262-5.

106. Huch M, Dorrell C, Boj SF, van Es JH, Li VS, van de Wetering M, et al. In vitro expansion of single Lgr5+ liver stem cells induced by Wnt-driven regeneration. Nature. 2013;494(7436):247-50.

107. Lancaster MA, Renner M, Martin CA, Wenzel D, Bicknell LS, Hurles ME, et al. Cerebral organoids model human brain development and microcephaly. Nature. 2013;501(7467):373-9.

108. Sato T, Stange DE, Ferrante M, Vries RG, Van Es JH, Van den Brink S, et al. Long-term expansion of epithelial organoids from human colon, adenoma, adenocarcinoma, and Barrett's epithelium. Gastroenterology. 2011;141(5):1762-72.

109. van de Wetering M, Francies HE, Francis JM, Bounova G, Iorio F, Pronk A, et al. Prospective derivation of a living organoid biobank of colorectal cancer patients. Cell. 2015;161(4):933-45.

110. Yui S, Nakamura T, Sato T, Nemoto Y, Mizutani T, Zheng X, et al. Functional engraftment of colon epithelium expanded in vitro from a single adult Lgr5(+) stem cell. Nat Med. 2012;18(4):618-23.

111. Iwasaki A, Medzhitov R. Regulation of adaptive immunity by the innate immune system. Science. 2010;327(5963):291-5.

112. Schirmer RH, Schollhammer T, Eisenbrand G, Krauth-Siegel RL. Oxidative stress as a defense mechanism against parasitic infections. Free Radic Res Commun. 1987;3(1-5):3-12.

113. Lipinski S, Till A, Sina C, Arlt A, Grasberger H, Schreiber S, et al. DUOX2-derived reactive oxygen species are effectors of NOD2-mediated antibacterial responses. J Cell Sci. 2009;122(Pt 19):3522-30.

114. Hartlova A, Erttmann SF, Raffi FA, Schmalz AM, Resch U, Anugula S, et al. DNA damage primes the type I interferon system via the cytosolic DNA sensor STING to promote anti-microbial innate immunity. Immunity. 2015;42(2):332-43.

115. Abe T, Harashima A, Xia T, Konno H, Konno K, Morales A, et al. STING recognition of cytoplasmic DNA instigates cellular defense. Mol Cell. 2013;50(1):5-15.

116. Zannetti C, Parroche P, Panaye M, Roblot G, Gruffat H, Manet E, et al. TLR9 transcriptional regulation in response to double-stranded DNA viruses. J Immunol. 2014;193(7):3398-408.

117. Hornung V, Ablasser A, Charrel-Dennis M, Bauernfeind F, Horvath G, Caffrey DR, et al. AIM2 recognizes cytosolic dsDNA and forms a caspase-1-activating inflammasome with ASC. Nature. 2009;458(7237):514-8.

118. Sun L, Wu J, Du F, Chen X, Chen ZJ. Cyclic GMP-AMP synthase is a cytosolic DNA sensor that activates the type I interferon pathway. Science. 2013;339(6121):786-91.

119. Kato H, Takeuchi O, Sato S, Yoneyama M, Yamamoto M, Matsui K, et al. Differential roles of MDA5 and RIG-I helicases in the recognition of RNA viruses. Nature. 2006;441(7089):101-5.

120. Moretti J, Roy S, Bozec D, Martinez J, Chapman JR, Ueberheide B, et al. STING Senses Microbial Viability to Orchestrate Stress-Mediated Autophagy of the Endoplasmic Reticulum. Cell. 2017.

121. Xia T, Konno H, Ahn J, Barber GN. Deregulation of STING Signaling in Colorectal Carcinoma Constrains DNA Damage Responses and Correlates With Tumorigenesis. Cell Rep. 2016;14(2):282-97.

122. Harding SM, Benci JL, Irianto J, Discher DE, Minn AJ, Greenberg RA. Mitotic progression following DNA damage enables pattern recognition within micronuclei. Nature. 2017;548(7668):466-70.

123. Nakagawa I, Amano A, Mizushima N, Yamamoto A, Yamaguchi H, Kamimoto T, et al. Autophagy defends cells against invading group A Streptococcus. Science. 2004;306(5698):1037-40.

124. Travassos LH, Carneiro LA, Ramjeet M, Hussey S, Kim YG, Magalhaes JG, et al. Nod1 and Nod2 direct autophagy by recruiting ATG16L1 to the plasma membrane at the site of bacterial entry. Nat Immunol. 2010;11(1):55-62.

125. Grootjans J, Kaser A, Kaufman RJ, Blumberg RS. The unfolded protein response in immunity and inflammation. Nat Rev Immunol. 2016;16(8):469-84.

126. Koritzinsky M, Levitin F, van den Beucken T, Rumantir RA, Harding NJ, Chu KC, et al. Two phases of disulfide bond formation have differing requirements for oxygen. J Cell Biol. 2013;203(4):615-27.

127. Malhotra JD, Miao H, Zhang K, Wolfson A, Pennathur S, Pipe SW, et al. Antioxidants reduce endoplasmic reticulum stress and improve protein secretion. Proc Natl Acad Sci U S A. 2008;105(47):18525-30.

128. Kharroubi I, Ladriere L, Cardozo AK, Dogusan Z, Cnop M, Eizirik DL. Free fatty acids and cytokines induce pancreatic beta-cell apoptosis by different mechanisms: role of nuclear factor-kappaB and endoplasmic reticulum stress. Endocrinology. 2004;145(11):5087-96.

129. Richardson CE, Kooistra T, Kim DH. An essential role for XBP-1 in host protection against immune activation in C. elegans. Nature. 2010;463(7284):1092-5.

130. Tschurtschenthaler M, Adolph TE, Ashcroft JW, Niederreiter L, Bharti R, Saveljeva S, et al. Defective ATG16L1-mediated removal of IRE1alpha drives Crohn's disease-like ileitis. J Exp Med. 2017;214(2):401-22.

131. Hassan I, Gaines KS, Hottel WJ, Wishy RM, Miller SE, Powers LS, et al. Inositol-requiring enzyme 1 inhibits respiratory syncytial virus replication. J Biol Chem. 2014;289(11):7537-46.

132. Myeni S, Child R, Ng TW, Kupko JJ, 3rd, Wehrly TD, Porcella SF, et al. Brucella modulates secretory trafficking via multiple type IV secretion effector proteins. PLoS Pathog. 2013;9(8):e1003556.

133. Oslowski CM, Urano F. Measuring ER stress and the unfolded protein response using mammalian tissue culture system. Methods Enzymol. 2011;490:71-92.

134. Pincus D, Chevalier MW, Aragon T, van Anken E, Vidal SE, El-Samad H, et al. BiP binding to the ER-stress sensor Ire1 tunes the homeostatic behavior of the unfolded protein response. PLoS Biol. 2010;8(7):e1000415.

135. Lee AH, Iwakoshi NN, Glimcher LH. XBP-1 regulates a subset of endoplasmic reticulum resident chaperone genes in the unfolded protein response. Mol Cell Biol. 2003;23(21):7448-59.

136. Kato H, Nakajima S, Saito Y, Takahashi S, Katoh R, Kitamura M. mTORC1 serves ER stress-triggered apoptosis via selective activation of the IRE1-JNK pathway. Cell Death Differ. 2012;19(2):310-20.

137. Niederreiter L, Fritz TM, Adolph TE, Krismer AM, Offner FA, Tschurtschenthaler M, et al. ER stress transcription factor Xbp1 suppresses intestinal tumorigenesis and directs intestinal stem cells. J Exp Med. 2013;210(10):2041-56.

138. Hollien J, Weissman JS. Decay of endoplasmic reticulum-localized mRNAs during the unfolded protein response. Science. 2006;313(5783):104-7.

139. Zucal C, D'Agostino VG, Casini A, Mantelli B, Thongon N, Soncini D, et al. EIF2A-dependent translational arrest protects leukemia cells from the energetic stress induced by NAMPT inhibition. BMC Cancer. 2015;15:855.

140. Heijmans J, van Lidth de Jeude JF, Koo BK, Rosekrans SL, Wielenga MC, van de Wetering M, et al. ER stress causes rapid loss of intestinal epithelial stemness through activation of the unfolded protein response. Cell Rep. 2013;3(4):1128-39.

141. Zinszner H, Kuroda M, Wang X, Batchvarova N, Lightfoot RT, Remotti H, et al. CHOP is implicated in programmed cell death in response to impaired function of the endoplasmic reticulum. Genes Dev. 1998;12(7):982-95.

142. Kaur J, Debnath J. Autophagy at the crossroads of catabolism and anabolism. Nat Rev Mol Cell Biol. 2015;16(8):461-72.

143. Cuervo AM, Wong E. Chaperone-mediated autophagy: roles in disease and aging. Cell Res. 2014;24(1):92-104.

144. Kissova I, Deffieu M, Manon S, Camougrand N. Uth1p is involved in the autophagic degradation of mitochondria. J Biol Chem. 2004;279(37):39068-74.

145. Bernales S, McDonald KL, Walter P. Autophagy counterbalances endoplasmic reticulum expansion during the unfolded protein response. PLoS Biol. 2006;4(12):e423.

146. Chu CT, Zhu J, Dagda R. Beclin 1-independent pathway of damage-induced mitophagy and autophagic stress: implications for neurodegeneration and cell death. Autophagy. 2007;3(6):663-6.

147. Khaminets A, Heinrich T, Mari M, Grumati P, Huebner AK, Akutsu M, et al. Regulation of endoplasmic reticulum turnover by selective autophagy. Nature. 2015;522(7556):354-8.

148. Wong YC, Holzbaur EL. Optineurin is an autophagy receptor for damaged mitochondria in parkin-mediated mitophagy that is disrupted by an ALS-linked mutation. Proc Natl Acad Sci U S A. 2014;111(42):E4439-48.

149. Kimura T, Jain A, Choi SW, Mandell MA, Schroder K, Johansen T, et al. TRIM-mediated precision autophagy targets cytoplasmic regulators of innate immunity. J Cell Biol. 2015;210(6):973-89.

150. Samie M, Lim J, Verschueren E, Baughman JM, Peng I, Wong A, et al. Selective autophagy of the adaptor TRIF regulates innate inflammatory signaling. Nat Immunol. 2018.

151. Kang R, Zeh HJ, Lotze MT, Tang D. The Beclin 1 network regulates autophagy and apoptosis. Cell Death Differ. 2011;18(4):571-80.

152. Jung CH, Ro SH, Cao J, Otto NM, Kim DH. mTOR regulation of autophagy. FEBS Lett. 2010;584(7):1287-95.

153. Lassen KG, Kuballa P, Conway KL, Patel KK, Becker CE, Peloquin JM, et al. Atg16L1 T300A variant decreases selective autophagy resulting in altered cytokine signaling and decreased antibacterial defense. Proc Natl Acad Sci U S A. 2014;111(21):7741-6.

154. Cadwell K, Liu JY, Brown SL, Miyoshi H, Loh J, Lennerz JK, et al. A key role for autophagy and the autophagy gene Atg16l1 in mouse and human intestinal Paneth cells. Nature. 2008;456(7219):259-63.

155. Massey DC, Parkes M. Genome-wide association scanning highlights two autophagy genes, ATG16L1 and IRGM, as being significantly associated with Crohn's disease. Autophagy. 2007;3(6):649-51.

156. Liu Z, Lee J, Krummey S, Lu W, Cai H, Lenardo MJ. The kinase LRRK2 is a regulator of the transcription factor NFAT that modulates the severity of inflammatory bowel disease. Nat Immunol. 2011;12(11):1063-70.

157. Talloczy Z, Jiang W, Virgin HWt, Leib DA, Scheuner D, Kaufman RJ, et al. Regulation of starvation- and virus-induced autophagy by the eIF2alpha kinase signaling pathway. Proc Natl Acad Sci U S A. 2002;99(1):190-5.

158. Hetz C, Thielen P, Matus S, Nassif M, Court F, Kiffin R, et al. XBP-1 deficiency in the nervous system protects against amyotrophic lateral sclerosis by increasing autophagy. Genes Dev. 2009;23(19):2294-306.

159. Qin L, Wang Z, Tao L, Wang Y. ER stress negatively regulates AKT/TSC/mTOR pathway to enhance autophagy. Autophagy. 2010;6(2):239-47.

160. Adolph TE, Tomczak MF, Niederreiter L, Ko HJ, Bock J, Martinez-Naves E, et al. Paneth cells as a site of origin for intestinal inflammation. Nature. 2013;503(7475):272-6.

161. Deuring JJ, Fuhler GM, Konstantinov SR, Peppelenbosch MP, Kuipers EJ, de Haar C, et al. Genomic ATG16L1 risk allele-restricted Paneth cell ER stress in quiescent Crohn's disease. Gut. 2014;63(7):1081-91.

162. Hasnain SZ, Tauro S, Das I, Tong H, Chen AC, Jeffery PL, et al. IL-10 promotes production of intestinal mucus by suppressing protein misfolding and endoplasmic reticulum stress in goblet cells. Gastroenterology. 2013;144(2):357-68 e9.

163. Hasnain SZ, Borg DJ, Harcourt BE, Tong H, Sheng YH, Ng CP, et al. Glycemic control in diabetes is restored by therapeutic manipulation of cytokines that regulate beta cell stress. Nat Med. 2014;20(12):1417-26.

164. Feng D, Park O, Radaeva S, Wang H, Yin S, Kong X, et al. Interleukin-22 ameliorates cerulein-induced pancreatitis in mice by inhibiting the autophagic pathway. Int J Biol Sci. 2012;8(2):249-57.

165. Hu M, Yang S, Yang L, Cheng Y, Zhang H. Interleukin-22 Alleviated Palmitate-Induced Endoplasmic Reticulum Stress in INS-1 Cells through Activation of Autophagy. PLoS One. 2016;11(1):e0146818.

166. Böck J. The role of ATG16L1 in chronic inflammatory bowel disease. Kiel, Germany: Kiel University; 2012.

167. Sauer JD, Sotelo-Troha K, von Moltke J, Monroe KM, Rae CS, Brubaker SW, et al. The N-ethyl-N-nitrosourea-induced Goldenticket mouse mutant reveals an essential function of Sting in the in vivo interferon response to Listeria monocytogenes and cyclic dinucleotides. Infect Immun. 2011;79(2):688-94.

168. Polykratis A, Hermance N, Zelic M, Roderick J, Kim C, Van TM, et al. Cutting edge: RIPK1 Kinase inactive mice are viable and protected from TNF-induced necroptosis in vivo. J Immunol. 2014;193(4):1539-43.

169. Murphy JM, Czabotar PE, Hildebrand JM, Lucet IS, Zhang JG, Alvarez-Diaz S, et al. The pseudokinase MLKL mediates necroptosis via a molecular switch mechanism. Immunity. 2013;39(3):443-53.

170. Yang H, Yamazaki T, Pietrocola F, Zhou H, Zitvogel L, Ma Y, et al. STAT3 Inhibition Enhances the Therapeutic Efficacy of Immunogenic Chemotherapy by Stimulating Type 1 Interferon Production by Cancer Cells. Cancer Res. 2015;75(18):3812-22.

171. Zijlstra FJ, Garrelds IM, van Dijk AP, Wilson JH. Experimental colitis in mice: effects of olsalazine on eicosanoid production in colonic tissue. Agents Actions. 1992;Spec No:C76-8.

172. Sato T, Vries RG, Snippert HJ, van de Wetering M, Barker N, Stange DE, et al. Single Lgr5 stem cells build crypt–villus structures in vitro without a mesenchymal niche. Nature. 2009;459(7244):262-5.

173. Shalem O, Sanjana NE, Zhang F. High-throughput functional genomics using CRISPR-Cas9. Nat Rev Genet. 2015;16(5):299-311.

174. Liang CC, Park AY, Guan JL. In vitro scratch assay: a convenient and inexpensive method for analysis of cell migration in vitro. Nat Protoc. 2007;2(2):329-33.

175. Siegmund B, Lehr HA, Fantuzzi G, Dinarello CA. IL-1 beta -converting enzyme (caspase-1) in intestinal inflammation. Proc Natl Acad Sci U S A. 2001;98(23):13249-54.

176. Lowry OH, Rosebrough NJ, Farr AL, Randall RJ. Protein measurement with the Folin phenol reagent. J Biol Chem. 1951;193(1):265-75.

177. Koressaar T, Remm M. Enhancements and modifications of primer design program Primer3. Bioinformatics. 2007;23(10):1289-91.

178. Untergasser A, Cutcutache I, Koressaar T, Ye J, Faircloth BC, Remm M, et al. Primer3--new capabilities and interfaces. Nucleic Acids Res. 2012;40(15):e115.

179. Iwakoshi NN, Lee AH, Vallabhajosyula P, Otipoby KL, Rajewsky K, Glimcher LH. Plasma cell differentiation and the unfolded protein response intersect at the transcription factor XBP-1. Nat Immunol. 2003;4(4):321-9.

180. Fribley A, Zhang K, Kaufman RJ. Regulation of apoptosis by the unfolded protein response. Methods Mol Biol. 2009;559:191-204.

181. Ather JL, Fortner KA, Budd RC, Anathy V, Poynter ME. Serum amyloid A inhibits dendritic cell apoptosis to induce glucocorticoid resistance in CD4(+) T cells. Cell Death Dis. 2013;4:e786.

182. Luo M, Wang H, Wang Z, Cai H, Lu Z, Li Y, et al. A STING-activating nanovaccine for cancer immunotherapy. Nat Nanotechnol. 2017;12(7):648-54.

183. Hasan M, Fermaintt CS, Gao N, Sakai T, Miyazaki T, Jiang S, et al. Cytosolic Nuclease TREX1 Regulates Oligosaccharyltransferase Activity Independent of Nuclease Activity to Suppress Immune Activation. Immunity. 2015;43(3):463-74.

184. Pokatayev V, Hasin N, Chon H, Cerritelli SM, Sakhuja K, Ward JM, et al. RNase H2 catalytic core Aicardi-Goutieres syndrome-related mutant invokes cGAS-STING innate immune-sensing pathway in mice. J Exp Med. 2016;213(3):329-36.

185. Lian LH, Jin Q, Song SZ, Wu YL, Bai T, Jiang S, et al. Ginsenoside Rh2 Downregulates LPS-Induced NF- kappa B Activation through Inhibition of TAK1 Phosphorylation in RAW 264.7 Murine Macrophage. Evid Based Complement Alternat Med. 2013;2013:646728.

186. Fan S, Liu B, Sun L, Lv XB, Lin Z, Chen W, et al. Mitochondrial fission determines cisplatin sensitivity in tongue squamous cell carcinoma through the BRCA1-miR-593-5p-MFF axis. Oncotarget. 2015;6(17):14885-904.

187. Niedzwiecka K, Dylag M, Augustyniak D, Majkowska-Skrobek G, Cal-Bakowska M, Ko YH, et al. Glutathione may have implications in the design of 3-bromopyruvate treatment protocols for both fungal and algal infections as well as multiple myeloma. Oncotarget. 2016;7(40):65614-26.

188. Chen X, Iliopoulos D, Zhang Q, Tang Q, Greenblatt MB, Hatziapostolou M, et al. XBP1 promotes triple-negative breast cancer by controlling the HIF1alpha pathway. Nature. 2014;508(7494):103-7.

189. Ma Y, Shimizu Y, Mann MJ, Jin Y, Hendershot LM. Plasma cell differentiation initiates a limited ER stress response by specifically suppressing the PERK-dependent branch of the unfolded protein response. Cell Stress Chaperones. 2010;15(3):281-93.

190. Dery MA, LeBlanc AC. Luman contributes to brefeldin A-induced prion protein gene expression by interacting with the ERSE26 element. Sci Rep. 2017;7:42285.

191. Wang Q, Mora-Jensen H, Weniger MA, Perez-Galan P, Wolford C, Hai T, et al. ERAD inhibitors integrate ER stress with an epigenetic mechanism to activate BH3-only protein NOXA in cancer cells. Proc Natl Acad Sci U S A. 2009;106(7):2200-5.

192. Slepak TI, Tang M, Slepak VZ, Lai K. Involvement of endoplasmic reticulum stress in a novel Classic Galactosemia model. Mol Genet Metab. 2007;92(1-2):78-87.

193. Martin M. Cutadapt removes adapter sequences from high-throughput sequencing reads. 2011. 2011;17(1).

194. Trapnell C, Roberts A, Goff L, Pertea G, Kim D, Kelley DR, et al. Differential gene and transcript expression analysis of RNA-seq experiments with TopHat and Cufflinks. Nat Protocols. 2012;7(3):562-78.

195. Anders S, Pyl PT, Huber W. HTSeq—a Python framework to work with high-throughput sequencing data. Bioinformatics. 2015;31(2):166-9.

196. Love MI, Huber W, Anders S. Moderated estimation of fold change and dispersion for RNA-seq data with DESeq2. Genome Biology. 2014;15(12):1-21.

197. Chen H, Boutros PC. VennDiagram: a package for the generation of highly-customizable Venn and Euler diagrams in R. BMC Bioinformatics. 2011;12(1):1-7.

198. Breuer K, Foroushani AK, Laird MR, Chen C, Sribnaia A, Lo R, et al. InnateDB: systems biology of innate immunity and beyond—recent updates and continuing curation. Nucleic Acids Research. 2013;41(D1):D1228-D33.

199. Robertson G, Bilenky M, Lin K, He A, Yuen W, Dagpinar M, et al. cisRED: a database system for genome-scale computational discovery of regulatory elements. Nucleic Acids Research. 2006;34(suppl 1):D68-D73.

200. Szklarczyk D, Franceschini A, Wyder S, Forslund K, Heller D, Huerta-Cepas J, et al. STRING v10: protein-protein interaction networks, integrated over the tree of life. Nucleic Acids Res. 2015;43(Database issue):D447-52.

201. Heijmans J, van Lidth de Jeude Jooske F, Koo B-K, Rosekrans Sanne L, Wielenga Mattheus CB, van de Wetering M, et al. ER Stress Causes Rapid Loss of Intestinal Epithelial Stemness through Activation of the Unfolded Protein Response. Cell Reports. 2013;3(4):1128-39.

202. Noda T, Ohsumi Y. Tor, a phosphatidylinositol kinase homologue, controls autophagy in yeast. J Biol Chem. 1998;273(7):3963-6.

203. Ahn J, Konno H, Barber GN. Diverse roles of STING-dependent signaling on the development of cancer. Oncogene. 2015;34(41):5302-8.

204. Murthy A, Li Y, Peng I, Reichelt M, Katakam AK, Noubade R, et al. A Crohn's disease variant in Atg16l1 enhances its degradation by caspase 3. Nature. 2014;506(7489):456-62.

205. Polykratis A, Hermance N, Zelic M, Roderick J, Kim C, Van T-M, et al. Cutting Edge: RIPK1 Kinase Inactive Mice Are Viable and Protected from TNF-Induced Necroptosis In Vivo. The Journal of Immunology. 2014;193(4):1539-43.

206. Murphy James M, Czabotar Peter E, Hildebrand Joanne M, Lucet Isabelle S, Zhang J-G, Alvarez-Diaz S, et al. The Pseudokinase MLKL Mediates Necroptosis via a Molecular Switch Mechanism. Immunity. 2013;39(3):443-53.

207. Welz PS, Wullaert A, Vlantis K, Kondylis V, Fernandez-Majada V, Ermolaeva M, et al. FADD prevents RIP3-mediated epithelial cell necrosis and chronic intestinal inflammation. Nature. 2011;477(7364):330-4.

208. Adolph TE, Tomczak MF, Niederreiter L, Ko H-J, Bock J, Martinez-Naves E, et al. Paneth cells as a site of origin for intestinal inflammation. Nature. 2013;503(7475):272-6.

209. Hernandez PP, Mahlakoiv T, Yang I, Schwierzeck V, Nguyen N, Guendel F, et al. Interferon-lambda and interleukin 22 act synergistically for the induction of interferon-stimulated genes and control of rotavirus infection. Nat Immunol. 2015;16(7):698-707.

210. Wang C, Gong G, Sheh A, Muthupalani S, Bryant EM, Puglisi DA, et al. Interleukin-22 drives nitric oxide-dependent DNA damage and dysplasia in a murine model of colitis-associated cancer. Mucosal Immunol. 2017.

211. Zheng Y, Danilenko DM, Valdez P, Kasman I, Eastham-Anderson J, Wu J, et al. Interleukin-22, a TH17 cytokine, mediates IL-23-induced dermal inflammation and acanthosis. Nature. 2007;445(7128):648-51.

212. Qin B, Zhou Z, He J, Yan C, Ding S. IL-6 Inhibits Starvation-induced Autophagy via the STAT3/Bcl-2 Signaling Pathway. Sci Rep. 2015;5:15701.

213. Shen S, Niso-Santano M, Adjemian S, Takehara T, Malik SA, Minoux H, et al. Cytoplasmic STAT3 represses autophagy by inhibiting PKR activity. Mol Cell. 2012;48(5):667-80.

214. Sabat R, Ouyang W, Wolk K. Therapeutic opportunities of the IL-22-IL-22R1 system. Nat Rev Drug Discov. 2014;13(1):21-38.

215. Tschurtschenthaler M, Wang J, Fricke C, Fritz TM, Niederreiter L, Adolph TE, et al. Type I interferon signalling in the intestinal epithelium affects Paneth cells, microbial ecology and epithelial regeneration. Gut. 2014;63(12):1921-31.

216. Grimm WA, Messer JS, Murphy SF, Nero T, Lodolce JP, Weber CR, et al. The Thr300Ala variant in ATG16L1 is associated with improved survival in human colorectal cancer and enhanced production of type I interferon. Gut. 2016;65(3):456-64.

217. Liang Q, Seo GJ, Choi YJ, Kwak MJ, Ge J, Rodgers MA, et al. Crosstalk between the cGAS DNA sensor and Beclin-1 autophagy protein shapes innate antimicrobial immune responses. Cell Host Microbe. 2014;15(2):228-38.

218. Ishikawa H, Ma Z, Barber GN. STING regulates intracellular DNA-mediated, type I interferon-dependent innate immunity. Nature. 2009;461(7265):788-92.

219. Jeremiah N, Neven B, Gentili M, Callebaut I, Maschalidi S, Stolzenberg MC, et al. Inherited STING-activating mutation underlies a familial inflammatory syndrome with lupus-like manifestations. J Clin Invest. 2014;124(12):5516-20.

220. Yu Q, Katlinskaya YV, Carbone CJ, Zhao B, Katlinski KV, Zheng H, et al. DNA-damage-induced type I interferon promotes senescence and inhibits stem cell function. Cell Rep. 2015;11(5):785-97.

221. Lan YY, Londono D, Bouley R, Rooney MS, Hacohen N. Dnase2a deficiency uncovers lysosomal clearance of damaged nuclear DNA via autophagy. Cell Rep. 2014;9(1):180-92.

222. Saitoh T, Fujita N, Hayashi T, Takahara K, Satoh T, Lee H, et al. Atg9a controls dsDNA-driven dynamic translocation of STING and the innate immune response. Proceedings of the National Academy of Sciences. 2009;106(49):20842-6.

223. Prabakaran T, Bodda C, Krapp C, Zhang BC, Christensen MH, Sun C, et al. Attenuation of cGAS-STING signaling is mediated by a p62/SQSTM1-dependent autophagy pathway activated by TBK1. EMBO J. 2018;37(8).

224. Gaidt MM, Ebert TS, Chauhan D, Ramshorn K, Pinci F, Zuber S, et al. The DNA Inflammasome in Human Myeloid Cells Is Initiated by a STING-Cell Death Program Upstream of NLRP3. Cell. 2017.

225. Lau L, Gray EE, Brunette RL, Stetson DB. DNA tumor virus oncogenes antagonize the cGAS-STING DNA-sensing pathway. Science. 2015;350(6260):568-71.

226. Goldring ES, Grossman LI, Krupnick D, Cryer DR, Marmur J. The petite mutation in yeast. Loss of mitochondrial deoxyribonucleic acid during induction of petites with ethidium bromide. J Mol Biol. 1970;52(2):323-35.

227. Kukat A, Kukat C, Brocher J, Schafer I, Krohne G, Trounce IA, et al. Generation of rho0 cells utilizing a mitochondrially targeted restriction endonuclease and comparative analyses. Nucleic Acids Res. 2008;36(7):e44.

228. Bradley JR. TNF-mediated inflammatory disease. J Pathol. 2008;214(2):149-60.

229. Linkermann A, Green DR. Necroptosis. N Engl J Med. 2014;370(5):455-65.

230. Hsu H, Huang J, Shu HB, Baichwal V, Goeddel DV. TNF-dependent recruitment of the protein kinase RIP to the TNF receptor-1 signaling complex. Immunity. 1996;4(4):387-96.

231. Grimm S, Stanger BZ, Leder P. RIP and FADD: two "death domain"-containing proteins can induce apoptosis by convergent, but dissociable, pathways. Proc Natl Acad Sci U S A. 1996;93(20):10923-7.

232. Mompean M, Li W, Li J, Laage S, Siemer AB, Bozkurt G, et al. The Structure of the Necrosome RIPK1-RIPK3 Core, a Human Hetero-Amyloid Signaling Complex. Cell. 2018.

233. Yeh WC, de la Pompa JL, McCurrach ME, Shu HB, Elia AJ, Shahinian A, et al. FADD: essential for embryo development and signaling from some, but not all, inducers of apoptosis. Science. 1998;279(5358):1954-8.

234. Yeh WC, Itie A, Elia AJ, Ng M, Shu HB, Wakeham A, et al. Requirement for Casper (c-FLIP) in regulation of death receptor-induced apoptosis and embryonic development. Immunity. 2000;12(6):633-42.

235. Varfolomeev EE, Schuchmann M, Luria V, Chiannilkulchai N, Beckmann JS, Mett IL, et al. Targeted disruption of the mouse Caspase 8 gene ablates cell death induction by the TNF receptors, Fas/Apo1, and DR3 and is lethal prenatally. Immunity. 1998;9(2):267-76.

236. Wu J, Huang Z, Ren J, Zhang Z, He P, Li Y, et al. Mlkl knockout mice demonstrate the indispensable role of Mlkl in necroptosis. Cell Res. 2013;23(8):994-1006.

237. Dondelinger Y, Declercq W, Montessuit S, Roelandt R, Goncalves A, Bruggeman I, et al. MLKL compromises plasma membrane integrity by binding to phosphatidylinositol phosphates. Cell Rep. 2014;7(4):971-81.

238. Duprez L, Takahashi N, Van Hauwermeiren F, Vandendriessche B, Goossens V, Vanden Berghe T, et al. RIP Kinase-Dependent Necrosis Drives Lethal Systemic Inflammatory Response Syndrome. Immunity. 2011;35(6):908-18.

239. Gunther C, Martini E, Wittkopf N, Amann K, Weigmann B, Neumann H, et al. Caspase-8 regulates TNF-[agr]-induced epithelial necroptosis and terminal ileitis. Nature. 2011;477(7364):335-9.

240. Welz P-S, Wullaert A, Vlantis K, Kondylis V, Fernandez-Majada V, Ermolaeva M, et al. FADD prevents RIP3-mediated epithelial cell necrosis and chronic intestinal inflammation. Nature. 2011;477(7364):330-4.

241. Robinson N, McComb S, Mulligan R, Dudani R, Krishnan L, Sad S. Type I interferon induces necroptosis in macrophages during infection with Salmonella enterica serovar Typhimurium. Nat Immunol. 2012;13(10):954-62.

242. Mouna L, Hernandez E, Bonte D, Brost R, Amazit L, Delgui LR, et al. Analysis of the role of autophagy inhibition by two complementary human cytomegalovirus BECN1/Beclin 1-binding proteins. Autophagy. 2016;12(2):327-42.

243. Hernandez PP, Mahlakoiv T, Yang I, Schwierzeck V, Nguyen N, Guendel F, et al. Interferon-[lambda] and interleukin 22 act synergistically for the induction of interferon-stimulated genes and control of rotavirus infection. Nat Immunol. 2015;16(7):698-707.

244. Kuriakose T, Man SM, Malireddi RKS, Karki R, Kesavardhana S, Place DE, et al. ZBP1/DAI is an innate sensor of influenza virus triggering the NLRP3 inflammasome and programmed cell death pathways. Science immunology. 2016;1(2):aag2045.

245. Goodall ML, Fitzwalter BE, Zahedi S, Wu M, Rodriguez D, Mulcahy-Levy JM, et al. The Autophagy Machinery Controls Cell Death Switching between Apoptosis and Necroptosis. Dev Cell. 2016;37(4):337-49.

246. Fink SL, Cookson BT. Caspase-1-dependent pore formation during pyroptosis leads to osmotic lysis of infected host macrophages. Cell Microbiol. 2006;8(11):1812-25.

247. Dixon SJ, Lemberg KM, Lamprecht MR, Skouta R, Zaitsev EM, Gleason CE, et al. Ferroptosis: an iron-dependent form of nonapoptotic cell death. Cell. 2012;149(5):1060-72.

248. Sperandio S, de Belle I, Bredesen DE. An alternative, nonapoptotic form of programmed cell death. Proc Natl Acad Sci U S A. 2000;97(26):14376-81.

249. David KK, Andrabi SA, Dawson TM, Dawson VL. Parthanatos, a messenger of death. Front Biosci (Landmark Ed). 2009;14:1116-28.

250. Byrne BG, Dubuisson JF, Joshi AD, Persson JJ, Swanson MS. Inflammasome components coordinate autophagy and pyroptosis as macrophage responses to infection. MBio. 2013;4(1):e00620-12.

251. Chassaing B, Aitken JD, Malleshappa M, Vijay-Kumar M. Dextran sulfate sodium (DSS)-induced colitis in mice. Curr Protoc Immunol. 2014;104:Unit 15 25.

252. Yazbeck R, Howarth GS, Butler RN, Geier MS, Abbott CA. Biochemical and histological changes in the small intestine of mice with dextran sulfate sodium colitis. J Cell Physiol. 2011;226(12):3219-24.

253. Orban PC, Chui D, Marth JD. Tissue- and site-specific DNA recombination in transgenic mice. Proc Natl Acad Sci U S A. 1992;89(15):6861-5.

254. Meng J, Vardar D, Wang Y, Guo HC, Head JF, McKnight CJ. High-resolution crystal structures of villin headpiece and mutants with reduced F-actin binding activity. Biochemistry. 2005;44(36):11963-73.

255. Neufert C, Becker C, Neurath MF. An inducible mouse model of colon carcinogenesis for the analysis of sporadic and inflammation-driven tumor progression. Nat Protoc. 2007;2(8):1998-2004.

256. Liu W, Liu X, Li Y, Zhao J, Liu Z, Hu Z, et al. LRRK2 promotes the activation of NLRC4 inflammasome during Salmonella Typhimurium infection. J Exp Med. 2017;214(10):3051-66.

257. Yan S, Shen H, Lian Q, Jin W, Zhang R, Lin X, et al. Deficiency of the AIM2-ASC Signal Uncovers the STING-Driven Overreactive Response of Type I IFN and Reciprocal Depression of Protective IFN-gamma Immunity in Mycobacterial Infection. J Immunol. 2018;200(3):1016-26.

# 10 Supplements

## 10.1 List of Abbreviations

| | |
|---|---|
| ADF | advanced DMEM/F12 medium |
| AHR | aryl hydrocarbon receptor |
| AIEC | adherent-invasive Escherichia coli |
| Akt (PKB) | protein kinase B |
| AMP | adenosine monophosphate |
| AMPK | 5’ AMP-activated protein kinase |
| ANOVA | analysis of variance |
| AOM | azoxymethane |
| ATF6 | activating transcription factor 6 |
| ATG | autophagy-related protein |
| ATG16L1 | autophagy-related 16-like 1 |
| BafA | bafilomycin A1 |
| BiP/GRP78/HSPA5 | 78 kDa glucose-regulated protein |
| BSA | bovine serum albumin |
| CD | cluster of differentiation |
| cDNA | complementary DNA |
| cGAMP | cyclic guanosine monophosphate-adenosine monophosphate |
| cGAS | cyclic GMP-AMP synthase |
| CHOP | C/EBP homologous protein |
| CRC | colorectal cancer |
| CRISPR | Clustered Regularly Interspaced Short Palindromic Repeats |
| Cas9 | CRISPR associated protein 9 |
| CXCL | C-X-C motif chemokine |
| CYBA | cytochrome b-245 light chain |
| DAB | 3,3’-diaminobenzidine |
| DAI | disease activity index |
| DAPI | 4’,6-diamino-2-phenylindole |
| DEG | differential expressed genes |
| DLB | denaturing lysis buffer |
| DMEM | Dulbecco’s Modified Eagle Medium |
| DMSO | dimethyl sulfoxide |
| DNA | deoxyribonucleic acid |
| DRAQ5™ | Deep Red Anthraquinone 5 |
| dsDNA | double stranded DNA |

| | |
|---|---|
| dsRNA | double stranded RNA |
| DSS | dextrane sodium sulphate |
| DTT | dithiothreitol |
| EDTA | ethylenediaminetetraacetic acid |
| EGF | epidermal growth factor |
| EGFR | epidermal growth factor-receptor |
| EIF2AK3/PERK | protein kinase R-like endoplasmic reticulum kinase |
| ELISA | enzyme-linked immunosorbent assay |
| ER | endoplasmic reticulum |
| ERN1 | endoribonuclease 1 |
| FACS | fluorescence assisted cell sorting |
| FADD | Fas-associated protein with death domain |
| FAM134B | family with sequence similarity 134, member B |
| FBS | foetal bovine serum |
| FLIP | FLICE-like inhibitory protein |
| FMT | faecal microbial transfer |
| FSC | forward scatter |
| GAPDH | glyceraldehyde 3-phosphate dehydrogenase |
| γH2AX | gamma H2A histone family, member X |
| GO | gene ontology |
| GvHD | graft-versus-host disease |
| HBSS | Hank’s Balanced Salt Solution |
| HEPES | 4-(2-hydroxyethyl)-1-piperazineethanesulfonic acid |
| HRP | horseradish peroxidase |
| HSC70 | heat shock cognate 71 kDa protein |
| HSV | herpes simplex virus |
| i.p. | intraperitoneal |
| IBD | inflammatory bowel disease |
| IEC | intestinal epithelial cells |
| IF | immunofluorescence |
| IFIT | interferon-induced protein with tetratricopeptide repeats 1 |
| IFN | interferon |
| IFNAR | interferon-α/β receptor |
| IgA | immunoglobulin A |
| IGF-1R | insulin-like growth factor 1 receptor |
| IHC | immunohistochemistry |
| IL | interleukin |

| | |
|---|---|
| IL22BP | interleukin-22-binding protein |
| IL23R | interleukin-23-receptor |
| IL7R | interleukin-7-receptor |
| ILC | innate lymphoid cells |
| IRE1 | inositol-requiring enzyme 1 |
| IRF3 | interferon regulatory factor 3 |
| IRGM | immunity-related GTPase family M protein |
| ISC | intestinal stem cells |
| ISG | interferon stimulated gene |
| JAK | Janus kinase |
| JNK | c-Jun N-terminal kinases |
| LAMP 2A | lysosome-associated membrane glycoprotein 2A |
| LC3 | microtubule-associated proteins 1A/1B light chain 3B |
| LRRK2 | leucine-rich repeat kinase 2 |
| LTi cells | lymphoid tissue inducer cells |
| MAVS | mitochondrial antiviral-signaling protein |
| MDA5 | melanoma differentiation antigen 5 |
| MEM | Modified Eagle Medium |
| MLKL | mixed lineage kinase domain like pseudokinase |
| mRNA | messenger RNA |
| mtDNA | mitochondrial DNA |
| mTOR | mechanistic Target of Rapamycin |
| mTORC1 | mechanistic Target of Rapamycin complex 1 |
| MUC2 | mucin 2 |
| NADPH | nicotinamide adenine dinucleotide phosphate |
| NCR | natural cytotoxicity receptor |
| NF-κB | nuclear factor kappa-light-chain-enhancer of activated B cells |
| NK cells | natural killer cells |
| NKT cells | natural killer T cells |
| NLRP3 | NOD-like receptor family pyrin domain-containing protein 3 |
| NOD2 | nucleotide-binding oligomerization domain-containing protein 2 |
| NOX1 | NADPH oxidase 1 |
| ORMDL3 | ORM1-like protein 3 |
| p40 | interleukin-12 subunit p40 |
| p53 | tumor protein 53 |
| PAGE | polyacrylamide gel electrophoresis |
| PAMP | pathogen-associated molecular pattern |

| | |
|---|---|
| PAR | poly(ADP-ribose) |
| PBC | primary biliary cirrhosis |
| PBS | phosphate-buffered saline |
| PCR | polymerase |
| PI | propidium iodide |
| PKR | protein kinase R |
| poly(I:C) | polyinosinic:polycytidylic acid |
| PSC | primary sclerosing cholangitis |
| PVDF | polyvinylidene fluoride |
| qPCR | quantitative (real time) PCR |
| REG3B/G | regenerating islet-derived 3 β/γ |
| RFP | red fluorescent protein |
| RIG-I | retinoic acid-inducible gene I |
| RIPK | receptor-interacting serine/threonine-protein kinase 1 |
| RNA | ribonucleic acid |
| RNASEH2B | ribonuclease H2, subunit B |
| RNAseq | RNA sequencing |
| ROS | reactive oxygen species |
| RPMI buffer | Roswell Park Memorial Institute buffer |
| S100A8/9 | S100 calcium-binding protein A8/9 |
| SDS | sodium dodecyl sulphate |
| SLE | systemic lupus erythematosus |
| SMAD7 | mothers against decapentaplegic homologous 7 |
| SNP | single nucleotide polymorphism |
| ssRNA | single stranded RNA |
| STAT | signal transducer and activator of transcription |
| STING | stimulator of interferon genes |
| STRING | Search Tool for the Retrieval of Interacting Genes/Proteins |
| TAC | transit amplifying cells |
| TBK1 | TANK-binding kinase 1 |
| TBS | Tris-buffered saline |
| TCF-4 | transcription factor 4 |
| TFBS | transcription factor binding site |
| TGF-β | transforming growth factor beta |
| TGS | Tris/glycine/SDS |
| $T_h$ cells | T helper cells |
| TLR | Toll-like receptor |

| | |
|---|---|
| TM | tunicamycin |
| TNFα | tumor necrosis factor alpha |
| TNFR1 | TNF receptor 1 |
| TRADD | TNF receptor type 1-associated death domain protein |
| TRIF | TIR-domain-containing adapter-inducing interferon-β |
| TRIM | tripartite motif family |
| T/TBS | TBS supplemented with Tween 20 (1%) |
| TUNEL | terminal deoxynucleotidyl transferase dUTP nick end labeling |
| TYK2 | tyrosine kinase 2 |
| UC | ulcerative colitis |
| UPR | unfolded protein response |
| WD40 | tryptophan-aspartic acid dipeptide repeats |
| WNT | Wingless-type MMTV integration site family |
| XBP1 | X-box binding protein 1 |
| XIAP | X-linked inhibitor of apoptosis protein |
| YAP | Yes-associated protein |
| ZO-1 | zonula occludens-1 |
| Z-VAD-FMK | carbobenzoxy-valyl-alanyl-aspartyl-(O-methyl)-fluoromethylketone |

## 10.2 List of Figures

## 10.3 List of Tables

## 10.4 Acknowledgements

Firstly, I am grateful to my principal investigator Prof. Dr. Philip Rosenstiel for giving me the opportunity to work in science. Your expertise, continuous motivation and advices were inspiring and layed the groundwork of my scientific training. Many thanks for your support of my work and academic career.

I would like to express my deepest gratitude to Dr. Konrad Aden for his encouraging and continuous guidance in scientific work, particularly for this project. I like to thank you for your precious advises for my academic career. I am pleased to share your enthusiasm and dedication on science.

I am grateful to Prof. Dr. Stefan Schreiber for promotion and support of my scientific work before and after my medical graduation. You are sharing your inspiring scientific and clinical visions which makes working in your department to a privilege.

I would like to thank the RTG 1743 *Genes, Environment, Inflammation* for financial and idealistic support of my work.

I like to thank Dr. Raheleh Sheibani-Tezerji for the support of the transcriptomic analysis as well as Dr. Go Ito for sharing his expertise in organoid cultures and fruitful discussions on this project. I like to thank Dr. Jan Kuiper for sharing his continuous and critical view on experimental details. I would like to acknowledge Dr. Kareen Bartsch for her help and discussion on dsDNA.

It was a pleasure for me to work with all of my colleagues in the lab. However, I like to point out Dr. Steffen Pfeuffer for introducing me into this lab and his proper in-lab-support. Thank you for your patience and your friendship.

A special thank goes to Markus Tschurtschenthaler, Svetlana Saveljeva and Joya Bhattacharyya during their time in Cambridge, who were warmly willing to help in this project without hesitation and steadily gave input to make the publication successful.

I deeply appreciate discussing and working with the technicians, namely Sabine, Dorina, Maren, Tanja, Katha, Melanie, Tatjana and Karina who helped me a lot with their immense expertise to make the experiments successful.

I need to thank Thomas for our deep friendship and our discussions. You are like a brother for me who shares the enthusiasm for science.

I would like to thank Cornelia for the last years of support during my work in the laboratory. Your love and patience kept my motivation alive. Thank you for your caring.

Finally, my deepest appreciation belongs to my family, especially my beloved mother, for their continuous and unconditioned love, patience and understanding. Thank you for everything.

## 10.5 Curriculum Vitae

### Personal Data

| | |
|---|---|
| First and last name | Florian Tran |
| Date of birth | 23rd April 1991 |
| Place of birth | Kiel, Germany |
| Nationality | German, Swedish |
| Address | Preußerstraße 12, 24105 Kiel, Germany |
| Contact | f.tran@ikmb.uni-kiel.de |

### Education and Training

| | |
|---|---|
| 02/2017 - now | Department of Internal Medicine I, University Hospital Schleswig-Holstein, Campus Kiel (Director: Prof. Dr. med. Schreiber)<br>- **clinical fellowship** |
| 02/2014 - now | Institute of Clinical Molecular Biology, Kiel, Germany<br>- **doctoral thesis**, Principal Investigator: Prof. Dr. med. Rosenstiel |
| 10/2015, 12/2016 | Christian-Albrechts-University Kiel, Germany<br>- **final exam**: very good (1,0) |
| 11/2015 - 10/2016 | **Clinical rotations**<br>- **Surgery**: Städtisches Krankenhaus, Kiel, Germany<br>- **Neurology**: Institute of Neurology, Queen Square, University College London, England<br>- **Internal Medicine**: University Hospital Schleswig-Holstein, Campus Kiel, Germany |
| 10/2012 - 09/2015 | Christian-Albrechts-University Kiel, Germany<br>- **clinical studies** |
| 10/2010 - 09/2012 | Christian-Albrechts-University Kiel, Germany<br>- **pre-clinical studies**, final result: very good (1,0) |
| 10/2007 - 09/2009 | Christian-Albrechts-University Kiel, Germany<br>- mathematics |
| 08/2001 - 06/2010 | Thor-Heyerdahl-Gymnasium, Kiel, Germany<br>- **secondary school**, grade: very good (1,2) |

### Scientific interests

Mucosal immunology, mono-/oligogenic IBD, immunodeficiencies, single cell transcriptomics, tissue regeneration, microbiome in IBD

## 10.6 Publications and scientific presentations

### 10.6.1 Publications

1. Aden K, Rehman A, Falk-Paulsen M, Secher T, Kuiper J, **Tran F**, Pfeuffer S, Sheibani-Tezerji R , Breuer A, Luzius A, Jentzsch M, Häsler R, Billmann-Born S, Will O, Lipinski S, Bharti B, Adolph T, Iovanna JL, Kempster SL, Blumberg RS, Schreiber S, Becher B, Chamaillard M, Kaser A and Rosenstiel P.
   **Epithelial IL-23R signaling licenses protective IL-22 responses in intestinal inflammation.**
   *Cell Reports. 2016, Aug 23; 16(8):2208-18.*
2. Aden K, Breuer A, Rehman A, Geese H, **Tran F**, Sommer J, Waetzig G, Reinheimer T, Schreiber S, Rose-John S, Scheller J, Rosenstiel P.
   **Classic IL-6R signalling is dispensable for intestinal epithelial proliferation and repair.**
   *Oncogenesis. 2016 Nov 21; 5(11):e270.*
3. Nikolaus S, Schulte B, Al-Massad N, Thieme F, Schulte DM, Bethge J, Rehman A, **Tran F**, Aden K, Häsler R, Moll N, Schütze G, Schwarz MJ, Waetzig GH, Rosenstiel P, Krawczak M, Szymczak S, Schreiber S.
   **Increased Tryptophan Metabolism Is Associated With Activity of Inflammatory Bowel Diseases.**
   *Gastroenterology, 2017 Dec; 153(6):1504-1516.e2*
4. Aden K*, **Tran F***, Ito G*, Sheibani-Tezerji R, Lipinski S, Kuiper J, Tschurtschenthaler M, Saveljeva S, Bhattacharyya J, Häsler R, Bartsch K, Luzius A, Jentzsch M, Falk-Paulsen M, Stengel S, Welz L, Schwarzer R, Rabe B, Barchet W, Krautwald S, Hartmann G, Pasparakis M, Blumberg RS, Schreiber S, Kaser A, Rosenstiel P.
   ***Atg16l1* orchestrates interleukin-22-signalling in the intestinal epithelium via cGAS/STING.**
   *Journal of Experimental Medicine. 2018, Nov 5; 215(11):2868-2886.*

### 10.6.2 Oral presentations

1. **Tran F**. *XBP1 und ATG16L1 koordinieren protektive Interleukin-22-Signale im intestinalen Epithel.* Presented at the Annual Meeting of the Deutsche Arbeitsgemeinschaft für chronisch-entzündliche Darmerkrankungen (DACED); 2015 Jun 19-20; Mainz, Germany.

2. Aden K*, **Tran F*** et al. *XBP1 und ATG16L1 koordinieren protektive Interleukin-22-Signale im intestinalen Epithel.* Presented at *Viszeralmedizin 2015*. Deutsche Gesellschaft für Viszeral- und Stoffwechselerkrankungen; 2015 Sep 21-24; Leipzig, Germany: Z Gastroenterol; 2015. Vol. 53(8), Abstract KG038
3. **Tran F**. *ATG16L1 and XBP1 coordinate protective IL-22 signals in the intestinal epithelium.* Presented at the Student Symposium of Life Sciences Nord 2015; 2015 Dez 5; Kiel, Germany.
4. **Tran F**. *The proregenerative role of Interleukin-22 signals in the intestinal epithelium depends on autophagy and ER stress*. Presented at the Annual Meeting of the Deutsche Arbeitsgemeinschaft für chronisch-entzündliche Darmerkrankungen (DACED); 2016 Jun 17-18; Mainz, Germany.
5. Aden K*, **Tran F*** et al. *Das Zusammenspiel aus Autophagie und ER-Stress koordiniert protektive IL-22-Signale im intestinalen Epithel***.** Presented at Viszeralmedizin 2016. Deutsche Gesellschaft für Viszeral- und Stoffwechselerkrankungen; 2016 Sep 21-24; Hamburg, Germany: Z Gastroenterol; 2016. Vol. 54(8), Abstract KV015
   - **Promotionsstipendium (DGVS)**
6. Aden K*, **Tran F*** et al. *The proregenerative role of Interleukin-22 signals in the intestinal epithelium depends on autophagy and ER stress*. Presented at the 24th United European Gastroenterology Week. United European Gastroenterology; 2016 Oct 15-19; Vienna, Austria: United European Gastroenterol J; 2016. Vol. 4(5), Abstract OP 306
   - **Basic Science Travel Grant, Oral Free Paper Prize**
7. Lipinski S, **Tran F** et al. *Die Rolle der NADPH-Oxidasen NOX1 und p22$^{phox}$ in frühkindlicher CED.* Presented at Viszeralmedizin 2017. Deutsche Gesellschaft für Viszeral- und Stoffwechselerkrankungen; 2017 Sep 13-16; Dresden, Germany: Z Gastroenterol; 2017. Vol. 55(8), Abstract KV064
8. Lipinski S, **Tran F** et al. *The role of the NADPH oxidases NOX1 and p22$^{phox}$ in (veo)IBD.* Presented at the 25th United European Gastroenterology Week. United European Gastroenterology; 2017 Oct 28 - Nov 1; Barcelona, Spain: United European Gastroenterol J; 2017. Vol. 5, OP271
   - **Basic Science Travel Grant**

## 10.6.3 Poster presentations

1. **Tran F** et al. *Interleukin-22 aggravates ER stress in intestinal epithelium.* Poster presented at the International 5th Annual Cluster Symposium of the Cluster of Excellence *Inflammation at Interfaces*. 2015 Feb 26-28; Kiel.
2. Aden K*, **Tran F*** et al. *An interplay between ER stress and autophagy coordinates protective IL-22 signaling in the intestinal epithelium.* Poster and poster talk presented at the 23rd United European Gastroenterology Week. United European Gastroenterology; 2015 Oct 15-19; Barcelona, Spain: United European Gastroenterol J; 2015. Vol. 3, Abstract P0287.
   - **Basic Science Travel Grant, Poster of Excellence, National Scholar Award**
3. **Tran F***, Aden K* et al. *Atg16L1 orchestrates interleukin-22-signalling in the intestinal epithelium via cGAS/STING.* Poster and Poster Prize Talk presented at the Falk Symposium 209: IX Gastro-Conference (Part II) - IBD 2017 - Therapeutic and Biological Barriers; 2017 Oct 6-7; Berlin, Germany.
   - **3rd Poster Prize**

## 10.7 Eidesstattliche Erklärung

Hiermit versichere ich, Florian Tran, an Eides statt, dass

- meine Dissertation, abgesehen von Ratschlägen meines Doktorvaters und meiner sonstigen akademischen Lehrer, nach Form und Inhalt meine eigene Arbeit ist, dass ich außer den in der Arbeit aufgeführten keine weiteren Hilfsmittel benutzt habe, und dass meine Arbeit bisher, weder ganz noch in Teilen, keiner anderen akademischen Stelle als Dissertation vorliegt.
- Veröffentlichungen nach den Richtlinien über Benotung von Dissertationen erfolgt sind.
- die zuständigen Behörden zugestimmt haben, dass Forschungsvorhaben an Tieren vorgenommen wurden.
- ich bis zum heutigen Tage 13 Semester an der Christian-Albrechts-Universität studiert habe.
- die Leiter des Instituts für klinische Molekularbiologie einverstanden sind, dass die Dissertation an deren Einrichtung geschrieben wurde.
- Für die Nutzung von Arbeitsmöglichkeiten der wissenschaftlichen Einrichtung durch mich das Einverständnis der Leitung der Einrichtung vorliegt.

Ich erkläre, dass die Arbeit unter Einhaltung der Regeln guter wissenschaftlicher Praxis der Deutschen Forschungsgemeinschaft entstanden ist.

Kiel, den 20.06.2018

Florian Tran